



Université Lille1

École Doctorale des Sciences Pour l'Ingénieur

Thèse

pour obtenir le grade de

Docteur de l'Université des Sciences et Technologies de Lille

Spécialité: Génie Électrique

**Sajjad A. SYED**

le 06 Juin 2012

ENERGETIC MACROSCOPIC REPRESENTATION AND MULTI-  
LEVEL ENERGY MANAGEMENT FOR HEAVY- DUTY HYBRID  
VEHICLES USING DOUBLE PLANETARY GEARTRAIN

Membres du jury :

M. BARRADE Philippe, *Invité*, EPF Lausanne

M. BOUSCAYROL Alain, *Directeur de la thèse*, Université Lille1

M. HOFMAN Theo, *Examineur*, TU Eindhoven

Mme. LEMAIRE-SEMAIL Betty, *Président*, Université Lille 1

M. LHOMME Walter, *Codirecteur de la thèse*, Université Lille1

M. PAPE Olivier, *Invité*, *NEXTER Systems*

Mme. PERA Marie-cécile, *Rapporteur*, FEMTO-ST Belfort

M. TRIGUI Rochdi, *Rapporteur*, IFFSTAR Bron



*Dedicated to my beloved mother  
“Zahra Syed”*



# Acknowledgment

At first, I would like to thank Prof. Dr. Alain BOUSCAYROL for providing me the opportunity to work under his supervision in the research group at Laboratoire d'Electrotechnique et d'Electronique de Puissance (L2EP), University of Lille1, France. He provided me with all the needed resources and allowed me autonomy to carry out my research work. His mentorship as well as wisdom and extensive experience in Modeling and Control helped to shape this paper and research. Despite his hectic research schedule, he always found time to discuss and review my work. Moreover, his help allowed for the progress of this research and the presentation of this work in its current form. Had it not been for his positive attitude and encouragement, this thesis might not have been completed.

I am also deeply grateful to my co-advisor Dr. Walter LHOMME, University of Lille1, for his constant guidance and support throughout the course of study. He is the most important influence on the successful completion of this thesis. He also had the greatest professional influence on my development as a researcher. He is an amazing scientist and mentor. He pushed me to develop my weaknesses and exploit my strengths. His courage to tackle new and difficult problems and his patience to withstand the many failures that accompany such risks is admirable.

All my friends at L2EP, especially Tony Letrouvé, Abdellatif Tinzefté, Yuan Cheng, Keyu Chen and Rindra Ramarotafika with whom I shared moments of stress and joy; and profound philosophical discussion regarding every perspective of thesis and life around us.

Most of all, I want to thank the people beyond university and academia, whose lives were affected by this work: my brothers and sisters for supporting me making this possible, my friends Azmat Hayat, Najeeb Sabir, Usman Bhatti, and Ali Shah for providing such a memorable company during the tough PhD years. They represent my “other life” during my stay in France, especially during weekends. And last but not least my wife for supporting and encouraging me for the timely completion of this thesis. Thank you, I could not have done this without all of you.



# Résumé

Actuellement, les Véhicules Electriques Hybrides (VEHs) sont considérés comme une partie essentielle du futur de l'industrie automobile. En effet, cette technologie permet de réduire la consommation de carburant et les émissions de gaz à effet de serre et ce, sans réduire les performances. Les VEHs sont composées de deux ou plusieurs sources d'énergie. Ces sources peuvent être organisées selon plusieurs architectures. Dans cette thèse, l'architecture série-parallèle est choisie pour des véhicules types militaires et de collecte d'ordures. Les VEHs étudiés contiennent un double train planétaire. Ce nouveau répartiteur de puissance rend le système très complexe. Par conséquent, dans cette thèse, la modélisation des VEHs étudiés avec un double train planétaire est faite. L'utilisation de la Représentation Macroscopique Energétique (REM), représentation graphique permettant de déduire la structure de commande, est effectuée pour les deux véhicules étudiés.

Cette thèse aborde également la problématique de la gestion de l'énergie des systèmes multi-sources pour les VEHs. Leur stratégie de gestion de l'énergie regroupe plusieurs disciplines et soulève différents challenges. Les défis résident principalement dans la gestion de la dépense d'énergie, la détermination de la répartition de l'énergie et l'établissement de méthode d'interface entre les différents systèmes de manière à répondre aux exigences de la propulsion et des autres exigences de la charge. Dans ce travail, une nouvelle organisation de la stratégie de gestion de l'énergie a été effectuée pour les véhicules étudiés (véhicules militaire et de collecte d'ordures) par une décomposition de cette gestion en 3 niveaux bien distincts.





# Abstract

Currently, Hybrid Electric Vehicles (HEVs) are considered to be a critical part of the future vehicle industry. This is because they allow for decreased fuel consumption and emissions without a decline in performance. HEVs are composed of two or more power sources and can be arranged in various topologies. In this thesis, a series-parallel architecture is chosen for military and garbage trucks. The studied HEVs contain a Double Planetary Geartrain as a Power Split Device (PSD), which makes the system very intricate and complex. Therefore, in this thesis, modeling of studied HEVs with a PSD is done. Later, through the assistance of Energetic Macroscopic Representation (EMR) it is graphically represented and local control structure for both vehicles are deduced.

This dissertation also addresses the problem of managing energy of multiple energy sources for the studied HEVs. The Energy Management Strategy (EMS) in application to HEVs encompasses several different disciplines and challenges. Primarily, the challenges lies in managing the energy expenditure, determining the proportional power splits and establishing methods to interface between the systems so as to meet the demands of the vehicle propulsion and other load requirements. In this work, an attempt has been made to provide a new organization of EMS by decomposition in 3 explicit levels for studied vehicles i.e. military and garbage truck.



# Table of Contents

<b>GENERAL INTRODUCTION .....</b>	<b>1</b>
<b>CHAPTER I HEAVY-DUTY HYBRID ELECTRIC VEHICLES .....</b>	<b>7</b>
<b>INTRODUCTION .....</b>	<b>9</b>
<b>I.1 CONTEXT AND CONCEPTS .....</b>	<b>10</b>
I.1.1 BACKGROUND.....	10
I.1.2 HYBRID ELECTRIC VEHICLES (HEVs).....	11
I.1.3 CLASSIFICATION OF VEHICLES .....	13
<b>I.2 POWERTRAIN AND POWER SPLIT DEVICES (PSDS) .....</b>	<b>21</b>
I.2.1 PLANETARY GEAR TRAINS .....	21
I.2.2 SINGLE PLANETARY GEAR TRAIN.....	22
I.2.3 COMPOUND PLANETARY GEAR TRAIN.....	23
<b>I.3 PRESENTATION OF THE STUDIED VEHICLES .....</b>	<b>25</b>
I.3.1 PROPOSED VEHICLES.....	25
I.3.2 KINEMATICS STUDY .....	27
I.3.3 ENERGETIC STUDY .....	29
<b>I.4 RESEARCH MOTIVATION AND OBJECTIVE .....</b>	<b>31</b>
I.4.1 BACKGROUND.....	31
I.4.2 RESEARCH MOTIVATION.....	32
I.4.3 RESEARCH OBJECTIVE .....	34
<b>CONCLUSION.....</b>	<b>36</b>
<b>CHAPTER II MODELING AND EMR OF STUDIED HEVS .....</b>	<b>37</b>
<b>INTRODUCTION .....</b>	<b>39</b>
<b>II.1 MODELING OF COMPLEX SYSTEMS.....</b>	<b>40</b>
II.1.1 MODELING, REPRESENTATION AND CONTROL .....	40
II.1.2 PRESENTATION OF THE VEHICLES .....	41
II.1.3 MODELING OF THE PSD .....	43
<b>II.2 EMR OF SUBSYSTEMS.....</b>	<b>47</b>
II.2.1 SOURCES .....	48
II.2.2 ENERGETIC ELEMENTS.....	54
<b>II.3 EMR OF BOTH HEVS.....</b>	<b>59</b>
II.3.1 DUAL-RANGE GEARBOXES WITH CLUTCH .....	60
II.3.2 FINAL EMR OF THE MILITARY TRUCK.....	64
II.3.3 FINAL EMR OF THE STUDIED VEHICLE .....	65
<b>CONCLUSION.....</b>	<b>67</b>
<b>CHAPTER III INVERSION-BASED CONTROL FOR STUDIED HEVS.....</b>	<b>69</b>
<b>INTRODUCTION.....</b>	<b>71</b>
<b>III.1 CONTROL OF THE STUDIED HEVS .....</b>	<b>72</b>
<b>III.2 INVERSION-BASED CONTROL FOR CONSIDERED HEVS.....</b>	<b>76</b>

III.2.1	INVERSION-BASED CONTROL OF SUBSYSTEMS .....	76
III.2.2	INVERSION-BASED CONTROL OF MILITARY TRUCK .....	80
III.2.3	INVERSION-BASED CONTROL OF GARBAGE TRUCK .....	81
<b>III.3</b>	<b>VALIDATION OF CONTROL SCHEME .....</b>	<b>82</b>
III.3.1	SIMULATION VALIDATION .....	82
III.3.2	SIMULATION RESULTS FOR MILITARY TRUCK .....	85
III.3.3	SIMULATION RESULTS FOR GARBAGE TRUCK .....	88
<b>CONCLUSION .....</b>		<b>92</b>
<b>CHAPTER IV ENERGY MANAGEMENT STRATEGY .....</b>		<b>93</b>
<b>INTRODUCTION .....</b>		<b>95</b>
<b>IV.1</b>	<b>ENERGY MANAGEMENT ANALYSIS .....</b>	<b>96</b>
IV.1.1	OVERVIEW .....	96
IV.1.2	CLASSIFICATION .....	98
IV.1.3	BASIC CONCEPTS OF ENERGY MANAGEMENT .....	100
<b>IV.2</b>	<b>PROPOSED GLOBAL ENERGY MANAGEMENT .....</b>	<b>102</b>
IV.2.1	PROPOSED MULTI-LEVEL ENERGY MANAGEMENT .....	102
IV.2.2	PROPOSED ENERGY MANAGEMENT REALIZATION .....	106
IV.2.3	ORGANIZATION OF MULTI-LEVEL EMS .....	109
<b>IV.3</b>	<b>VALIDATION AND SIMULATION RESULTS .....</b>	<b>113</b>
IV.3.1	VALIDATION IN STATEFLOW .....	113
IV.3.2	SIMULATION RESULTS FOR MILITARY TRUCK .....	117
IV.3.3	SIMULATION RESULTS FOR GARBAGE TRUCK .....	122
<b>CONCLUSION .....</b>		<b>126</b>
<b>FINAL CONCLUSION .....</b>		<b>127</b>
<b>APPENDIX A:</b>	<b>EMR AND INVERSION-BASED CONTROL .....</b>	<b>135</b>
<b>APPENDIX B:</b>	<b>STATIC MAPS .....</b>	<b>137</b>
<b>APPENDIX C:</b>	<b>EQUIVALENT SHAFTS .....</b>	<b>138</b>
<b>APPENDIX D:</b>	<b>POWER FLOWS .....</b>	<b>144</b>
<b>APPENDIX E:</b>	<b>STATE TRANSITION DIAGRAM .....</b>	<b>149</b>
<b>ACRONYMS AND ABBREVIATIONS .....</b>		<b>151</b>
<b>LIST OF SYMBOLS .....</b>		<b>155</b>
<b>REFERENCES .....</b>		<b>159</b>

# **General Introduction**



# General Introduction

In the modern economy, efficient transportation, i.e. road vehicles is a matter of vital importance. Increased concern about fuel economy and emissions coupled with the ever-depleting natural resource of oil has put increased emphasis on developing alternatives modes of eco-friendly transport. With a part estimated at approximately at 20% of global carbon dioxide (CO<sub>2</sub>) emissions, the transport sector is one of the main contributors to global warming [IEA 2009]. In order to help lower carbon dioxide emissions and save energy to prevent global warming, focus has been on developing new technology and improvements in fuel efficiency. One of the most promising solutions towards efficient and clean land transportation can be achieved with the transition from Internal Combustion Engine (ICE) based vehicles to ones equipped with electric propulsion (Electric Machines (EMs) with batteries) or a mix between both, known as Hybrid Electric Vehicle (HEV) [Chau 2007] [Chan 2010]. Though HEVs do not completely rule out the use of crude oil, they do decrease its usage to a considerable extent.

In last decade, the hybridization of all kinds of vehicles has attracted tremendous attention as a commercially viable alternative to both traditional and electric vehicles. Battery- powered electric vehicles are very environmentally friendly but have strong limitations such as a short driving range, a high cost for batteries and a long charge time [Raskin 2006] [Chan 2011]. Furthermore, in the heavy-duty class, electric vehicles are not a viable alternate due to the large weight and power requirements needed. Therefore, to meet these challenges, HEVs offers the best solution to overcome the limitations of both vehicles i.e. ICE based and battery based, for application to large weight vehicles. The other significant advantage of HEVs is its flexibility in optimal power distribution due to its multiple power sources, while satisfying the performance requirements.

In this context, MEGEVH (Modelisation Energetique et Gestion d'Energie de Vehicules Hybrides / Energy Modeling and Energy Management of Hybrid Vehicles) was established in 2005. This network is based on different academic institutions and industrial partners that work on HEVs in France. The objective of MEGEVH is to foster collaboration regarding ener-

getic modeling, energy management and energy optimization of HEVs. In the MEGEVH network, there are many ongoing and operational projects such as MEGEVH-strategy, MEGEVH-macro etc. This dissertation is also a part of MEGEVH network in the project named ARCHYBALD (ARChitectures HYBrides Adaptées aux véhicules Lourds à forte Disponibilité / Hybrid Drive Systems for Heavy-Duty Vehicles). This project is funded by ANR (Agence Nationale de la Recherche) for the development of a hybrid vehicle for the New Generation Heavy Trucks and managed by NEXTER Systems.

There are many different modeling topologies or formalisms that have been used to represent complex systems such as HEVs. In this research work, Energetic Macroscopic Representation (EMR) is taken into account in order to represent the casual functional modeling of the studied vehicles. The EMR representation gives in-depth information about the energetic functions of the system through its macroscopic energetic view. The other main reason for using this formalism is its inversion rules. The inversion rules of EMR lead to build the local control structure of complex systems in a systematic way. Thanks to these features, EMR and its inversion-based control contribute significantly to the control design and energy management of HEVs. From many years EMR has been successfully applied to different HEVs [Lhomme 2007] [Chen 2010] [Letrouvé 2010] and other applications such as wind energy conversion systems [Bouscayrol 2002] [Delarue 2003] [Bouscayrol 2005-a] [Peng 2009], fuel cell systems [Chrenko 2009] [Boulon 2009-a] [Boulon 2010], photovoltaic system [Locment 2010], electric subway [Verhille 2006] [Allègre 2010-a], hybrid railway powertrain [Baert 2011], multi-drive paper processing systems [Wankam 2006], two arranged EM drives (split E-CVT) [Chen 2008] [Cheng 2010], gantry drive system [Kestelyn 2009] and helicopter systems [Bienaimé 2011].

The ARCHYBALD project deals with the research and development for the hybridization of heavy-duty vehicles for military and civil applications. In this research work a series-parallel architecture is chosen for the hybridization of these vehicles. To achieve this architecture, a special geartrain called the double planetary geartrain is utilized. Both considered HEVs have a similar architecture but are different in the sizing of their components and subsystems. The partners involved in ARCHYBALD project are two industrial (NEXTER Systems and BATSCAP) and three research laboratories FEMTO-ST (Belfort), IFFSTAR (Arcueil, Ile de France) and L2EP (Lille). In this pro-



ject, two other PhDs have been undertaken. One focuses on the development of energy storage systems such as batteries and ultra capacitors [Butterbach 2010] and the other focuses on the design of electric machines [Wu 2012].

The objective of this thesis work to perform modeling, simulation and propose an organization of multi-level Energy Management Strategy (EMS), solution for the new type of vehicle proposed in the project i.e. military and garbage trucks. Although the architecture of both vehicles is similar, the design constraints and limitations vary. Consequently, these differences will have an impact on the final energy management of the system. Because of this, the second goal of this research is to assess and compare these differences by implementing the same modeling and control structure through EMR and its inversion-based control not using the same energy management. EMR is used because it is an efficient and flexible tool that can handle the issues related to both HEVs very effectively. The global energy management or EMS in vehicles, specifically HEVs, is an important and key issue because it can significantly influence the performance of the vehicle. Improving energy management in vehicles can also deliver important benefits such as reducing fuel consumption, decreasing emission, lower running cost, reducing noise pollution, improving driving performance and facilitate easy usage.

Chapter I is dedicated to characterizing typical HEVs and their key components for the heavy-duty vehicles specifically for application to military and garbage trucks. Later, in light of these characterizations, the objective of this thesis is defined.

Chapter II presents the modeling and graphical representation of the two considered HEVs through EMR. In this, the detailed features of both vehicles and their containing components are discussed by highlighting the requirements and constraints of each vehicle.

Chapter III builds an inversion-based control for the studied HEVs, using the inversion principle of EMR and modeling presented in Chapter II. Simulation results are presented through a simple strategy.

Chapter IV proposes a new organization of multi-level EMS and its implementation for complex systems such as studied HEVs. An organization of multi-level EMS is thus proposed and realized and simulation results are provided for studied HEVs.



# **Chapter I**

## **Heavy-Duty Hybrid Electric Vehicles**



## Introduction

The conventional vehicle based on Internal Combustion Engine (ICE) uses gasoline or diesel as fuel for the energy source. Because of its fuel only base, this vehicle presents a problem due to its increased oil consumption with minimum oil resources and an increase in hazardous emissions in the air. Therefore, for future road transportation there should be new alternative which should address these challenges. Various alternatives have been proposed to alleviate these issues such as: an improvement in an ICE based vehicle, use of new alternative fuels called biofuels, increased in development of Electric Vehicles (EVs), Fuel Cell vehicles (FC) and Hybrid Electric Vehicles (HEVs) [Granovskii 2006].

Battery based EVs are arguably one of the best solutions to the current energy crisis and the environment because EVs do not consume any oil and have no local emissions during driving. However, these vehicles have limitations such as a short driving range, high cost due to batteries and a long charge time [Chan 2011] [Raskin 2006]. Furthermore, amongst other reasons, a battery based EVs are not practical for big trucks due to the large weight and required power of the vehicle. Therefore, to meet the above discussed challenges, HEVs offers an interesting solution to overcome the limitations of both vehicles i.e. ICE based and battery based, for application to heavy weight vehicles.

The aim of this chapter is to characterize typical HEVs and their key components for the heavy-duty vehicles specifically for application to military and civil trucks. Later, in light of these characterizations, the objective of thesis will be defined. To do so, this chapter is organized in four sections. The first section deals the basic context and concepts involved in vehicle engineering. The second section details the powertrain and the power split devices for HEVs. In the third section, the presentation of the vehicle will be done for the chosen architecture of the HEV. The fourth and final section will summarize the objective of this thesis.

## **I.1 Context and Concepts**

The field of vehicle engineering has had and continues to have a great impact on our daily lives, methods and ease of transportation. One of the greatest achievements in this field was the evolution of the Internal Combustion Engine (ICE) which changed the face of vehicles altogether. However, despite the many benefits and conveniences derived from vehicles equipped with an ICE, the ICE has come under increasing criticism due to environmental concerns and fossil fuel depletion. In the last few decades, growing attention has been devoted by governments and international agencies to try and resolve this issue and make an environmentally friendly alternative.

### **I.1.1 Background**

The first internal-combustion four-stroke cycle ICE was created in 1876 by the German inventor Nicholas A. Otto. In the early stages of its manufacture, the only drawback to Otto's ICE was the noise. The harm associated with the exhaust was considered nothing more than an unpleasant scent. The first known incident of pollution happened in the summer of 1946 in Los Angeles, United States of America. There, people noticed that the air seemed to be thickened and the visibility of nearby mountains reduced. Later, this phenomenon was called smog which is a portmanteau of smoke and fog [Sokhi 2008]. Crops began to show a bronzing of their foliage, car tires shown premature aging and health-related problems had drastically increased. It was termed "gas attack" by local officials [Allaby 2003].

Today, more than a century after Otto's invention, smog still presents a vast problem. The far-reaching environmental disturbance due to ICE based vehicle emissions includes direct health concerns for humans, animals and plants, as well as lasting health problems due to phenomena such as smog, acid deposition, and toxic pollution. According to the United States Environmental Protection Agency (EPA) and United Nations Framework Convention on Climate Change (UNFCCC) this pollution contains more than 40 substances that are listed as hazardous air pollutants and more than 30 epidemiological researches have correlated exhaust fumes to cancer [Fiveland 2000].

Throughout the history of ground vehicles, ICEs have been one of the main power sources. However, following the oil crisis in the 1970's, engine

developers have shifted their focus to fuel economy and emission reduction. In the 1980s, researchers introduced both the electronic ignition and fuel injection systems, which allowed developers a far greater capability of ICE control than before. The biggest limitation in ICE control development lies in the available information about the controlled process and the combustion. The development of ICE efficiency is driven by its fuel economy, which includes optimal ignition timing and fuel amount for any given operating condition. Emission reduction drives the development of air-fuel ratio control, misfire detection and purge control (controls the fuel vapor flow into the ICE) [Docquier 2002] [Guzzella 2004].

Solutions towards efficient and clean land transportation can be achieved with the transition from ICE based vehicles to ones equipped with electric propulsion or a mix between both thermal and electric vehicles known as Hybrid Electric Vehicle (HEV). However, the combination of these differing propulsion systems makes the system increasingly complex. This complexity is due to the prevalence of energy sources (electric and fuel) and converters i.e. Electric Machines (EMs) and the ICE, compared to conventional vehicles (ICE only) [Eshani 2005] [Raskin 2006] [Bellis 2009].

### **1.1.2 Hybrid Electric Vehicles (HEVs)**

The first concept for a HEV dates back to 1901 when Ferdinand Porsche at Lohner Coach Factory designed the 'Mixte', a series HEV (see section 1.1.3) modeled after his earlier electric vehicle. This hybrid vehicle utilized a gasoline ICE combined with an electric generator and an electric motor with a small battery for increased reliability. The start of the contemporary HEVs as we know today began in 1972 when Viktor Wouk installed his prototype hybrid Powertrain into a Buick Skylark given by General Motors (GM). This was the turning point for modern HEVs and the concept grew increasingly popular and research branched out into many other varying aspects such as regenerative braking issues, fuel consumption considerations, emission, and battery wear [Anderson 2010] [Callery 2009].

In HEVs, the EM(s) play the critical role of optimizing the productivity of the ICE (increase the efficiency) as well as energy recovery during braking or coasting. HEVs also utilize the excess power from the ICE to charge the battery if the power demands on the final drive is lower than the power con-

verted by the ICE. Another function of the EM is to aid the ICE in the case that the ICE alone cannot fulfill the demands of the driver.

There are a number of advantages in hybridizing a conventional vehicle; however four significant advantages are listed below [Miller 2003]:

1. ICE Downsizing: the main advantage of hybridization is the downscaling of the ICE due to the addition of an EM. This allows the ICE to be sized for mean power instead of the peak power demand. With this, the batteries can make up for the lack of power in high power demand stages of driving through the EM. Therefore, when a vehicle has a smaller ICE it can be driven more efficiently than when it has large ICE under normal driving conditions.
2. regenerative Braking possibility: the dispersed energy in conventional vehicles released during braking can be regenerated and saved in the batteries using the EM in its generator mode.
3. pure Electric Drive: one advantage of having an EM alongside the ICE is that the ICE is able to shut down when the vehicle is at low speeds so that the controller shuts the ICE down and the EM propels the vehicle at a low speed. This also greatly reduces fuel consumption and local emissions.
4. improved performance efficiency of the ICE: the HEV is able to obtain the propulsion power demand from a mixing of power from the ICE and battery. Due to this, the control of the ICE operating point, i.e., ICE torque and speed, can be completed with a much larger degree of freedom with comparison to a conventional vehicle. Furthermore, due to the smaller time constant than an ICE, the EM in the propulsion system is able to respond to sudden changes in the demand for propulsion power and helps to avoid transient ICE utilization.

While the advantages of HEVs are excellent, there are some limitations as well. The first is their increased cost, weight and volume due to the presence of EMs, batteries, and electric converters. Other problems include some safety issues due to existence of high voltage electricity and Electro-Magnetic Interference (EMI) because of high frequency switching circuits of the electric converters.



### I.1.3 Classification of Vehicles

The classification of the vehicles can be done in different ways. However, in this section the classification of vehicle has been arranged on the basis of architectures and degree of hybridization for HEV, the duty classes of the vehicle with existing designs of HEV in heavy-duty.

#### A) Architecture of HEV

As previously mentioned, any HEV contains at least two sources of energy. These two sources are able to be combined together in several different configurations according to the application. The most common and basic configurations are series, parallel and series-parallel HEVs [Eshani 2005] [Chan 2009]. The existing architectures of all HEVs are based on these basic configurations. Therefore, a brief description of each basic configuration is highlighted below.

**Series HEV:** in this structure (Fig. I.1), all of the traction power is converted from electricity and the ICE is not directly connected to the final transmission. Here, the ICE output is first converted into electrical energy using an EM in the generator mode and then this electric energy can either charge the battery when needed or bypass the batteries and propel the vehicle through a distinct EM in motor mode. In this architecture, the energy sum of the power sources is an electric node through a DC bus.

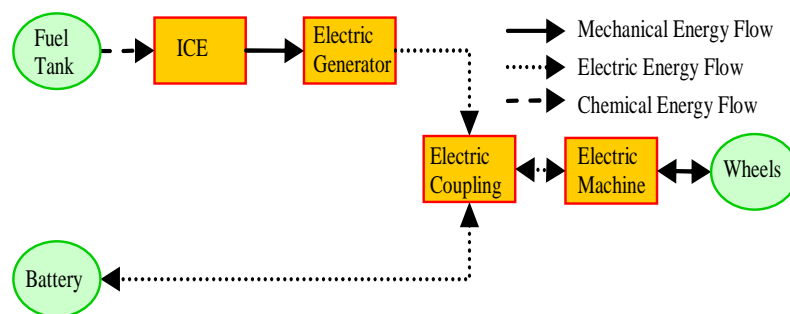
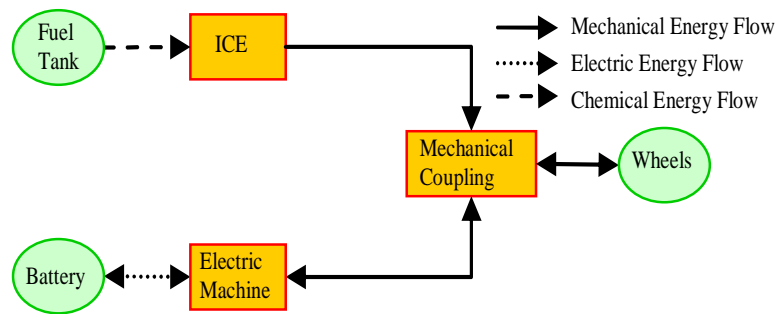


Fig. I. 1 - Series HEV architecture

In series HEV, at least three machines are needed: one ICE, one electric generator and one electric machine. Because of having three machines, the vehicle becomes more expensive. Another drawback of a series HEV is that it is lower in efficiency due to many electro-mechanical conversions. On

the other hand, the major benefits of this configuration are to work ICE in good consumption area, ease in being able to place the ICE anywhere in the vehicle and the extension in the driving range (range extender) in comparison with EV.

**Parallel HEV:** in this architecture (Fig. I.2), the EM and ICE deliver the propulsion energy to the final drive via two separate parallel paths. These two power sources are connected through a mechanical coupling. This coupling can either be a common shaft or a connection of two shafts through gears, pulley-belt units, etc. The primary propulsion unit can be the ICE and the EM is considered an assistant to it.

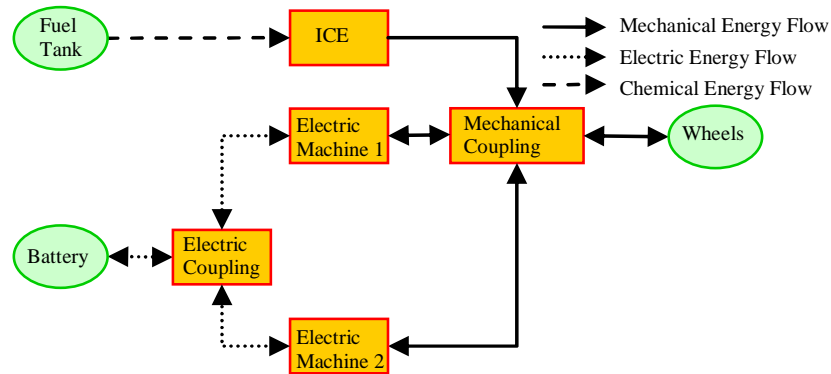


**Fig. I. 2 - Parallel HEV architecture**

In its simplest form, parallel HEVs require two machines (ICE and EM) rather than the three for the series HEVs. The EM of parallel HEVs can operate as a generator to charge the battery by regenerative braking or absorb power from the ICE and also as a motor to tract the vehicle. Due to the mechanical coupling between the ICE and the transmission, the ICE cannot operate at its optimal region. Clutches and multi-gear transmissions are commonly necessary for achieving higher efficiency [Eshani 2005].

**Series-Parallel HEVs:** the series-parallel HEV (Fig. I.3) is the combination of the above two architectures. It combines the merits of both these above discussed architectures. In this architecture, both coupling i.e. mechanical and electrical is used to achieve both energy nodes i.e. electrical and mechanical. The DC bus achieves the electrical energy node and the mechanical node is achieved by adding the Power Split Devices (PSDs). Due to these PSDs, the speed ratio between the ICE shaft and the transmission shaft is

continuous and variable and is called an Electric CVT (E-CVT) [Miller 2006] [Chan 2010].



**Fig. I. 3 - Series-Parallel HEV architecture**

In the series parallel HEV, either the battery powers the vehicle or the ICE energy supplied to battery is done through an EM (EM1, EM2 or both). The ICE can also power the vehicle directly or through the EM(s). The series-parallel architecture strictly depends on which type of power split device is being used in the architecture (see detail in section I.2). In spite of blending different features from both the series and parallel HEVs, three machines are necessary. This makes the drivetrain rather expensive and complex.

For this configuration several other architectures can be used. In recent years many researchers have been investigating Electric Variable Transmission (EVT) architecture. It was realized that the series-parallel function can be realized in an electromagnetic way and for doing so both electric machines (EM1 and EM2) are concentrically arranged [Hoeijmakers 2006] [Cheng 2010]. Nevertheless, in this thesis the series-parallel vehicle is considered with the PSD.

## **B) Degree of Hybridization of HEV**

The degree of hybridization is illustrated by a number between zeros to one, which indicates the ratio of the maximum power output of the energy converters of two energy domains. Therefore, in the case of HEVs, the degree can be defined as the ratio of the maximum electric power of the EM to the sum of the maximum power of ICE by burning the fuel and electric power of EM [Baumann 2000] [Maggetto 2000]. Furthermore, the more electric sub-

systems utilized in the vehicle, the greater the degree of hybridization is that can be achieved. Due to this, the fuel economy of the vehicle will be increased [Feroldi 2009] [Boulanger 2011] [Chan 2011]. Hence, after finding the degree of hybridization, the following types of HEVs are possible:

**Micro HEVs** - Micro HEVs contains an EM that is utilized as a start-er-alternator [Chai 2005] which helps the ICE achieve increased vehicle performance during the start and stop functions. It is well established that any EM has faster dynamics than the ICE, which ensures better start and stop functions in micro HEVs. In contrast, conventional vehicles equipped with an ICE, are always running once started, even if the vehicle is stopped. Therefore, equipping the conventional vehicle with small EM gives an increased fuel economy around 2% to 10% in urban driving cycles [Bruyere 2009].

**Mild HEVs** – Mild HEVs provides an additional boost function with the start and stop function of micro HEVs. This boost function is achieved by increasing the size of EM. Due to the size increment, the EM will boost the ICE during acceleration and braking by applying an additional torque. The estimated fuel economy improvement in mild HEVs is around 10% to 20% [Bruyere 2009].

**Full HEVs** – In full HEVs, the size of the EM is greater in comparison to micro and mild HEVs. Due to the larger size of the EM, this HEV is able to operate the vehicle alone. This type of HEV has no emissions when the vehicle is running in pure electric function. Therefore, the fuel economy of these HEVs is significantly higher than the two HEVs mentioned above. The estimated fuel economy ranges from 20% to 50% [Burke 2007].

**Plug-in HEVs** – Plug-in HEVs are based on the batteries and can be charged externally by plugging into an electric outlet source. In its hybrid structure, a limited power ICE is installed which helps to charge the batteries and extend the pure electric driving range [Burke 2007].

### C) Duty Class Vehicles

Following the demands and desires of the market, the automotive industry has grown and produced an increasingly diverse product range. To classify these vehicles many different classification schemes have been put forward. These classifications are normally based on the number of axles, axles spacing, weight and length of the vehicle. The most used and prominent

method of classification is called the Gross Vehicle Weight Rating (GVWR). In this method, the vehicles are divided into three categories according to their weight: light-duty, medium-duty and heavy-duty (see Fig. I.4)[Walsh 1999] [Woodrooffe 2000].The GVWR method includes the gross vehicle weight with the limitation of both (front and rear) axle capacities, suspension, wheels, and brake. According to this method, the vehicle registration authority calculates vehicle taxes and emission standards. The Environmental Protection Agency (EPA) also uses the same method to distinguish the emission regulations for light, medium and heavy-duty vehicles.

This method contains eight classes (shown in Fig. I.4) in total. A light-duty vehicle is comprised of two classes, medium-duty vehicles four and heavy-duty vehicles two. Classes 1 and 2 are designated for lighter duty vehicles with a gross weight less than 4,500 kg. This generally includes passenger cars, light trucks such as pickups, small vans, and sport utility vehicles. Classes 3 to 6 are mainly medium-duty vehicles and include single rear axles like city buses, delivery vans, conventional vans, etc. Classes 7 and 8 are the heavy-duty vehicle classes and include all municipal trucks including garbage, fire brigade and construction vehicles, military vehicles and big trailers. For this specific heavy-duty class, all vehicles have 2 or more axles [Diegel 2002] [Reitze 2010].

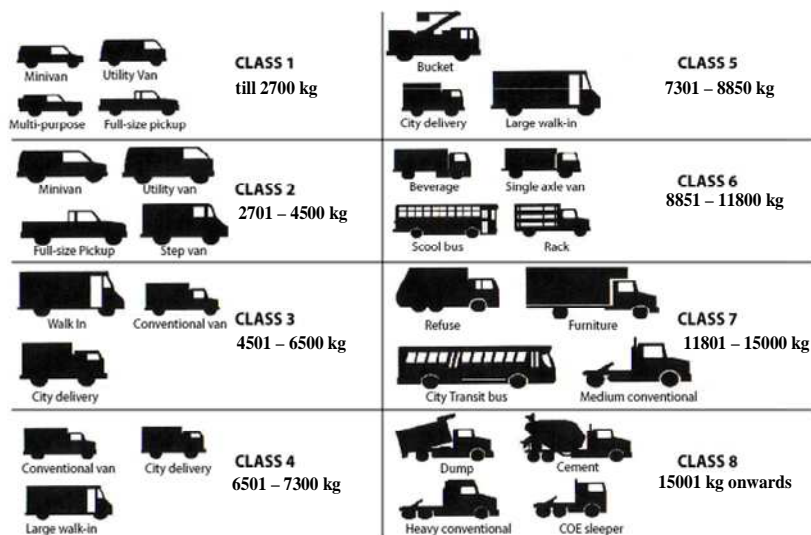


Fig. I. 4 - Duty Vehicle Classification [Ravelco 2011]

## **D) Existing Heavy-Duty HEVs**

HEVs have been designed and introduced for duty- class vehicles including cars, trucks, busses, purpose vehicles and vehicles for military application. Therefore, there are many models of HEVs available with different architectures for application to light and medium-duty. Although, some models of HEVs for heavy-duty application are available, most of them are still in progress.

Some of the available models for light-duty vehicles of Class 1 and Class 2 are the Toyota Prius, Honda Insight, Ford Fusion Hybrid, and the Daihatsu Hijet Cargo Hybrid, Chevrolet Silverado 1500 Hybrid, GMC Sierra Hybrid, respectively. Similarly, for medium-duty vehicle from class 3 to 6 available models include the Hino Ranger Hybrid, Navistar International Durastar, Nissan Condor Hybrid, Mitsubishi Fuso, Isuzu Elf Hybrid, etc.

To reiterate, many laboratories and industries are still working to make HEVs for application to heavy-duty classes viable for future transportation. Applying hybridization to these vehicles can offer significant advantages in terms of fuel economy and emission reduction but these vehicles have constraints due to their large weight. This thesis deals with the HEV in application to heavy-duty vehicles more specifically to those with a series-parallel architecture. Therefore, in this section a brief overview is sketched for existing heavy-duty HEVs for different applications with their architectures.

**Hybrid Trucks and Buses** – According to the International Energy Agency (IEA) 23% of the pollution is made by the transportation sector, with a major part coming from trucks and buses. Therefore, to aim for green land transportation it is necessary to hybridize these sectors [IEA 2009]. Following in this direction, many local governments have partnered with different companies, to introduce hybrid buses (Nova Bus LFS HEV Artic, IC Bus HC Series hybrid, Gillig hybrid-electric bus, Daimler Orion VII Hybrid etc.) [Gover 2010]. These buses are introduced specifically in heavy-duty class of 7 and 8. As far as heavy-duty trucks, much research is still ongoing and sufficient numbers of HEVs have not been introduced. Some of the heavy-duty trucks that are in existence are detailed in Table .1

**Table 1 - Heavy-Duty HEV Trucks**

Company	Model	Class	Application	Architecture
Freightliner	Business Class M2e Hybrid	Class 7 & 8	Mild	Parallel
Kenworth	T370	Class 7	Full	Parallel
Navistar, Inc	4300	Class 7 & 8	Plug-in	Parallel
	DuraStar Hybrid	Class 7	Full	Parallel
	International WorkStar Hybrid	Class 7	Full	Parallel
Peterbilt	386 Hybrid	Class 8	Full	Parallel

**Hybrid Military and Special Purpose Vehicles** - Hybrid technology has also been introduced to military and special purpose (waste collection, digger derrick, recovery towing, landscape dump etc.) vehicles. Most of the models for special purpose vehicles are same as those detailed in Table I.2, although some specific models are mentioned in Table I.2.

Heavy-duty HEVs of different architectures, specifically series-parallel, are still in the developing stages within many research laboratories and industries. Although, for medium-duty classes 3 to 6 for military application have been introduced such as the GM Hybrid Military Army Pickup, MP Hybrid, SmarTruck III, Stealth Hybrid Vehicle and The Shadow RST-V. This research work surrounds the heavy-duty vehicles in application to military and waste collection trucks, therefore, in below some of the existing heavy-duty military HEVs with waste collection trucks are listed.

In literature, due to secrecy of company data most hybrids or alternate solution to hybrids in application to military vehicles are not clearly specified. Although in application to garbage truck many manufacturers are working in hybridization, total electric, alternate fuels or traction only with ICE but rest of the system including auxiliaries powered by hydraulic or batteries. As an example, Renault Gamme GNV, Scania EEV and GDF-SUEZ-GNVERT are totally natural gas based vehicles. Furthermore, Gdfsuez-GNVERT has the capability to work on biofuel as well. The other garbage trucks alternative to

hybrid are Geesink Norba, Eurovoirie-ECOLYMPUS, Faun Environment, etc. In these trucks traction power is given by the ICE but remaining system including all auxiliaries on batteries or hydraulic power.

**Table I. 2 - Military and Waste Collection HEVs**

Company	Model	Class	Application	Architecture
OSHKOSH	HEMTT A3 Diesel Electric	Class 7 & 8	Military	Series
General Dynamics	AHED- Electric Drive Technology	Class 7	Military	Series
NEXTER	DPE 6X6	Class 8	Military	Series
Mack/Volvo	TerraPro Hybrid	Class 8	Garbage Truck	Parallel
Peterbilt	337 Hybrid	Class 7	Garbage Truck	Parallel
	320 Hybrid	Class 8	Garbage Truck	Parallel
Renault	Hybrys	Class 8	Garbage Truck	Parallel
Volvo	Fe Hybrid	Class 8	Garbage Truck	Parallel
BAE Systems (HybridDrive)	HDP - 600 HDP - 700 HDP - 750 HDP - 800	Class 7 & 8	Garbage Truck	Parallel

In the above discussion it is clear that most of the HEVs in application for heavy-duty usage utilize the series or parallel architecture for hybridization or other solutions. There is no series-parallel drive-train currently being used due to its complexity. This complexity is mainly due to the need for split devices within this architecture. To address these issues, in the next section powertrains and power split devices are detailed.



## **I.2 Powertrain and Power Split Devices (PSDs)**

The function of a gear train is to transmit motion and/or power from one rotating shaft to another. A large number of gear trains are used in various applications such as robots, clocks, vehicle engineering and so on. One of the earliest known gear trains applications was the South Pointing Chariot invented by the Chinese around 2600 B.C [Tsai 2000]. Over time, the gear train evolved into many different types for a wide number of applications. In the automotive field, gear trains are mostly utilized in the transmissions. Transmissions are an essential part of the driveline and are used to transmit torque and rotary motion from a power source to an output device. A vehicle powertrain essentially contains the driveline along with onboard energy sources. In some cases the powertrains also includes related parts of the vehicle such as fuel system, exhaust systems, etc. In other words, the conventional and the hybrid vehicle can also be known as the conventional and hybrid powertrain respectively [Husain 2003] [Cho 2006].

Hybrid powertrains have been discussed in section I.1. Within the series-parallel hybrid powertrain there is an essential drive element known as the Power Split Device (PSD). This PSD divides all of the power coming from various power sources into the drivetrain into two separate paths: all mechanical that has high efficiency and electro-mechanical that has lower efficiency [Guzzella 2007] [Liu 2008]. Furthermore, these PSDs are also able to achieve Electric Variable Transmission (EVT) by adding separate power inputs to produce single output [Beresford 2006]. In this section a detailed description of these PSDs is given.

### **I.2.1 Planetary Gear trains**

The most common gear train used in PSDs is known as the epicyclic or planetary gear train. The original concept for this gear train was given in 1781 by James Watt for application to steam engines for railways. The planetary gear trains are transmission systems of high kinematic complexity and challenging visualization [Ceccarelli 2007]. They have many advantages: they are compact, light, allow high-speed reductions, and possess high reliability because of their constant engagement. They also have a bifurcating capacity, power splits and allow for multiple transmission ratios [Miller 2006]. There are numerous types of planetary gear trains available. The most well-known

being the single planetary gear train such as those used in the Toyota Prius. This type of the gear train is a three wheel type although more complex gear trains consisting of four wheels or more called compound planetary gear trains are available, which have also been considered in this dissertation. Descriptions about single and compound planetary gear trains and how they are beneficial to hybrid vehicles, especially heavy-duty trucks are described in the next sections.

## I.2.2 Single Planetary Gear train

Single planetary gear trains are the simplest form of planetary gears (Fig. I.5), and are comprised of a sun gear, a number of pinion gears with planet-carrier and a ring gear. The ring gear is an internal gear. The pinions are mounted on shafts and bearings to a structural member called a planet carrier. These pinions revolve on their own axis or around the sun gear if the carrier is free to rotate. The gears are meshed with a parallel axis. This gear train can increase speed or torque, reverse the direction of operation or perform as a coupling device in direct drive [Litvin 2004].

The most significant feature of this type of planetary gear is that the input and output shafts lie on the same axis. This means that input and output align with each other which minimizes the offset of the shafts. Also, due to the simple design structure, the noise and other losses are lower.

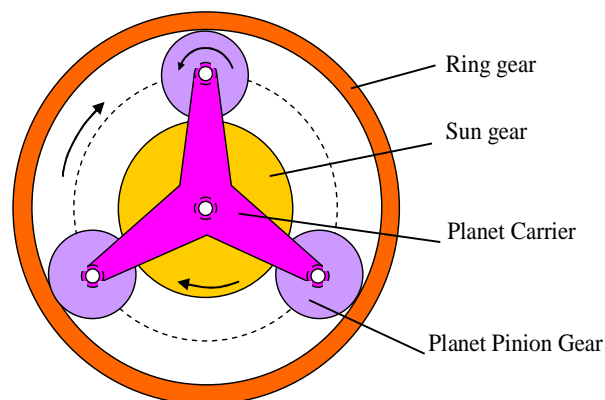


Fig. I. 5 – Single PGT [Kessels 2007]

This type of PSD is good for limited power applications such as the Toyota Prius. However, this PSD is not ideal for heavyweight, high power or torque transmission vehicles due to mechanical constraints such as size,

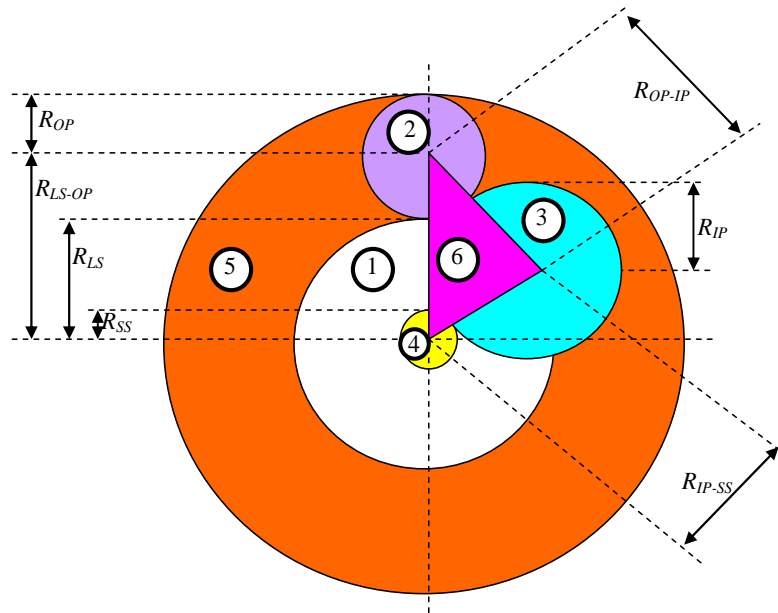
weight, etc. But when high power or torque is needed, two or more of this type of PSD can be used.

This research deals with heavy-duty vehicles in which the vehicle has a large weight. Due to the heavy weight of these vehicles, a larger power is needed for propelling or absorbing. For these reasons, the compound planetary gear train is used instead of the single as the PSD to fulfill the required power requirements.

### **I.2.3 Compound Planetary Gear train**

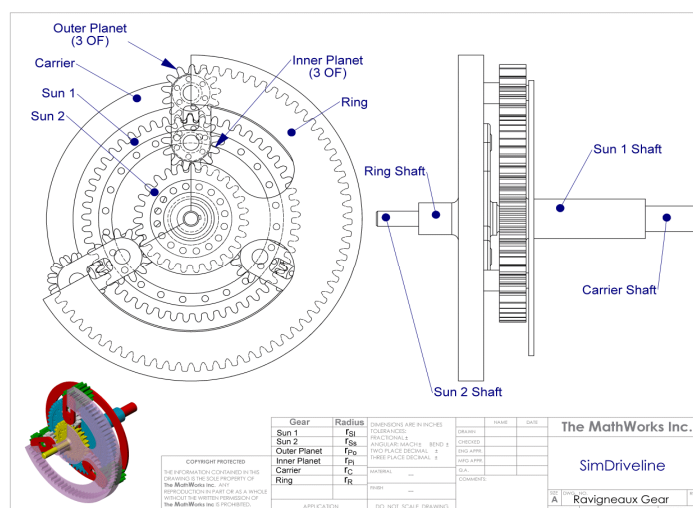
The compound planetary gear trains are the mechanisms of several degrees of freedom. In its composition, one element of the compound planetary gear train has two rotational movements. For this type of gear train different configurations can be achieved. The most renowned types are the gear trains of the Simpson, Wilson, Lepelletier and Ravigneaux. In this dissertation, the Ravigneaux gear train (Fig. I.6) is taken into consideration to achieve higher performance efficiency for the large power requirement [Miller 2003] [Naunheimer 2011].

The design of the Ravigneaux gear train has two layers of pinion gears, two suns, a ring gear and a planet-carrier. In Fig. I.6, it is shown that the two layers of pinion gears i.e. outer ② and inner ③ are meshed with each other. In addition, the outer pinion gears are meshed with a common ring gear ⑤ and a large sun ① with a fixed gear ratio. The inner pinion gear is engaged with the small sun ④ and has a fixed gear ratio. Also, the inner and outer pinion gears are connected independently with the planet-carrier ⑥.



**Fig. I. 6 – Ravigneaux Geartrain Arrangement**

Typical to this gear train, one of the elements (ring, carrier or suns) is kept in place while the other one is driven. The output comes out of the fourth element. By varying these arrangements, different ratios can be achieved. Driving two of the elements simultaneously yields a direct drive. Various combinations of the simple and compound planetary gear train may be used to create the required speeds and torques. A view of the elements from SimDriveline for the Ravigneaux arrangement is shown in Fig. I.7.



**Fig. I. 7 – Elements of Ravigneaux Gear train [MathWorks 2011-b]**

The Ravigneaux gear train, like other planetary gear trains, provides gear reductions, overdrives, direct drive and reverse combination. It offers additional advantages such as space reduction, compactness and increased torque loading capacity due to high gearing.

### **I.3 Presentation of the Studied Vehicles**

In this dissertation, a series-parallel HEV propulsion system is taken into consideration with application to heavy-duty vehicles of class 7 and 8 for civil and military applications, respectively. To reiterate, the series-parallel HEV is the most complex design because it consists of an ICE, one or more batteries or super-capacitors, EMs, power converters, a transmission and various driveline linkages. A complex device called the PSD fills a key role within this architecture. For this PSD role, a Ravigneaux compound planetary gear train has been utilized. In heavy-duty vehicles the most significant characteristic is its power due to its large weight [O’Keefe 2002] [Serrao 2006], therefore, for satisfying the system’s power requirements this specific types of gear trains was implemented. Furthermore, this specific type of PSD helps to divide the power coming from various power sources into the drivetrain according to a suitable energy management strategy [Gao 2006].

#### **I.3.1 Proposed Vehicles**

In this research, the proposed vehicle (Fig. I.8) was taken into consideration for military and civil applications. This is an HEV of series-parallel architecture. In this series-parallel layout some additional gearboxes are introduced for different reasons: the first being to achieve a higher system performance, the second to avoid failure of the system in any circumstances and the third to reduce the volume of machines.

In the system below (Fig. I.8), the ICE drives the Small Sun wheel (SS), while the Large Sun gear (LS) is connected to the electric machine EM2 (Motor/Generator) through an additional gearbox. The Ring gear (R) is connected to the other electric machine EM1 (Motor/Generator) through an additional gearbox. In the beginning of the project, high rated electric machine was considered without the gearbox. But later, due to the additional gearboxes, this rated power of each machine gets reduced.

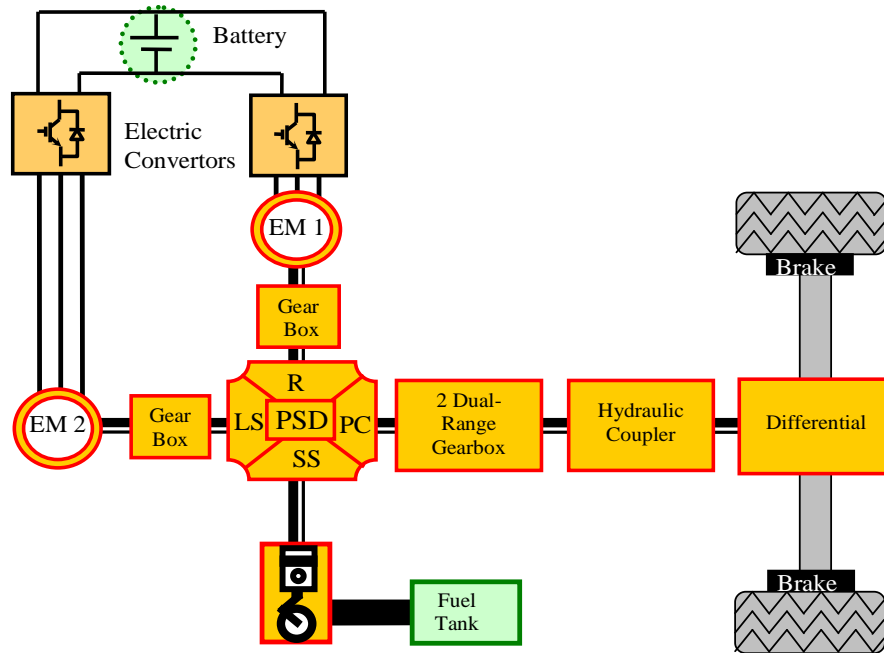


Fig. I. 8 – Studied System Layout

The Planet-Carrier (PC) provides the resultant torque and is connected through two dual-range gearboxes with the wheels of the vehicle. The planet-carrier output shaft transmits the summation power to the vehicle driveline. In the vehicle driveline between the gearbox assembly and the differential, a fluid coupling or hydraulic coupler is placed. This coupler is added to replace the mechanical clutch and can operate only when a certain amount of slippage difference in rotation speed between the driving and the driven member exists. Also, due to prolonged slipping, the ordinary clutch sometimes gets damaged due to overheating but if a hydraulic coupler is used it is not impacted. Furthermore, the coupler provides an excellent cushioning effect in picking up the load [Dagoon 2000] [Garret 2001].

The above presented architecture is patented by NEXTER Systems [Le Trouher 2009]. What makes this architecture unique is that the ICE is able to start in any circumstance (by incarcerating the shaft of an EM), unlike other architectures such as the Toyota Prius which does not utilize an ICE only start feature as all of its operations are combined with both the ICE and EMs. In the above architecture, two dual-range gearboxes (four gears with two clutches) are installed on the transmission line which allows the ICE to be available in all circumstances, even if the batteries and/or EM(s) fail. Also, this helps the vehicle to reverse with the ICE instead of the EMs.

The gearbox assembly in the driveline of the proposed vehicle shown in Fig. I.8 can be simplified for civil application. For civil application, the higher securities and assurances of the system in case of any failure needed for military vehicles are not necessary. Therefore at the first stage, for a civil truck, instead of four gears of dual-range gearboxes assembly in the driveline only one gear is considered.

It should be noted that this consideration does not have any impact on the modeling of the entire system (see chapter II). Before beginning the modeling of the complete vehicle it is necessary to understand or analyze the kinematics and energetic studies of the PSD as it occupies a key role in the modeling of the vehicle. The kinematics and energetic studies are analyzed in the section below.

### I.3.2 Kinematics Study

At first, to better understand the dynamics of the PSD and to further simplify the studied system shown in Fig. I.8, only the PSD is taken into account with its connected shafts. These connected shafts of each part has its own torque, resulting in the speed (Fig. I.9).

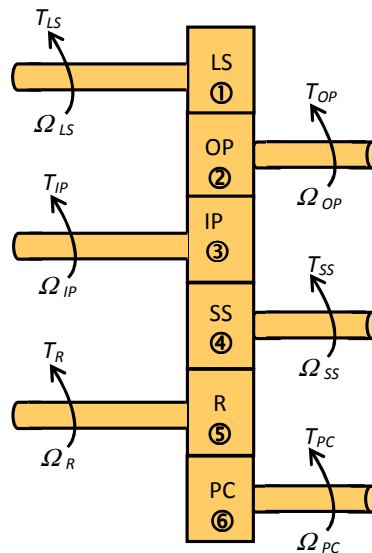


Fig. I. 9 – Element of the PSD with Speed and Torque

If taking the Willis equation principle, one of the elements (ring, carrier or suns) would be kept stationary as a reference. In this case, by keeping the planet-carrier fixed with reference to the other elements, the gear train

imposes four kinematic constraints (speeds) and as well as four geometric constraints (radiuses) with the outer and inner pinion gears. From Fig. I.6 and Fig. I.9 these constraints can be determined as follows:

$$\begin{aligned}
R_{IP-SS}\Omega_{PC} &= R_{SS}\Omega_{SS} + R_{IP}\Omega_{IP} && \text{with} \\
R_{IP-SS} &= R_{IP} + R_{SS}, && \text{and} \\
-\frac{R_{IP}}{R_{SS}} &= \frac{\Omega_{SS} - \Omega_{PC}}{\Omega_{IP} - \Omega_{PC}}
\end{aligned} \tag{1.1}$$

$$\begin{aligned}
R_{LS-OP}\Omega_{PC} &= R_{LS}\Omega_{LS} + R_{OP}\Omega_{OP} && \text{with} \\
R_{LS-OP} &= R_{LS} + R_{OP}, && \text{and} \\
-\frac{R_{OP}}{R_{LS}} &= \frac{\Omega_{LS} - \Omega_{PC}}{\Omega_{OP} - \Omega_{PC}}
\end{aligned} \tag{1.2}$$

$$\begin{aligned}
R_{OP-IP}\Omega_{PC} &= R_{OP}\Omega_{OP} + R_{IP}\Omega_{IP} && \text{with} \\
R_{OP-IP} &= R_{OP} + R_{IP}, && \text{and} \\
-\frac{R_{IP}}{R_{OP}} &= \frac{\Omega_{OP} - \Omega_{PC}}{\Omega_{IP} - \Omega_{PC}}
\end{aligned} \tag{1.3}$$

$$\begin{aligned}
R_R\Omega_R &= R_{LS-OP}\Omega_{PC} + R_{OP}\Omega_{OP} && \text{with} \\
R_{LS-OP} &= R_{LS} + R_{OP} = R_R - R_{OP}, && \text{and} \\
\frac{R_R}{R_{OP}} &= \frac{\Omega_{OP} - \Omega_{PC}}{\Omega_R - \Omega_{PC}}
\end{aligned} \tag{1.4}$$

By substituting the value of  $R_{OP}$  in equation (1.3) through (1.2) and then dividing the result with the equation (1.1), the following result will be deduced:

$$R_{LS}\Omega_{LS} = (R_{LS} + R_{SS})\Omega_{PC} - R_{SS}\Omega_{SS} \tag{1.5}$$

Similarly, by first substituting the value of  $R_{OP}$  in equation (1.4) and then placing the value of  $R_{LS-OP}$  in the result, the following equation is realized:

$$R_{LS}\Omega_{LS} = \Omega_{PC} 2(R_{LS} + R_{OP}) - (R_{LS} + 2R_{OP})\Omega_R \tag{1.6}$$



By further resolution of the above equations (1.5) and (1.6), the two gear ratios of the Ravigneaux geartrain can be expressed as follows:

$$k_{LS} = -\frac{(R_{LS} + 2R_{OP})}{R_{LS}} = -\frac{R_R}{R_{LS}} \quad \text{and} \quad (1.7)$$

$$k_{SS} = \frac{(R_{LS} + 2R_{OP})}{R_{SS}} = \frac{R_R}{R_{SS}} \quad (1.8)$$

The interior and exterior contacts represent how the gears are meshed internally or externally with each other. The negative sign in equation (1.7) shows the interior contact between part ② and part ⑤ and the exterior contacts between parts ① and ② of Fig. I.6, respectively. In this (Fig. I.6), the gear part ② plays an intermediary role between parts ① and ⑤ which must have an interior and exterior contact. Similarly, the positive sign in equation (1.8) is due to the exterior contact between parts ④ and ③ or parts ③ and ② and the interior contact between parts ② and ⑤. From this, the above two equations (1.5) and (1.6) can be rewritten as follows:

$$\Omega_{LS} - k_{LS}\Omega_R + (k_{LS} - 1)\Omega_{PC} = 0 \quad (1.9)$$

$$\Omega_{SS} - k_{SS}\Omega_R + (k_{SS} - 1)\Omega_{PC} = 0 \quad (1.10)$$

From the above two equations, (1.9) and (1.10), it can be clearly seen that there are two independent state variables because if two speeds are known then the other speeds can be deduced.

These equations (1.9) and (1.10) are similar to the single planetary gear train but in the single planetary gear train only one gain or gear ratio is needed. This is due to the fact that single planetary gear trains have three shafts and are a system of two degrees of freedom. Contrarily, the Ravigneaux gear train has four shafts and two degrees of freedom.

### 1.3.3 Energetic Study

The energy lost in any gear systems among many other losses is due to the friction of the teeth during their meshing with each other and wear and abrasion between the teeth. Therefore, not all parts of the gear trains are de-

formable; since the total or summation of all powers of their own efforts i.e. PSD, should be zero:

$$\sum P_i = 0 \quad \text{including losses} \quad (1.11)$$

The respective speeds of the four shafts of the PSD are constants with respect to the frame and the total of these will lead to zero. The energy lost in this gear train is due to the teeth friction during the meshing of the gears. Therefore, by adding the frictional power  $P_F$ , the total power is given as:

$$\begin{aligned} \sum P_i &= P_{LS} + P_{SS} + P_R + P_{PC} + P_F = 0 \quad \text{and,} \\ &= T_{LS}\Omega_{LS} + T_{SS}\Omega_{SS} + T_R\Omega_R + T_{PC}\Omega_{PC} + P_F = 0 \end{aligned} \quad (1.12)$$

According to the basic principle of statics, for any isolated system to be in balance as compared to a reference, the sum of all the external mechanical actions exerted on this system will be zero. So:

$$\begin{aligned} \sum T_i &= 0 \\ \text{so, } T_{LS} + T_{SS} + T_R + T_{PC} &= 0 \\ \text{and } T_{PC} &= -T_{LS} - T_{SS} - T_R \end{aligned} \quad (1.13)$$

By simplifying equations (1.12) and (1.13) by neglecting the frictional power ( $P_F = 0$ ), the following result is achieved:

$$T_{LS}(\Omega_{LS} - \Omega_{PC}) + T_{SS}(\Omega_{SS} - \Omega_{PC}) + T_R(\Omega_R - \Omega_{PC}) = 0 \quad (1.14)$$

Further simplifying the above equation (1.14) with (1.1), (1.3) and (1.4), the following results will be deduced:

$$T_R = - (k_{LS}T_{LS} + k_{SS}T_{SS}) \quad (1.15)$$

$$T_{PC} = T_{LS}(k_{LS} - 1) + T_{SS}(k_{SS} - 1) \quad (1.16)$$

Finally, the key relationships needed in order to interact with the external connected devices are (1.9), (1.10), (1.15) and (1.16). In these relationships between speed and torque, if any two speeds and torques are known, then all of the remaining variables can be determined easily.

## I.4 Research Motivation and Objective

### I.4.1 Background

The promotion of the HEV research requires multiple expertise due to the fact that different field of sciences are involved such as electrical, mechanical, chemical etc. Although in this the electrical engineering laboratories are playing a vital role due to more electrification of components in the vehicle. Therefore, interdisciplinary collaboration with other disciplines is needed to succeed. In this context different academics departments and industries makes collaboration to progress in this research. In France, a national research network of named MEGEVH (Modélisation Énergétique et Gestion d'Énergie des Véhicules Hybrides) has been established in 2005. In this network 10 laboratories and 7 industrial partners are incorporated (Fig. I.10) [MEGEVH 2007]. The aim of this network is to promote collaboration regarding energetic modeling, energy management and energy optimization of HEVs.



Fig. I. 10 – MEGEVH Partners [MEGEVH 2011]

## **MEGEVH Network and Projects**

The MEGEVH network is based on different industrial and academic partners. Therefore, for organizing the projects, it is further divided into two levels: one the theoretical level and second the application level. The first level deals with the development of theoretical methodologies. It aims to develop generic methodologies for modeling energy management and energy optimization. Later, at the application level, the theoretical methodologies are validated on real vehicles or sub-systems.

In the MEGEVH network, there are many ongoing projects are operational such as MEGEVH-strategy, MEGEVH-macro etc. This dissertation is also a part of MEGEVH network in the project named ARCHYBALD. This project is funded by ANR (Agence Nationale de la Recherche) for the development of a hybrid vehicle for the New Generation Heavy Trucks.

### **ARCHYBALD project**

The ARCHYBALD project deals with the heavy-duty vehicle for both urban transport and military applications. The partners involved in ARCHYBALD project are 2 industrial (NEXTER Systems and BATSCAP) and 3 research laboratories FEMTO-ST (Belfort), IFFSTAR (Arcueil, Ile de France) and L2EP (Lille) [Pape 2010].

The L2EP is in charge of the simulation and the energy management of the vehicle, while other partners are in charge of developing new components (storage, traction, transmission, etc.) [Pape 2010]. The L2EP is also responsible for the formalism of modeling, synthesis of control and control structures. Industrial partner NEXTER Systems is coordinating the project and also in charge of building the electrical and mechanical transmission [Sautter 2010]. BATSCAP is developing the batteries and super capacitors for the vehicle. FEMTO-ST is designing the electric machines with the associated power electronics used for the vehicle [Wu 2010] [Wu 2012]. IFFSTAR is in charge of research on batteries with associated power electronics [Butterbach 2010].

## **I.4.2 Research Motivation**

In the conventional vehicles (powered by ICE), the final torque at the wheels strictly depends on the amount of the fuel injected in combustion

chamber. By strict regulation of controlling the pollution in transport sector, different improvements have been done such as EGR (Exhaust Gas Recirculation), DPF (Diesel Particulate Filter) and to control the exact and specific amount of fuel as according to the vehicle speed through more usage of actuators and sensors. Contrarily, all these improved technologies to conventional vehicle did not satisfy to lemmatize the pollution content and to get more energy from the chemical energy of the fuel. Therefore, in this dissertation instead of conventional vehicle a series-parallel HEV in application to heavy-duty class (for civil and military application) is taken into consideration.

The proposed heavy-duty vehicle for ARCHYBALD for both application have some common features, which allows to address some key issues to be identified in it like:

- reducing consumption and emissions,
- achieving high performance,
- achieving high availability even in case of failure.

To satisfy the above discussed issues in ARCHYBALD HEVs, the modeling and the control part of these vehicles are the key concern. This is because the dynamics involved due to the presence of multi-sources such as EMs and an ICE with multiple subsystems such as compound planetary gear train, different gearboxes, batteries, clutch etc.

## **Modeling and Formalisms**

For the development of control design of any complex system based on multisource and multi subsystem such as HEV have two challenges to tackle: one to reduce the development time and second to handle the design complexity of the system. Therefore, to coop with these challenges, model-based control design processes are being used which provides an efficient way of carrying out control design. The model-based control design process involves system modeling, system analysis, control tuning, system and control simulation, experimental validation, and finally control deployment.

Different graphical modeling formalisms have been introduced for the system modeling such as Bond Graph [Paynter 1961] [Karnopp 1975], Power Oriented Graph (POG) [Zanasi 1996], Causal Ordering Graph (COG) [Hautier 1996] [Hautier 2004] and Energetic Macroscopic Representation (EMR) [Bouscayrol 2000] [Bouscayrol 2003-a]. These all modeling formalisms or approaches deal with the organization of the models but the COG and

EMR yield the control structure directly using the inversion-based rules (see Appendix A) [Barre 2006].

In comparison with COG, the EMR offers a more global energetic view of the system. Moreover, EMR and its inversion-based control significantly contribute the control structure and energy management of the whole system. Therefore, in this dissertation EMR formalism is being used to organize the modeling of the vehicle and later an inversion principle has been used to find the control structure of the system.

EMR is strictly based on integral causality and one of its distinct features is to respect physical causality and provide allow for functional modeling of the system. Thus, EMR aids in the building of a control structure and developing energy management for complex systems such as HEVs. EMR and its inversion-based control are used in this dissertation to show the functional modeling of the ARCHYBALD system as well as to find the control structure.

### **I.4.3 Research Objective**

The aim of MEGEVH is to establish HEV modeling using energetic descriptions for control purposes. As part of this network, many research involving different Ph. Ds and Postdoctoral fellowships has already been done or is still in progress involving different kinds of HEVs. Similarly, keeping with the same objective of MEGEVH, the ARCHYBALD project has been designed specifically for the modeling and control of HEVs for application to the heavy-duty class. In this project, cooperation have been done between L2EP (Lille), FEMTO-ST (Belfort), IFFSTAR (Versailles), and BATSCAP (Quimper) and NEXTER Systems (Versailles).

In MEGEVH, the first research work to apply EMR formalism to HEVs was carried out from 2004 to 2007 [Lhomme 2007]. It was incorporated with former LTE-INRETS and in this project an EMR and its inversion-based control was utilized to find the control design and energy management of series, parallel and series-parallel HEVs. Afterwards, other research and studied work was carried out mainly with focus on energy sources with the drive train of HEVs [Boulon 2009-b]. This project was incorporated with NEXTER Systems from 2006 to 2009 and in this work a military vehicle equipped with fuel cell was studied. Moreover, the PhD of K. Chen was focused on EMR of

different drivetrain [Chen 2010] and the PhD of A. Allègre on hybrid energy storage systems [Allègre 2010-b]

In the ARCHYBALD project, the scientific challenge is to propose a new architecture for multi-use hybrid trucks in order to provide the market with a viable alternative. The proposed structure and power management model developed would provide all of the necessary indicators for an implementation of a prototype.

Leading to above mentioned objective, this thesis aims to perform modeling, simulation and propose an energy management solution for this new type of vehicle proposed in the project. To reiterate, there are two vehicles being considered for two different applications i.e. civil and military. Although the architecture of both vehicles are similar, the design constraints and limitations vary. Consequently, these differences will have an impact on the final energy management of the system. Because of this, the second goal of this research is to assess and compare these differences by implementing the same modeling and control structure through EMR and its inversion-based control but not the same energy management.

## Conclusion

Chapter I presented the intention behind and an overview of this research. This chapter was divided into four main sections that highlighted the different concerns regarding heavy-duty HEVs.

The first section of this chapter explained the basic concepts about vehicle engineering and the context behind this research. In this, the importance of HEVs was explained. Various reasons were given including the desire to address the current challenges of the transportation sector such as energy security, climate change and fuel depletion. Furthermore, in this section the various types of HEV types with different duty-class vehicles were described in detail.

The second section of this chapter dealt with the powertrain and power split devices. Their importance in vehicle engineering, specifically in series-parallel HEVs is detailed. Both the single planetary gear train used in Toyota Prius and compound planetary gear trains was presented and described. Furthermore, in this section, the importance of using a compound planetary gear train in application to heavy-duty class vehicle was explained.

The third section included the presentation of the vehicle used in this research. The vehicle and its all components were detailed. Later, the modeling of the key component i.e. compound planetary gear train used in this architecture was presented. For this, the energetic and kinematic studies have to be done for the sake of better understanding of whole vehicle.

The fourth and the final section introduced the research objective and motivation behind this Ph. D work. In this section the importance of the MEGEVH network for collaboration with different partners i.e. industrial or academics for HEVs have been elaborated on. This PhD is part of the ARCHYBALD project within MEGEVH network which deals with the modeling and energy management of proposed HEV using a compound PSD.

Before beginning the energy management, the modeling and control design of the vehicle must be studied. This is detailed in chapter II.



# **Chapter II**

## **Modeling and EMR of Studied HEVs**



## Introduction

Modeling is the mathematical description of any system in which a model is created that sufficiently and accurately represents a target system to permit the study or simulation of those systems. Its importance becomes vital when it is applied to complex systems. One of the definitions for complex systems modeling is from ACS<sup>1</sup> which considers that complex systems are usually comprised of number of interacting entities, processes, or agents that need to be understood. Once a system has been modeled, the next step is organizing the system in such a way that the specific properties of the system can be elucidated. This elucidation leads to the idea of representing the system through state-space, transfer function etc. or graphical formalisms such as Bond Graph [Paynter 1961], Power Oriented Graph (POG) [Zanasi 1996], Causal Ordering Graph (COG) [Hautier 1996] [Hautier 2004] or Energetic Macroscopic Representation (EMR) [Bouscayrol 2003-a] [Bouscayrol 2005-b].

Hybrid Electric Vehicles (HEVs) are one example of a complex system because they contain many different multi-physical components such as batteries, Electric Machines (EMs), Internal Combustion Engine (ICE), Power Split Device (PSD), etc. Furthermore, when hybridization is applied to heavy-duty vehicles, the modeling becomes increasingly complex due to the alteration of the dynamics of the system when its components are changed [Serrao 2006]. Therefore, representation tools such as EMR help to understand the complexity in modeling while helping to simplify the building of the control structure of the system. In this research work, two heavy-duty hybrid trucks are taken into consideration for two different applications i.e. military and civil. Each of these has different requirements and constraints.

This chapter is dedicated to presenting the modeling and graphical representation of the two considered HEVs through EMR. The first section emphasizes the modeling of the complex systems through a presentation of the studied HEV. The second and third sections deal with the modeling and EMR of both considered HEVs for waste collection and military application. In this, the detailed features of both vehicles and their containing components are discussed by highlighting the requirements and constraints of each vehicle.

---

<sup>1</sup> An Advance Complex Systems Journal (ACS) is a peer-reviewed journal published by World Scientific providing a multidisciplinary perspective to the study of complex systems since 1997.

## II.1 Modeling of Complex Systems

This section will present the causal representation of the considered series-parallel HEV discussed in Chapter I. In the first part of this section, the characteristic features of the vehicle will be presented. In this, for the sake of accurate modeling and a better understanding of the presented vehicle, the system will be simplified through some assumptions. These assumptions also enable increased ease in the complete modeling of the considered HEV. The second part of this chapter highlights the representation of the system through EMR and the last section presents a control design through EMR where the inversion-based control of the considered vehicle is determined and discussed.

### II.1.1 Modeling, Representation and Control

A mathematical description of a system by means of a number of variables which are defined to represent the inputs, outputs, and internal states of the system or a process is called modeling [McGraw-Hill 2002]. This representation is a way to organize the models. Although the same modeling can be depicted by different representations or formalisms in order to highlight the different properties of the system, all representations differ from one and another by having their own philosophy, specific notions and rules. In this thesis, EMR formalism is taken as the representation tool to present the modeling of the considered HEV.

EMR has the global capability of representing complex systems as well as deducing control schemes. The energetic properties of the system are highlighted through EMR. An inversion-based control can be deduced directly and systematically from the EMR of the system (see Appendix A). EMR has been successfully applied to different complex systems such as wind energy conversion systems [Bouscayrol 2002] [Delarue 2003] [Bouscayrol 2005-a] [Peng 2009], fuel cell systems [Chrenko 2009] [Boulon 2009-a] [Boulon 2010], photovoltaic system [Locment 2010], electric subway [Verhille 2006] [Allègre 2010-a], hybrid railway powertrain [Baert 2011], multi-drive paper processing systems [Wankam 2006], two arranged EM drives (split E-CVT) [Chen 2008] [Cheng 2009], gantry drive system [Kestelyn 2009], helicopter

systems [Bienaimé 2011] and HEVs [Lhomme 2008] [Chen 2011] [Letrouvé 2010].

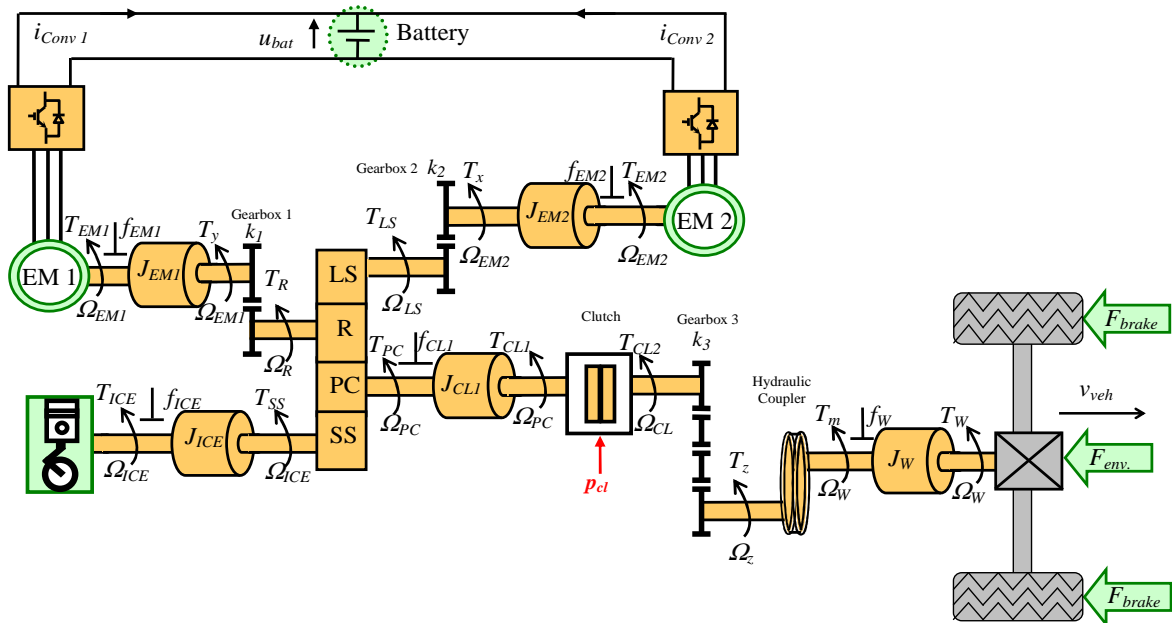
In this research, the EMR is being used as graphical formalism to represent the considered HEVs. However, before representing the system through EMR, the modeling should be completed. Therefore, in the next sections, the modeling of the considered HEV will be discussed and later the EMR and its inversion-based control will be deduced (see Chapter III).

## II.1.2 Presentation of the Vehicles

Chapter I describes in detail the two vehicles taken into consideration for different applications i.e. one for the military application and the other for the municipal waste collection. Both vehicles have the same series-parallel architecture and belong to the same class 8 of heavy-duty vehicles. In this section detailed description of both vehicles with respect to modeling will be described.

### II.1.2.1 Military Truck

The presentation of any system with its state variables is an initial and crucial step because it permits an ease in the modeling of the system. A series-parallel HEV propulsion system for a military truck with its variables is presented below in Fig. II.1.



### **Fig. II. 1– Military Truck Layout**

The above presented architecture (Fig. II.1) illustrates that the system is very complex and difficult to resolve because of its many variables. Because of this, some modeling assumptions are taken into account to simplify the system which will be detailed in the next sections.

In this architecture, electric machines (EM1 & EM2) are connected by the inverters, which are powered by the battery. The energy of the EM(s) and ICE, after passing through the compound planetary gear train, is utilized for traction. All components in the vehicle are permanently connected and as a result, power can be split or combined through the gear train (compound planetary gear train). Thus, in this system, multi-energy paths are possible or the vehicle can be powered by more than one energy source. Here, the importance of energy management arises which ensures that the energy of different components is generated for optimal performance.

The compound planetary gear train is mounted with shafts connected to two electric machines (EM1 and EM2) through gearboxes, an ICE and wheels through transmission and two dual-range gearboxes. The two dual-range gearboxes consist of four gears and two clutches in total. Although, in Fig. II.1, instead of two clutches a single equivalent clutch is shown to improve the functionality of this part. Normally, clutches are used in the system for the efficient engagement and/or disengagement of the shaft or allow for a smooth shift from one gear ratio to another. Here, the clutches are being used during gear shifting for changing the gear ratios. This assumption will not make any effect on the modeling of complete system nor on the clutch.

#### **II.1.2.1 Waste Collection or Garbage Truck**

This section will present the architecture of the series-parallel HEV for a waste collection or garbage truck for civil application. As shown in Fig. II.2, the architecture of this vehicle is similar to the vehicle used for a military truck except for some changes in the transmission line. These changes include the removal of the hydraulic coupler and the two dual-range gearboxes with clutch and the addition of one gear without any clutch.

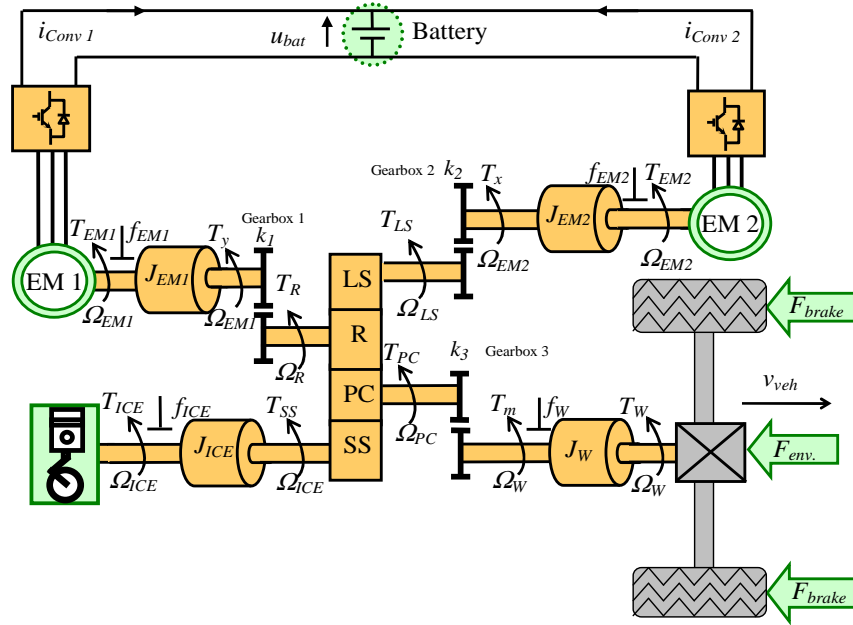


Fig. II. 2 – Garbage Truck Layout

The purpose of the removal of the hydraulic coupler and the two-dual range gearboxes in the waste collection truck is due to the application requirement and to avoid complexity of the system. To elaborate on this difference, the vehicle used for military application needs a large torque for propulsion due to the heavy weight of the vehicle itself and the ammunitions contained along with it. The other requirement for a military vehicle is an availability for use at all times, even in the case of failure of an EM. Contrarily, in civil application these requirements are not mandatory because this vehicle would theoretically have access to repair and maintenance on a regular basis. Therefore, on the basis of these constraints and requirements, instead of the two dual-range gearboxes on the transmission line, only one gear ratio without any clutch is taken for waste collection trucks.

### II.1.3 Modeling of the PSD

The compound planetary gear train is used as the PSD and is a mechanism of several degrees of freedom. Earlier, the application of these gear trains was mainly used for automatic transmissions or in mechanical differentials. This research work is unique in that it utilizes this component as the PSD and connects four energy sources with it. A key advantage of this geartrain is its higher gear ratios over small dimensions (see section I.2 –I.3).

The studied system shown in Fig. II.1 is very elaborate and is simplified by considering only the compound planetary gear train as the PSD. This modeling is done by taking the assumption that the sources i.e. ICE, EM1, EM2 and wheels are directly connected with the compound planetary gear train without gearboxes, clutch or a hydraulic coupler. The simplified system after consideration is presented in Fig. II.3.

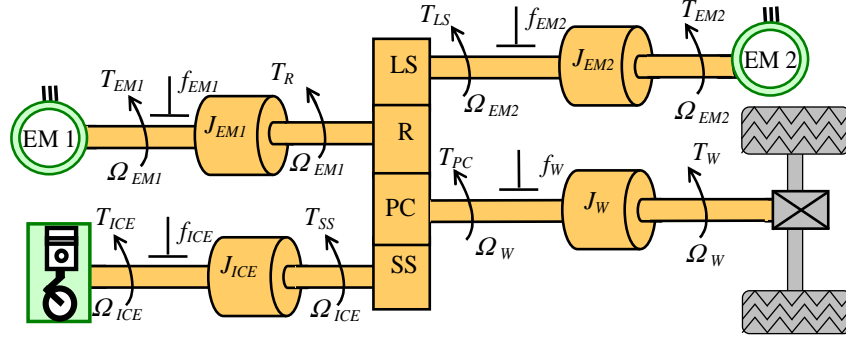


Fig. II. 3 – Compound Planetary Gear Train with Sources

The equations of the four shafts connected to the geartrain are:

$$T_{EM1} - T_R = J_{EM1} \frac{d}{dt} \Omega_{EM1} + f_{EM1} \Omega_{EM1} \quad (2.1)$$

$$T_{ICE} - T_{SS} = J_{ICE} \frac{d}{dt} \Omega_{ICE} + f_{ICE} \Omega_{ICE} \quad (2.2)$$

$$T_{EM2} - T_{LS} = J_{EM2} \frac{d}{dt} \Omega_{EM2} + f_{EM2} \Omega_{EM2} \quad (2.3)$$

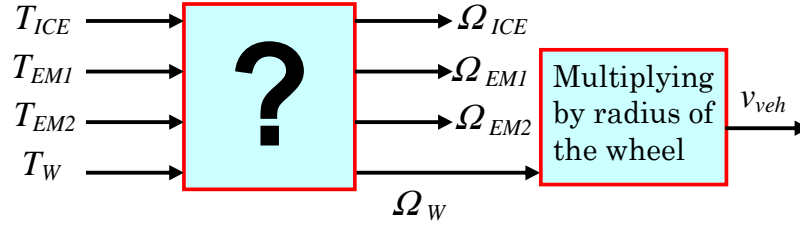
$$T_W - T_{PC} = J_W \frac{d}{dt} \Omega_W + f_W \Omega_W \quad (2.4)$$

where  $J_{EM1}$ ,  $J_{EM2}$ ,  $J_{ICE}$ ,  $J_W$ ,  $f_{EM1}$ ,  $f_{EM2}$ ,  $f_{ICE}$  and  $f_W$  represents the moment of inertia and viscous friction of the connected part i.e. EM1, EM2, ICE and Transmission with the chassis respectively. The consideration takes into account that all parts are mounted on the same shaft connected to the compound planetary geartrain and that their moment of inertias and viscous frictions are considered the same as their sources.

The studied system shown in Fig. II.2 has four speeds ( $\Omega_{EM1}$ ,  $\Omega_{EM2}$ ,  $\Omega_{ICE}$  and  $\Omega_W$ ) and four torques ( $T_{EM1}$ ,  $T_{EM2}$ ,  $T_{ICE}$  and  $T_W$ ). Universally it is



known that when torque is applied on any rigid shaft, after a period of time it will influence the speed. Similarly, in this case, when the machine's torques ( $T_{EM1}$ ,  $T_{EM2}$  and  $T_{ICE}$ ) are applied then it will result in ( $\Omega_{EM1}$ ,  $\Omega_{EM2}$  and  $\Omega_{ICE}$ ), as shown in Fig. II.4. It is also known that the wheels are not the source which generates torque. The rotation speed of the wheels will give the speed of the vehicle ( $v_{veh}$ ) after multiplying with its radius.



**Fig. II. 4 – Objective of the Modeling**

As described previously, only two speeds are independent (see section I.3). The objective of this modeling is to find two optimum speeds that when are applied to two torques, all other speeds can be determined. Therefore, derived equations for torque and speed in (1.9), (1.10), (1.15) and (1.16) will lead to the following solutions:

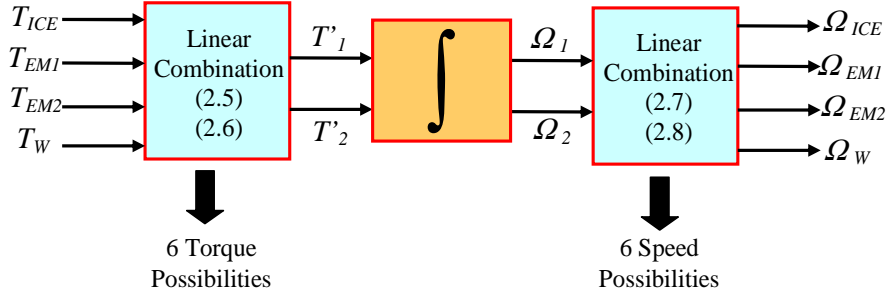
$$T_R = - (k_{LS}T_{LS} + k_{SS}T_{SS}) \quad (2.5)$$

$$T_{PC} = T_{LS}(k_{LS} - 1) + T_{SS}(k_{SS} - 1) \quad (2.6)$$

$$\Omega_{EM2} - k_{LS}\Omega_{EM1} + (k_{LS} - 1)\Omega_W = 0 \quad (2.7)$$

$$\Omega_{ICE} - k_{SS}\Omega_{EM1} + (k_{SS} - 1)\Omega_W = 0 \quad (2.8)$$

The above equation from (2.5) to (2.8) clearly shows the linear combination of torques and speeds of energy sources. For the choice of two optimum speeds ( $\Omega_1$  and  $\Omega_2$ ), the Fig. II.4 is decomposed and shown in Fig. II.5. In this assumption, it is taken into consideration that the torque ( $T_1', T_2'$ ) will be the combination of other torques. For the speed there are six possible combinations ( $[\Omega_{ICE}, \Omega_W]$ ,  $[\Omega_W, \Omega_{ICE}]$ ,  $[\Omega_{ICE}, \Omega_{EM1}]$ , etc.). Here, the choice  $[\Omega_{ICE}, \Omega_W]$  is taken as a state variable for the modeling purposes.



**Fig. II. 5 – Decomposition of the system to find best solution**

The reason for the choice of the state variables  $\Omega_{ICE}$  and  $\Omega_w$  is because the ICE points of operation ( $T_{ICE}$  and  $\Omega_{ICE}$ ) can be determined directly from the curves and the  $\Omega_w$  directly reflects the speed of vehicle. This combination also helps to reduce the cross effect in such a way that the summation of torque ( $T'_1$ ) will avoid the  $T_{ICE}$  for  $\Omega_w$  and the other summation of torque ( $T'_2$ ) will avoid  $T_w$  for  $\Omega_{ICE}$ . These relationships will look like:

$$\begin{bmatrix} T'_1 \\ T'_2 \end{bmatrix} = f \begin{bmatrix} T_{ICE}, T_{EM1}, T_{EM2} \\ T_w, T_{EM1}, T_{EM2} \end{bmatrix} \quad (2.9)$$

From the above discussion, it is obvious that for the modeling of the compound planetary gear, there are six different categories of torques and speeds, which are a combination of any three torques and any two speeds combinations. Due to these six categories of torques and speeds, the system can be modeled in thirty-six different ways. Table 1 depicting all of these combinations is shown below.

In the above discussion, the modeling of the PSD is done without considering the clutch, gearbox and the hydraulic coupler. This modeling is the foundation for the modeling of whole system. Therefore, through exploiting the benefits of above discussed modeling, the modeling of whole vehicle can be done and is discussed in the next section.

**Table II.1 – Input – Output Possible Combinations**

Speeds Torques	$\begin{bmatrix} \Omega_{ICE} \\ \Omega_{EM1} \end{bmatrix}$	$\begin{bmatrix} \Omega_{ICE} \\ \Omega_{EM2} \end{bmatrix}$	$\begin{bmatrix} \Omega_{ICE} \\ \Omega_W \end{bmatrix}$	$\begin{bmatrix} \Omega_{EM1} \\ \Omega_{EM2} \end{bmatrix}$	$\begin{bmatrix} \Omega_{EM1} \\ \Omega_W \end{bmatrix}$	$\begin{bmatrix} \Omega_{EM2} \\ \Omega_W \end{bmatrix}$
	$\begin{bmatrix} T_{EM1}, T_{ICE}, T_{EM2} \\ T_{EM1}, T_{ICE}, T_W \end{bmatrix}$	1	2	3	4	5
$\begin{bmatrix} T_{EM1}, T_W, T_{EM2} \\ T_{EM1}, T_W, T_{ICE} \end{bmatrix}$	7	8	9	10	11	12
$\begin{bmatrix} T_{EM1}, T_{EM2}, T_{ICE} \\ T_{EM1}, T_{EM2}, T_W \end{bmatrix}$	13	14	15	16	17	18
$\begin{bmatrix} T_{EM2}, T_W, T_{ICE} \\ T_{EM2}, T_W, T_{EM1} \end{bmatrix}$	19	20	21	22	23	24
$\begin{bmatrix} T_{EM2}, T_{ICE}, T_W \\ T_{EM2}, T_{ICE}, T_{EM1} \end{bmatrix}$	25	26	27	28	29	30
$\begin{bmatrix} T_{ICE}, T_W, T_{EM1} \\ T_{ICE}, T_W, T_{EM2} \end{bmatrix}$	31	32	33	34	35	36

## II.2 EMR of Subsystems

This section will present the EMR of each subsystem in both HEVs i.e. military truck and garbage truck. As previously discussed (Chapter I) both HEVs have the same architecture but the differences lie in the component sizes such as the PSD, EMs, Battery, ICE and gearboxes. Furthermore, the other key difference between both HEVs is that military truck consists of two additional component in the transmission line i.e. two dual-range gearbox with clutch and the hydraulic coupler. The design differences will not make any effect on the representation of the system through EMR but it will impact the impression on the vehicle characteristic profile. Therefore, the EMR for both vehicles will be the same except to add the dual-range gearboxes with clutch.

EMR is the modeling formalism that can be used to model the systems in such a way that the interactions between the components of the system are highlighted. EMR has been developed to describe complex electromechanical systems since the 2000s [Bouscayrol 2003-a]. It is based on the principles of action and reaction and an integral causality. It uses normalized shapes and

colors to represent energy sources, conversion elements, storage elements and distribution elements (or couplings) (see Appendix A). The first part of this section details the energetic sources while the second presents the converters and accumulation elements that exist in both HEVs.

## **II.2.1 Sources**

This section deals with a discussion about the energetic sources in the system. The sources generate an output, which does not accept discontinuity [Foch 1989]. It has a single input (or input vector) and a single output (or output vector). This output can be influenced by the source input.

There are four main sources in the architecture (see Fig. II.1) i.e. battery, fuel tank, environment and the mechanical brakes. In reality, the EM(s) and the ICE are converters which convert the energy from one form to another. In this research work, the EM(s) are taken as electric converters while ICE plus fuel tank is taken as an equivalent source. This assumption is made to avoid the complexity of dynamic model of ICE. The environment is also considered as a source that represents all of the external resistances on the vehicle such as air drag, rolling drag, etc. The fourth source in the studied system is mechanical brakes which stop the vehicle through frictional force. Further descriptions of each source are described in the following:

### **II.2.1.1 Battery**

A battery is a device that converts chemical energy into electrical energy and vice versa. Complete modeling of a battery is a very complex procedure and requires a thorough knowledge of electrochemistry. For the military truck a Li-ion battery is chosen while for the garbage truck Lead-acid batteries are being utilized. The general specification of each battery module in garbage truck is: the voltage of 12 V for one hour discharge rate of capacity rate 80 Ah and for ten hour discharge rate the maximum capacity of 110 Ah. However the total weight of battery module is 40 kg with 2 Ah/kg energy density and specific energy of 24 Wh/kg. The characteristics of batteries, specifically in application to garbage trucks, are discussed in further detail in [Butterbach 2010]. The battery module used in military truck is of voltage 12, maximum discharge capacity of 260 Ah and specific energy is 200 Wh/kg.

There are many models available for the battery [Martinet 2010]. One common type of battery model is electric circuit-based which represents an electrical characteristic of the battery [Chan 2000] [Liawa 2004]. In this study, an equivalent electric-circuit based model is used to determine the battery characteristics. Equivalent circuit-based models are further subdivided into many types, but all of them are based on the Thevenin battery model. This battery model is unique due to its simplicity in determining key factors such as the State Of Charge (SOC), battery storage capacity, Depth Of Discharge (DOD), temperature and stealth of the battery [Gates 1997]. For the battery modeling, the first assumption taken into consideration is to ignore the factors of temperature and age. The reason this assumption is taken is to avoid the complexity of the system through simple modeling.

The SOC of the battery strongly depends on the Open Circuit Voltage (OCV) in the considered battery model. An OCV is the voltage at the battery terminals when no load is applied and the SOC is an expression of the present battery storage capacity as a percentage of maximum capacity. The SOC is always calculated as a percentage and it is proved that a narrow band of SOC ensures better performance and longer life [Burke 2007] [Pop 2008]. The relationship between the OCV and the SOC is determined as follows [Pang 2001] [Allègre 2010-b]:

$$OCV = a(SOC) + u_{bat} \quad (2.10)$$

$$SOC = 100 - DOD \quad (2.11)$$

$$DOD = 100 \frac{Q_P}{Q_R} \quad (2.12)$$

$$Q_P = Q_O + \frac{1}{3600} \int i_{bat} dt \quad \text{with rate of charge } 0 \leq i_{bat} / \text{discharge } i_{bat} \geq 0 \quad (2.13)$$

$$Q_O = \frac{Q_R}{DOD_O} \quad (2.14)$$

whereas the  $a$  is battery constant,  $u_{bat}$  reflects the battery nominal voltage (V),  $Q_P$  is the present storage capacity (Ah) at the time of estimation,  $Q_R$  is the reference or designed capacity of the battery (Ah),  $Q_O$  is the initial capacity (Ah),  $DOD_O$  is the initial rate of discharge (%) and  $i_{bat}$  the battery

current (A). Furthermore, a low level of discharge of the battery will be defined by a low level of *DOD* (or high level of SOC) and a high level of discharge leads to high level of *DOD* (or low level of the SOC).

The efficiency of a battery depends on the value of the internal series resistance. This means that the internal resistances are directly related to the DOD of the battery. In addition, the resistance value varies depending on the direction of energy transfer (charge or discharge). In the following equation, the internal resistance of battery is estimated through the SOC percentage as follows:

$$R = x(SOC)^2 - y(SOC) + z \quad (2.15)$$

In the above equation (2.15),  $x$ ,  $y$  and  $z$  are the unit-less designed value of the battery in which the internal resistance  $R$  is determined through SOC of the battery.

From the above discussion, it is clear that batteries are voltage sources. Therefore, the electric output of the model is a voltage and the input is a current. The equation for the battery model will be:

$$u_{bat} = OCV - Ri_{Conv} \quad \begin{cases} OCV = f(SOC) \\ R = f(SOC) \\ SOC = f(i_{Conv}) \end{cases} \quad (2.16)$$

In EMR the batteries can be represented as a source element, which is shown in Fig. II.6 below with relationship of equation (2.16).

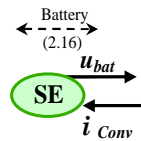


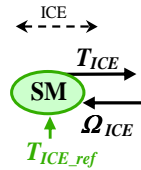
Fig. II. 6 – EMR of the Battery

### II.2.1.2 Internal Combustion Engine (ICE)

The ICE converts the chemical energy of fuel with oxygen in the air into mechanical energy. This mechanical energy leads to the traction of the

vehicle. The ICE can be categorized in a variety of different ways such as by fuel, operating cycles, combustion patterns, design etc. [Srinivasan 2007] However, the ICEs used commonly in HEVs or conventional vehicles are based on a four-stroke Spark Ignition (SI) or Compression Ignition (CI) engines. The SI engines are based on gasoline and CI engines are based on diesel. In heavy-duty application, most of the ICEs are CI with diesel as the fuel being used. The choice of diesel as a fuel is mainly due to its reduced cost [Kavalov 2004] [Olah 2006]. The price factor of fuel is also very important, especially in heavy-duty HEVs, because the hybridization of these vehicles greatly increases the cost of additional components such as the EM, electric converters, batteries, etc. [O’Keefe 2002] [Serrao 2006].

In EMR, the ICE is represented as a mechanical source (Fig. II.7) instead of a mechanical converter due to the basis of energetic modeling. In this, the ICE delivers the torque as an output to the system and in reaction it receives the angular velocity.



**Fig. II. 7 – EMR of the ICE**

For the ICE, static modeling by mapping is done. Mapping is very useful in ICE modeling because it helps to determine the position of the fuel injector directly according to the required torque and speed. Furthermore, this mapping represents the empirical numerical quantification of ICE. Moreover, mappings are becoming more commonly used in simulation models because instead of considering the whole modeling dynamics of ICE, just the final operating points are taken in steady state. The mapping of both ICEs are given in Appendix B and the efficiency of the ICE for both applications can be determined as follows:

$$\eta_{ICE} = \frac{100}{BSFC \frac{E_D}{1000}} \quad (2.17)$$

where  $\eta_{ICE}$ ,  $BSFC$  and  $E_D$  are the efficiency of ICE, Brake Specific Fuel Consumption and Energy density of the fuel. The average calorific value of diesel is about 42.1 MJ/kg and energy density is an average of 11.7 kWh/kg. The ICE used for military truck is taken from Mercedes and for garbage truck is made by Detroit Diesel Corporation.

### II.2.1.3 Mechanical Brakes

During the transmission of energy to the wheels, the braking element will help to slow down the vehicle. The mechanical brakes are the elements which act on the vehicle body closest to the road i.e. wheels. Normally the brake model is always next to each wheel. For simplification, a single model of four wheels is considered. Therefore, in a similar way, a single model for brakes is taken into account, shown in Fig. II.8 below.

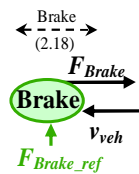


Fig. II. 8 – EMR of the Mechanical Brakes

The mechanical brakes deliver a braking force to the vehicle chassis and are controlled by an attached entry control (Fig. II.8). The model adopted for the brake is an energetic type that is designed to hasten the dynamics of the system. Therefore, the braking source is considered as perfectly delivering the desired braking force.

The relationship for the braking force can be determined by the total force exerted on the vehicle and the environmental force (see section II.2.1.4). However, in Fig. II.8, the brake force ( $F_{Brake}$ ) is equal to the reference brake force ( $F_{Brake\_ref}$ ) exerted by the driver.

$$F_{Brake} = F_{Brake\_ref} \quad (2.18)$$

### II.2.1.4 Environment

The environment represents the external resistance to propel the vehicle on a longitudinal plane. There are three main resistances: rolling (rolling



resistance), drag (air resistance) and resistance due to slopes or grade resistance. The relationship of rolling force for sand and road are described as follows [Galland 2008]:

$$\begin{aligned}
 F_{Rolling} &= f_R M_{veh} g \cos(\alpha) && \text{with} && (2.19) \\
 f_R &= (0.02 + 0.00025 v_{veh}) && \text{for road} && \\
 f_R &= (0.075 + 0.0005 v_{veh}) && \text{for sand} &&
 \end{aligned}$$

with  $f_R$  being the coefficient of rolling resistance which depends on the ground surface,  $M_{veh}$  the mass of vehicle,  $g$  the acceleration due to gravity ( $m/s^2$ ),  $\alpha$  the slope angle and  $v_{veh}$  the vehicle speed ( $m/s$ ).

The drag refers to forces that oppose the relative motion of a vehicle through air. It gives frontal thrust on the vehicle. The resistance due to the slopes (grade resistance) characterizes the slope of the rise of a vehicle.

$$F_{Drag} = 0.5 \rho c_x A (v_{veh} + v_{wind})^2 \quad (2.20)$$

$$F_{Grade} = M_{veh} g \sin(\alpha) \quad (2.21)$$

where  $\rho$  is the air density ( $kg/m^3$ ),  $c_x$  is the drag coefficient,  $A$  is the maximum cross section area ( $m^2$ ) and  $v_{wind}$  is the opposite wind speed ( $m/s$ ).

All resistance forces can be represented by a single force as follows:

$$F_{env.} = F_{Rolling} + F_{Drag} + F_{Grade} \quad (2.22)$$

The vehicle environment is represented by a mechanical source providing a resistance force  $F_{env.}$  by receiving the vehicle speed (Fig. II.9). Also, the resistance forces of environment and braking force ( $F_{Brake}$ ) summation gives the total forces ( $F_{Tot}$ ) as follows:

$$\left\{ \begin{array}{l} v_{veh} \\ F_{Tot} = F_{Brake} + F_{env} \end{array} \right. \quad \text{common} \quad (2.23)$$

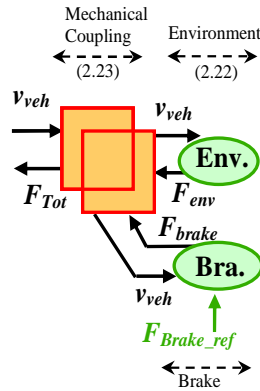


Fig. II. 9 – EMR of the Environment with Mechanical Brakes

## II.2.2 Energetic Elements

This section deals with discussion about energetic elements in both HEVs. According to the physical causality these energetic elements can be classified into two categories. One is based without time (rigid relation) and the other is based with time (casual relation) between the inputs and outputs of the elements. In the energetic elements based on rigid relationship, the output follows the input without any storage or accumulation effect. However, in energetic elements, the inputs and outputs are transposable. Contrarily, in the energetic element based on causal relationship, the transposability between the inputs and the output is derivative, which is against physical phenomena. Therefore, in this, the inputs and outputs are defined internally in such a way that it assures non-transposability with accumulation effect [Hautier 2004].

In EMR, the rigid elements can be mono-physical or multi-physical elements. The mono-physical elements can couple or convert the energy in the same field of physics without accumulation such as coupling or conversion blocks. While the multi-physical elements convert the energy form one to other types of energy without any accumulation elements such as converters or distribution elements (see Appendix A).

### II.2.2.1 Electric Drives

Electric machines (EMs) are electromechanical or multi-physical energy converters elements. In automotive applications mostly synchronous and induction machines are being used as the EM. The electric drives can be dis-

tinguished by the materials used, certain key construction features, or the underlying principles of operation [Taylor 2002]. In the ARCHYBALD project, the Permanent Magnet Synchronous Machine (PMSM) is utilized due to its high power density, higher efficiency, low noise and less vibration.

In any HEV, the EMs have a much faster response time than the ICE because of their higher availability and performances. The main issues with EMs lie in their energy management and control. To handle this, different models such as dynamic, static and quasi-static models are being used. All modeling methods have their advantages and disadvantages but here static modeling is used to build the map of EM. This modeling method is taken into consideration because it will take less simulation time and will allow for an easier study of power and energy during the steady states for global optimization [Letrouvé 2010].

Static models has no time constant and has the ability to take into account the whole EM with its inverter and control. Furthermore, the EMs are directly controlled by a reference torque such as:

$$T_{EM} = T_{EM\_ref} \quad (2.24)$$

For the military and garbage truck, two surface-mounted PMSM electric machines of are utilized of different design power (see Appendix B). For the military truck, the average mass and volume of each machine is 44.3 kg and 10.6 liters, respectively. The detailed distinct features of these machines are detailed in [Wu 2009] [Wu 2010] [Wu 2012].

Mapping is done for the energetic modeling of EMs in application to military and garbage truck, shown in Appendix B. Also, at the initial stages, the electrical drives (electric machine, inverter and local control) are modeled by the following global equation in a static way:

$$u_{bat} i_{Conv} = T_{EM} \Omega_{GB} + losses \quad (2.25)$$

or

$$i_{Conv} = \frac{T_{EM} \Omega_{GB} + losses}{u_{bat}}$$

$T_{EM}$  and  $\Omega_{GB}$  are the torque of electric machine (Nm) and speed through gearbox, ( $rad/s$ ) respectively. The EMR of the electric drives can be symbolized by an electromechanical conversion with the reference input torque (Fig. II.10).

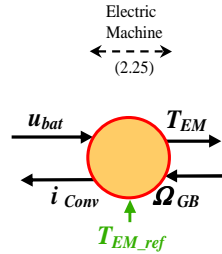


Fig. II. 10 – EMR of the Electric Machine

### II.2.2.2 Common DC Bus

The electric machines EM1 and EM2 are fed by inverters, supplied by the same DC bus. An electrical coupling (mono-physical element) is then defined, with the battery voltage as common variable (Fig. II.11):

$$\begin{cases} u_{bat} & \text{common} \\ i_{Conv} = i_{Conv1} + i_{Conv2} \end{cases} \quad (2.26)$$

$u_{bat}$  and  $i_{Conv}$  are the voltage (V) and current (A) respectively. The DC bus voltage can be considered as the bus which is supplied by the batteries.

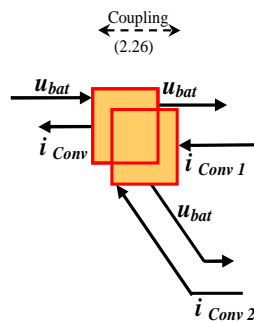


Fig. II. 11 – EMR of the Common Supply

### II.2.2.3 Gearboxes

The gearbox adjusts the output torque to the load torque. In vehicles, the torque depends on several parameters like vehicle weight, desired accel-

eration, slope, drag coefficient, rolling resistance, etc. The gearbox must be chosen in such a way that the torque capacity is always greater than the load torque. In both vehicles i.e. military and garbage truck, three gearboxes are utilized to step-up the torque capacity. Two gearboxes are used with each electric machines and one in the transmission line. For military truck, neglecting the clutch phenomena the associated equations for gearboxes in both HEVs will be:

$$\begin{cases} \Omega_R = \frac{\Omega_{EM1}}{k_1} \\ T_y = \frac{T_R}{k_1} \end{cases} \quad (2.27)$$

$$\begin{cases} \Omega_{LS} = \frac{\Omega_{EM2}}{k_2} \\ T_x = \frac{T_{LS}}{k_2} \end{cases} \quad (2.28)$$

$$\begin{cases} \Omega_{PC} = k_3 k_4 \Omega_w \\ T_m = k_3 k_4 T_{PC} \end{cases} \quad (2.29)$$

where  $k_1$ ,  $k_2$  and  $k_3$  represent the gear ratios of the connected gear to EM1, EM2 and planet-carrier of the PSD respectively. The  $k_4$  gain shows the differential gear ratio of the vehicle. In EMR, a mono-physical converter can be used to represent these gearboxes (see example of (2.27) in Fig. II.12).

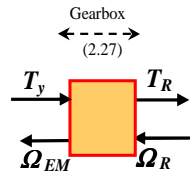


Fig. II. 12 – EMR of the Gearbox

#### II.2.2.4 Wheels

The wheels are mono-physical elements that link the road and chassis of the vehicle (Fig. II.13). These transform the differential rotation into the

linear movement of the vehicle. Based on the assumption that the road is straight and there is no slipping, a unique equivalent wheel is considered.

$$\begin{cases} T_W = R_W F_{Tot} \\ v_{veh} = R_W \Omega_W \end{cases} \quad (2.30)$$

with  $R_W$  is the radius of the wheels of (m) and  $F_{Tot}$  is the total force exerted on the vehicle. The EMR of the wheels is:

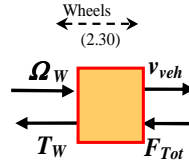


Fig. II. 13 – EMR of the Wheels

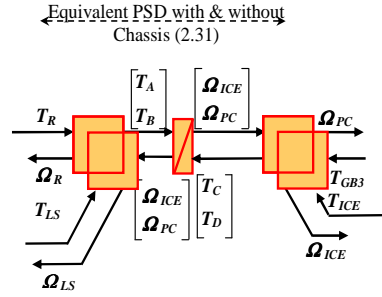
### II.2.2.5 Equivalent Shaft with Chassis

The equivalent shafts with the chassis are resolved in the same methodology which is discussed in section II.I.2 and discussed in [Chen 2010] and [Lhomme 2007]. The complete resolution of the system is given in Appendix C and the formulations have been defined to have two speeds  $\Omega_{ICE}$  and  $\Omega_{PC}$  with two torques  $T'_1$  and  $T'_2$ . Since the torques  $T'_1$  and  $T'_2$  are based on the four input torques of the energy sources i.e. EM1, EM2, ICE and wheels. The final result from Appendix C is given in equation (2.31), and its EMR representation is given in Fig. II.14.

$$\begin{bmatrix} T'_1 \\ T'_2 \end{bmatrix} = C \frac{d}{dt} \begin{bmatrix} \Omega_{ICE} \\ \Omega_{PC} \end{bmatrix} + D \begin{bmatrix} \Omega_{ICE} \\ \Omega_{PC} \end{bmatrix} \quad (2.31)$$

with,

$$\begin{aligned} T'_1 &= T_A + T_C = f(T_{ICE}, T_{EM1}, T_{EM2}) \\ T'_2 &= T_B + T_D = f(T_W, T_{EM1}, T_{EM2}) \\ C &= - \begin{bmatrix} J_1 & -J_2 \\ -J_3 & J_4 \end{bmatrix} \quad \text{and} \quad D = \begin{bmatrix} f_1 & -f_2 \\ -f_3 & f_4 \end{bmatrix} \end{aligned}$$



**Fig. II. 14 – EMR of the Equivalent Shafts with Chassis**

The above modeling is done with the equivalent shaft with chassis when the clutch is in a locked position. This assumption is taken into consideration to avoid the complexity and the non-linear behavior of the whole clutch. In the next section, the modeling of the clutch with connected parts in both positions i.e. slipped and locked is discussed. Also, the problems associated with connecting the elements within EMR are detailed.

### II.3 EMR of both HEVs

In this section, the final EMR of both HEVs are described based on the discussion in Section II.2. Furthermore, the EMR of each element, presented above, is difficult to connect directly with the part next to it in the physical system. This is due to the causality and constraints of the system. To overcome this problem, the permutation and merging rules of EMR [Bouscayrol 2003-a] are taken into account to build the studied HEVs.

In EMR, two elements can be connected directly if their exchange variables are of the same field and nature. Other possibilities of direct connection are: the input/output of the first element corresponds to the output/input of the second element or the variables have the same value at the connection moment. But in this case, when there is no direct connection because of a state variable conflict between the elements then the merging rule can be implemented. The other rule utilized for building the EMR of the studied HEV is the permutation rule. This helps when any two elements, mono-physical or accumulation with exchange variables, have continuous evolutions. The equivalent fictitious elements have to produce the same effect that the initial association (same global outputs) under the same requests (same global inputs). In that case, the parameters of the equivalent elements are defined in function of the initial elements parameters. The same rules have

been utilized for the modeling of the PSD (Appendix C) and clutch assembly (section II.3.1). Due to the existence of many state variables or accumulation elements, the rules i.e. merging and permutation solve the state variable conflict by reducing it in the studied vehicles. Thus, the same representation includes only a single accumulation element, which produces the common state variable. However, while these rules resolve the causality conflict, they reduce the coherency with the structural representation of the system.

### **II.3.1 Dual-Range Gearboxes with Clutch**

This section deals with the modeling and EMR of the dual-range gearboxes with clutch for the military truck. The two dual-range gearboxes consist of two clutches. The hydraulic coupler acts as a clutch and helps during startup or in case of failure of the mechanical clutches. In the modeling perspective, all of these clutches are considered as one only. This is due to the clutch's functionality i.e. to change the one gear ratio to another [Bennett 2005] and makes no difference in the modeling of the clutches itself or as a whole.

The clutch helps to allow a breakable connection between two rotating shafts. Furthermore, this connection should be smooth and allows the power to flow from one inertia to another according to the relative speed between the two inertias of the shaft. The torque transmission is achieved through friction between two surfaces or disks. When applied to automotives, clutches typically ensure the smooth transfer of power between the transmission and the rest of the system all the while avoiding extra jerks, shocks and excessive wear [Vasca 2008]. Furthermore, when applied to HEVs, clutches are used for the actuation of energy flow management [Lee 2000].

In literature, several approaches are used to model the clutch and signify its complex phenomenon such as [Otter 1997] [Wipke 1999] [Nobrant 2001] [Serrarens 2004] [Lhomme 2007] and [Lhomme 2008-a]. The complexity is due to the nonlinear behavior of clutches and its ability to have three states i.e. opened, slipped and closed. The opened and slipped state of clutch can be considered the same because both contain the same number of state variables i.e. two. Therefore, when the clutch is slipped or opened, the inertias of the both shafts i.e. driven and driving, must be taken into account. Contrarily, when two disks of the clutch are locked with each other, the sys-



tem must be considered as a single unit and have an equivalent inertia that induce a unique state variable. This locking of the two shafts and having an equivalent inertia causes the system torque to be transmitted to the wheels via the transmission. For clutch modelling in the studied system (see Fig. II.1), only the transmission line until the wheels (Fig. II.15). For the clutch modelling, the friction and dissipation losses, vibration, abrasion and temperature effects are neglected.

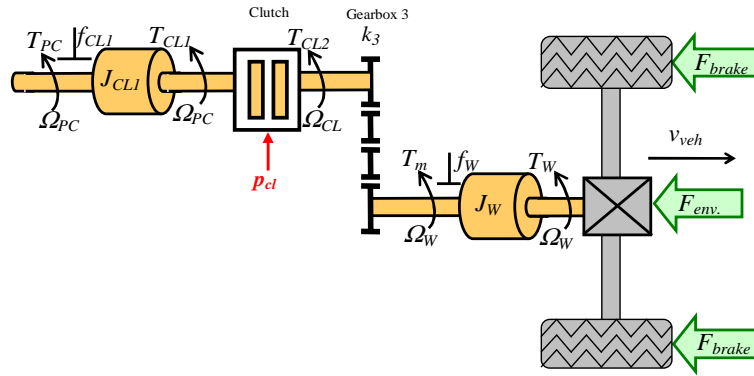


Fig. II. 15– Transmission line

**Model ①: Slipped Clutch** – For finding the behaviour of the clutch in the slipped position, the studied system (Fig. II.1) is divided into two parts—one before the clutch and the other after the clutch. The part before the clutch includes the PSD, ICE, and EMs with converters and gearboxes. The part after the clutch mainly includes the chassis, dual-range gearbox, differential, brakes and the wheels. At the initial stage, it is assumed that the part before the clutch can be considered as an equivalent mechanical source represented as MS1 (Fig. II.16). This assumption is based on the fact that the sources EM and ICE supply the final torque passed through the clutch for final traction of the vehicle. On the other hand, the part after the clutch including wheels and the brakes with environmental drag, are considered as a second equivalent mechanical source and represented as MS2 (Fig. II.16).

As shown above (Fig. II.15), when the torques ( $T_{CL1}$  and  $T_{CL2}$ ) is applied to the upstream and downstream of the clutch then the corresponding speeds of primary and secondary shafts after and before the clutch are  $\Omega_{CL}$  and  $\Omega_{PC}$ . Therefore in the case where the clutch is slipped, the equation of the shaft will be [Lhomme 2008-a]:

$$T_{PC} - T_{CL1} = J_{CL1} \frac{d}{dt} \Omega_{PC} + f_{CL1} \Omega_{PC} \quad (2.32)$$

$$T_{CL1} = T_{CL2} = 2F_n R_{clutch} \mu \text{SIGN}(\Omega_{PC} - \Omega_{CL}) \quad (2.33)$$

$$F_n = F_{n\_max} \left[ 1 - \sqrt{1 - \left( \frac{p_{cl}}{100} - 1 \right)^2} \right] \quad (2.34)$$

$$\mu = \mu_{stat} - \alpha_{dyn} |\Omega_{PC} - \Omega_{CL}| \quad (2.35)$$

$$T_{CL\_o} = T_{CL1} \quad (2.36)$$

where  $f_{CL}$  and  $J_{CL}$  are the friction coefficient and the inertia of the shaft, respectively;  $\mu$  is the friction coefficient of the clutch;  $\mu_{stat}$  is the static friction coefficient of the clutch;  $\alpha_{dyn}$  is a parameter for the dynamic friction coefficient of the clutch;  $R_{clutch}$  is the average radius of the clutch friction plate;  $p_{cl}$  is the position of the clutch in percentage from 0 (closed) to 100 (open) and  $F_n$  is the normal actuation force.

In the EMR of clutch representation (Fig. II.16) there are two accumulation elements. For the slipped position of the clutch, the accumulation element connected with the MS1 represents all of the relationships before the planet-carrier including the inertias and viscous friction of the connected shafts with attached gearboxes and PSD. Another accumulation element after Gearbox 3 represents the equivalent shaft of the vehicle.

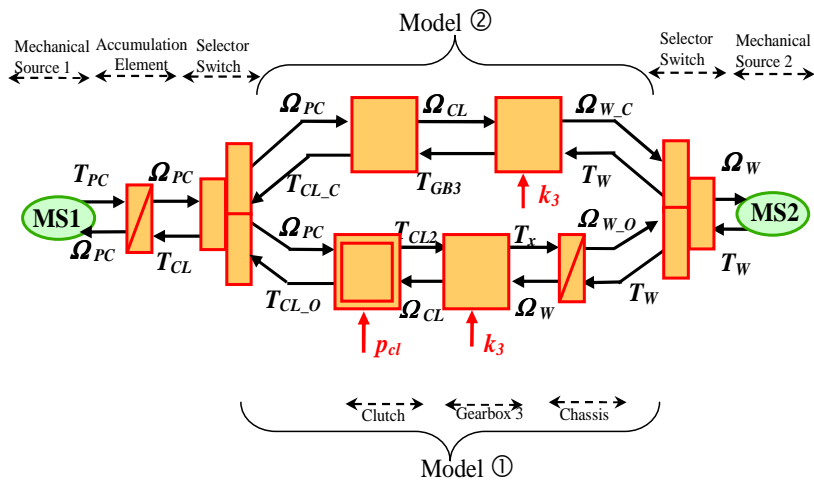


Fig. II. 16 - Modeling of the clutch by EMR approach

**Model ②: Locked Clutch** - When the clutch is locked, it means that the disks are rigidly coupled with each other. During this, the entire system should be considered as one single unit. Therefore for the energy accumulation, a single accumulation element (see Fig. II.16) is enough to hold all inertias, viscous friction and chassis of the vehicle. Furthermore, during the locked position of the clutch, the torques i.e.  $T_{CL1}$  and  $T_{CL2}$ , and the speeds i.e.  $\Omega_{CL}$  and  $\Omega_{PC}$  on both the up and downstream of the clutch will be equal to each other.

$$T_{PC} - T_{CL\_C} = J_{lock} \frac{d}{dt} \Omega_{CL} + f_{lock} \Omega_{CL} \quad (2.37)$$

$$T_{CL1} = T_{CL2} = T_{GB3} \quad (2.38)$$

$$\Omega_{PC} = \Omega_{CL} \quad (2.39)$$

$$T_{Max} = 2F_n R_{clutch} \mu = 2F_n R_{clutch} \mu_{stat} \quad (2.40)$$

As  $\Omega_{CL}$  and  $\Omega_{PC}$  are equal, the differential equation (2.32) will no longer be independent and the maximal torque value of the clutch ( $T_{Max}$ ) will be static which is expressed in equations (2.37) and (2.40) respectively. Furthermore, in equation (2.37),  $J_{lock}$  represents the moment of inertias including total mass of the system.

**Selector Switch:** Later, a selector switch is defined using a Petri net [Wang 1998], [Stremersch 2001] (Fig. II.17) to ensure the physical energy flow and the activation of both models ① and ②. In this, the state  $P_1$  (slipped clutch) represents the active model when the conditions at transition state  $\tau_2$  are validated. Similarly, state  $P_2$  (locked clutch) also represents the active model and it will be active when the transition state  $\tau_1$  becomes true. Both models are depicted using the EMR with two switch selectors (Fig. 11.16).

In the selector switch to switch the model from locked to slipped, torque  $T_{CL1}$  will be compared to the maximum transmissible torque through the clutch ( $T_{Max}$ ). However, these two torques will not appear in EMR (Fig. II.16) because they represent the local properties of the clutch. The other reason for their disappearance is that EMR is a macroscopic description and it represents only the global features or properties of the system.

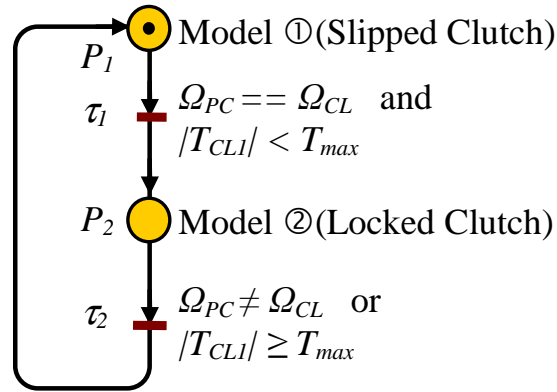


Fig. II. 17 - Petri net for the model switch

### II.3.2 Final EMR of the Military Truck

The final EMR of the studied system for a military truck is organized in EMR (Fig. II.18). This representation highlights the exchange variables of the elements for an energetic conversion. The EMR is built according to the above expression derived with respect to two state variables i.e. speed of ICE ( $\Omega_{ICE}$ ) and planet-carrier ( $\Omega_{PC}$ ). The final EMR of the military truck is built on the discussion of each element, presented in section II.2. But as mentioned previously, it is difficult to directly connect these two elements by considering the structural layout of the studied HEV. Therefore, by utilizing the merging and permutation rule, the final EMR of the studied vehicle is presented in Fig.II.18. Due to these rules of EMR, the conflict between state variables is solved and common chosen state variables i.e.  $\Omega_{ICE}$  and  $\Omega_{PC}$  are produced with a single accumulation element.

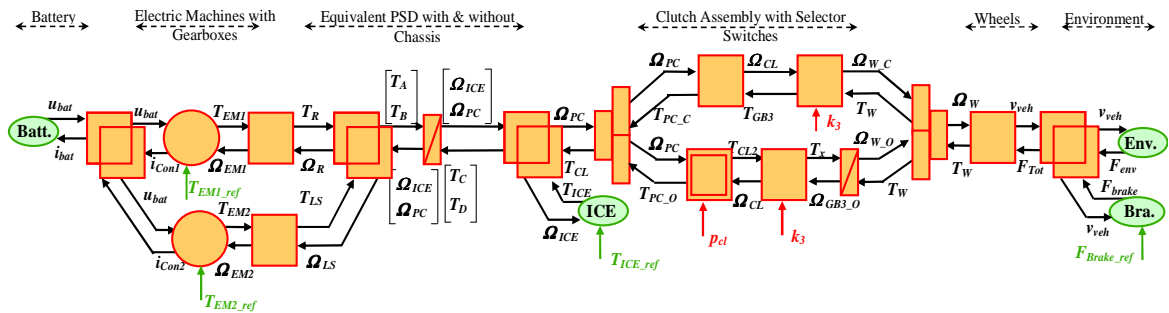


Fig. II. 18 - EMR of the Military Truck

In Fig. II.18, the dual-range gearboxes with the clutch in the transmission line have an input  $k_3$  and  $p_{cl}$ . This input reflects the gear change and the clutch pedal of the vehicle which is controlled by the driver.

In Fig. II.18, the mechanical coupling before the accumulation element is used to combine the made up torques  $T_A$  and  $T_B$  that are associated with sources EM1 and EM2. Similarly, the other mechanical coupling after the accumulation element is used to combine the made up torques  $T_C$  and  $T_D$  associated with the ICE and wheels. These torques are added to get  $T'_1$  and  $T'_2$  which were discussed in Appendix C an section II.2.2.5. Later, scalar torques  $T'_1$  and  $T'_2$  are vectored to apply energy into the accumulation element. In the above representation, a vectorial accumulation element bears the equivalent mass, moment of inertia and viscous friction. This equivalent represents the mass of the total vehicle with passengers and the equivalent moment of inertia represents all moments of inertia i.e. EMs, ICE, chassis and wheels.

### II.3.3 Final EMR of the Studied Vehicle

The final EMR of the studied system for a garbage truck is organized in Fig. II.19. This EMR is very similar to the EMR of a military truck (see section II.3.2). Here, in building the EMR for a garbage truck, the same permutation and rules are taken into consideration to produce the same state variables i.e. speed of ICE ( $\Omega_{ICE}$ ) and planet-carrier ( $\Omega_{PC}$ ). Furthermore, the similar state variables of both HEVs i.e. military and garbage truck will provide an easier route in building a similar control structure for both vehicles.

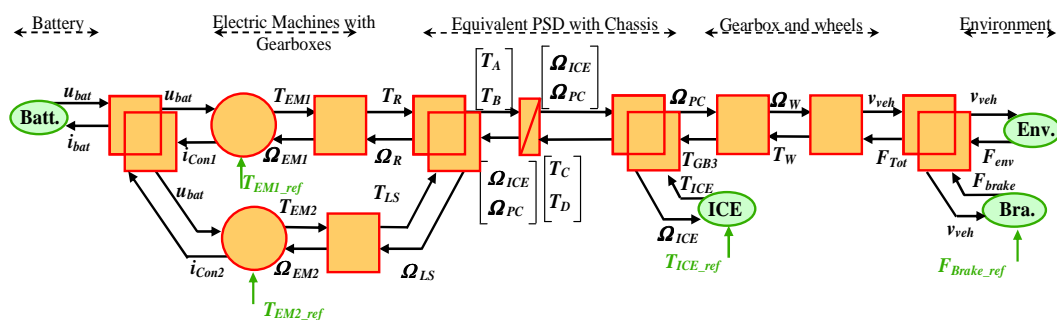


Fig. II. 19 – EMR of the Garbage Truck

By comparing the above EMR shown in Fig. II.19 with the EMR shown in Fig. II.18 it can be determined that when the clutch is closed (in Fig. II.18), the EMR will be the same as shown in Fig. II.19. Therefore, it can be con-

cluded that the same modeling and EMR of the military truck can be used for the garbage truck with the exception of the dual-range gearboxes with clutch. This similarity in the modeling and EMR of the both HEVs will also make it easier to build a similar kind of local control structure i.e. inversion-based control and global control structure i.e. Energy Management Strategy (EMS). In the next chapter, a detailed discussion is given about the local and global control structures of both HEVs (see Chapter III and IV).

## Conclusion

In this chapter, detailed modeling and graphical description through EMR for two considered HEVs have been done. Although both vehicles have a similar architecture i.e. series-parallel, there are differences in their additional components and sizes. The main difference between the components in both vehicles is that the military truck contains two dual-range gearboxes with clutch while the waste collection truck does not.

This chapter explained the modeling of the studied HEVs with a more complex device i.e. double planetary geartrain. Structurally, this geartrain connects 4 shafts, which mean there are a total of 4 rotation speeds and torques. However, the internal relationships demonstrate that 2 rotation speeds are enough to be considered as the state variable. Thus, the modeling of this geartrain has been reorganized with the equivalent torques as input and 2 rotation speeds as output. A vectorial element has then been used in EMR. Moreover, for the military truck, a clutch switching model was used to take the clutch model into account [Lhomme 2007].

During the building of EMR of the studied HEVs, the association rules were used to solve the conflict of state variables. The EMR of the military truck can be considered as a general model as the second vehicle i.e. garbage truck, can be deduced from this by considering the clutch in a closed position.

A single planetary geartrain connects 3 shafts and has 2 state variables [Lhomme 2007] [Chen 2011]. The double planetary geartrain connects 4 shafts and has same number of state variables i.e. 2. This is the key point for this modeling and also for building control structures. The EMR highlights this critical property in next chapters (Chapter III and IV) in which the local control structures and EMS are built on the basis of EMR of both studied HEVs in this chapter.





# **Chapter III**

## **Inversion-based Control for Studied HEVs**



## Introduction

The objective of this chapter is to determine a control structure for studied HEVs i.e. military and garbage truck through EMR. As explained and shown earlier in Chapter II, both vehicles have a very complex structure due to a multitude of energy sources and subsystems. Therefore, the build-ings of control structures of these HEVs are difficult and an important tasks [Chan 2010]. When working with the multiple sources and subsystems in studied HEVs, individually or collectively, a control scheme plays a critical role in realizing the driver's requirement along with other performances. Normally, the control schemes are divided into two levels, local and global [Bouscayrol 2003-a] [Delarue 2003]. The local control refers to the control of the individual subsystem components while global control is the energy management strategy of the whole system. Global control is detailed in Chapter IV, while in this chapter only the local control schemes or local energy man-agements of the studied HEVs are detailed. The local control structures can be achieved in different ways but in this research work only model-based lo-cal control structure through EMR is taken into consideration. This control structure through EMR is based solely on its inversion principle. Indeed, this graphical description enables facing the complexity of the control for these complex new vehicles.

In this chapter, an inversion-based control for the studied vehicles, military and garbage trucks, using the inversion principle of EMR and model-ing presented in Chapter II is built. The first section of this chapter details how to determine the control structures along with the definition of the tun-ing and control paths of the studied HEVs. The second section is an explana-tion of the inversion of each subsystem within the entire vehicle. The third section presents the simulation results following the validation of the inver-sion-based control structure in the MATLAB-Simulink® environment through a simple energy management strategy.

## III.1 Control of the Studied HEVs

The control structure of HEVs is multi-sourced and contains multiple subsystems. The central issue is the development of these complex systems [Gao 2006] [Chan 2010]. When building the control structures for complex systems the challenge is to do so with less computation time and minimal errors. A more efficient way of carrying out the control structure is the model-based control design process [Chen 2010]. The general steps involved in a model-based control design process are: system modeling, system analysis, control tuning, system and control simulation, experimental validation, and finally, control deployment.

### III.1.1 Control Structure

In model-based control structures, modeling is the first step in building a control structure. Using different objectives, various models and modeling approaches can be utilized to build different control structures for the same real system. EMR allows for the control system to be deduced systematically. After analyzing the studied system with its EMR, the control objectives and constraints must be defined. The control objective can either be a local or global variable. Furthermore, it is possible to set many local variables in which to achieve a single global objective. The constraints are a choosing a variable that can be controlled to achieve a goal [Bouscayrol 2003-a].

Building the control structures and/or energy management is one of the main concerns in HEVs. This is because building a control structure allows for the control of many energy sources and subsystems. When using model-based control structures to achieve satisfactory energy management, two control levels can be considered: local control or local energy management and global control or Energy Management Strategy (EMS) [Bouscayrol 2003-a]. The first level must be ensured in fast-dynamic and, the second level must be ensured at the system level in order to coordinate the power flows in each subsystem.

**Local control Structure** – When building a local control for any considered system; two methods are normally used i.e. heuristic control and model-based control. Heuristic control requires prior expertise while model-based control is based on causal models of studied systems [Hautier 2004]

[Barre 2006] [Chan 2010]. In model-based control a key feature is the ability to locate controllers and degrees of freedom along the causal model.

In EMR topology, controllers are used in its inversion. Components are based on the controller and on integral causality or time-based relationships. For casual elements (time-based relationships) the control consists in a closed-loop. Furthermore, supplementary inputs (degrees of freedom) can be added to the inversion of the components that have connection analogies [Bouscayrol 2003-b]. Additionally, in EMR, the direct inversions of the components are used for other instantaneous relationships. Through this it is possible to determine a local control of the system in a systematic way. Furthermore, this method helps to indicate the number of controllers, measurements or estimators and degrees of freedom. By utilizing the same inversion topology, a systematic inversion based on the local control of both considered HEVs is deduced. This is detailed in following sections.

**Global control Structure (EMS)** – Generally, global control produces references for local control loops. The energy management of HEVs can be classified into the following two types: rule-based solutions and optimization-based solutions [Salmasi 2007]. The energy management strategy should meet the driver's requirements regarding traction power, sustaining or depleting the battery charge, optimization of drivetrain efficiency, fuel consumption, and emissions. The main feature in rule-based energy management approaches is their efficiency in real-time supervisory control of power flows in a hybrid drive train. The rules are built on heuristics, intuition, human expertise, as well as mathematical models. They are also normally made without prior knowledge of a predefined driving cycle [Salmasi 2007]. These rules can be further classified into deterministic [Anderson 1995] and fuzzy rule-based methods [Lee 1998]. In optimization-based strategies, the optimal torque and gearbox ratios are calculated by minimizing the cost function connected to the consumption. If this optimization is performed over a fixed driving cycle, a global optimum solution can be reached. The definition of an instantaneous cost function is key in obtaining a real-time optimization-based control strategy [Sciarretta 2004]. A detailed analysis of different energy management strategies as well as a new proposal will be discussed in Chapter IV.

### **III.1.2 Inversion of Elements in EMR**

In EMR topology, before inverting the elements it is necessary to determine the tuning and control paths of the system. Afterwards, an inversion-based control structure can be obtained from EMR in a systematic way. The inversion can be done directly by inverting the elements of EMR.

In EMR, the only elements that can be directly inverted are mono or multi-physical converters. This is because these elements are not time-based and generally contain linear and stationary relationships. Therefore the accumulation element cannot be inverted due to the fact that it represents a time-dependent relationship that cannot be inverted physically. Because of this, a close-loop control is needed to handle this issue. The controller can be of any type such as P controller, PI controller, or other kinds of controllers. Also, if sensors are required for the measurement of variables, it is also possible to represent those with small circle on the measurable variable. Inversion of distribution elements is made using criteria or disturbance rejection.

The inversion of all elements in EMR is illustrated by light blue parallelograms. The EMR provides insights into the real energy operation of the system and allows for a more complete understanding of its potentials from a dynamic point of view. Other advantages are it gives a more energetic view and yields a direct control structure.

Control schemes of systems from EMR are yielded from specific inversion rules. This control scheme ensures local control. At the same time, the local control of each subsystem takes the whole system into account. This is because the EMR of the system, from which this control scheme is deduced, is created according to the whole system function, and not only the structure. Because of this, the degrees of freedom of the system naturally appear where they act on the energy management level.

### **III.1.3 Tuning and Control Paths for considered HEVs**

In EMR, the first step before inversion is to analyse the tuning and control paths. After these paths are defined, the inversion-based control scheme can be deduced. The tuning paths can be defined according to the objectives and constraints of the system. At first, these paths start from the tuning variables before approaching the objective variables. Later, control paths can be determined by the inversion of the tuning paths.

The EMR shown in Fig. II.8 and Fig. II.9 (chapter II) for garbage and military truck is nearly the same. The only difference is the 4 gears used in the clutch assembly for the military truck. Both EMRs contain a maximum of 5 tuning variables which include the reference torques for EM1 and EM2 ( $T_{EM1\_ref}$  and  $T_{EM2\_ref}$ ), the torque reference for ICE ( $T_{ICE\_ref}$ ), the mechanical braking force reference ( $F_{Brake\_ref}$ ) and the third gearbox gear ratios ( $k_3$ ).

In the garbage truck, the gear ratio  $k_3$  is fixed and contains only one gear ratio. Therefore, for this vehicle there are only 4 tuning variables i.e.  $T_{EM1\_ref}$ ,  $T_{EM2\_ref}$ ,  $T_{ICE\_ref}$  and  $F_{Brake\_ref}$ . For military truck, the gear ratio  $k_3$  (4 gears with a clutch assembly) is not a tuning input because the speed ratio is chosen by the driver using a manual gear. Therefore, this ratio will be an uncontrolled input for the control scheme. Similarly, like the garbage truck, this vehicle contains only 4 tuning variables i.e.  $T_{EM1\_ref}$ ,  $T_{EM2\_ref}$ ,  $T_{ICE\_ref}$  and  $F_{Brake\_ref}$ . To avoid complexity, the clutch position  $p_{cl}$  is not taken into account at this stage because it is directly controlled by the driver through clutch pedal. Therefore, in both HEVs the tuning and control paths are the same and  $k_3$  and  $p_{cl}$  are just a disturbance for the control.

Here, the primary objective is to control the vehicle speed  $v_{veh}$  which is proportional to  $\Omega_{PC}$ . The secondary objective is to reduce fuel consumption by finding the optimum points of  $\Omega_{ICE}$  and  $T_{ICE}$ . The operation points for ICE:  $T_{ICE\_ref}$  and  $\Omega_{ICE\_ref}$  are directly chosen from the strategy level through the performance chart of ICE in such a way that it should work under its optimal region. The tuning variable  $F_{Brake\_ref}$  is used to achieve the mechanical braking through brake pedal, which is also directly given input from the strategy.

The tuning paths are defined in Fig. III.1 according to the objectives. After finding the tuning paths for the system, the control paths can be determined through a mirror effect as shown in Fig. III.2.

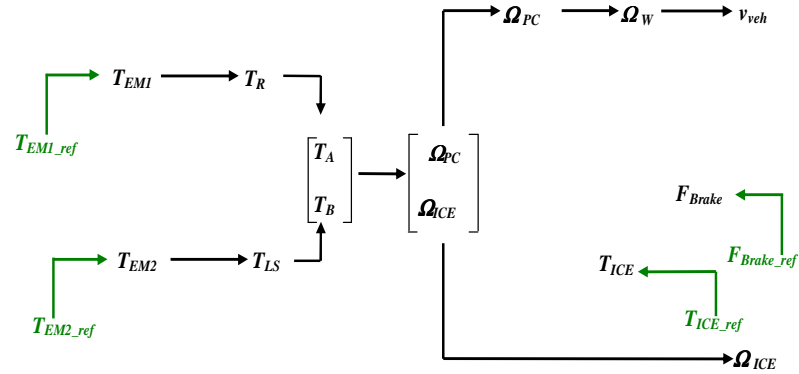


Fig. III.1 – Tuning Path: Military and Garbage Truck

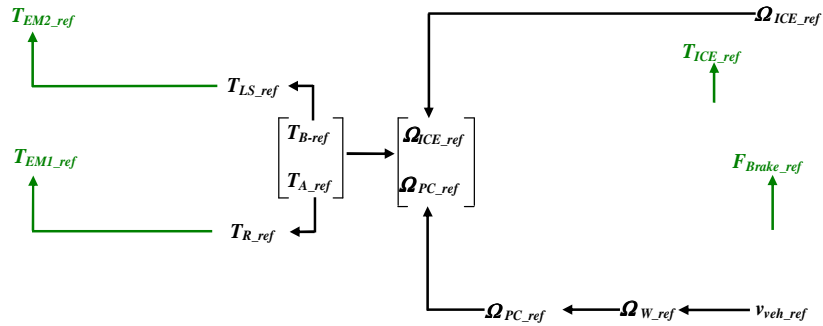


Fig. III. 2 – Control Path: Military and Garbage Truck

## III.2 Inversion-based Control for Considered HEVs

In this section the inversion-based control of both HEVs are discussed. To reiterate previous chapters, to achieve series-parallel architecture, a complex PSD is used i.e. compound planetary geartrain. In the first section, the inversion of elements in EMR being used to represent considered HEVs subsystems are discussed. In second and third sections, inversion-based control of both HEVs and energy management are detailed.

### III.2.1 Inversion-based Control of Subsystems

Both HEVs consist of subsystems such as energy sources (battery, ICE, etc.), converters (electric machines), gearboxes, wheels and a power split device. With application to a military vehicle, a set of four gears is used in the transmission line with additional clutch assembly. In EMR topology, the energy sources are not inverted because they are the terminal of the system



[Bouscayrol 2003-a]. The detail of inversion for each subsystem in considered HEVs are as follows:

**Inversion of Electric Drives** – Two EMs are used in the studied HEVs, to convert the electrical energy to mechanical energy. As discussed earlier (see section II.2.1) static modeling through mapping has been chosen. This is due to the fact that this type of modeling has no time constant and has the ability to take into account the whole EM with inverters and control. Furthermore, this modeling helps to circumvent the dynamic behavior of the system. Therefore, no inversion of this subsystem is needed because both EMs can be directly controlled through imposing the reference torque for EM1 and EM2 such as  $T_{EM1\_ref}$  and  $T_{EM2\_ref}$  respectively.

**Inversion of Gearboxes and Wheels** – Previously, in section II.2.2 the modeling and representation with EMR for the gearboxes and wheels is detailed. These subsystems hold non-time-based or stationary relationships therefore the direct inversion of this subsystem will be shown by blue parallelograms (see Fig. III.3). After the inversion of the associated equation for the gearboxes and wheels from (2.27) – (2.30), the results will be:

$$T_{EM1\_ref} = \frac{1}{k_1} T_{R\_ref} \quad (3.1)$$

$$T_{EM2\_ref} = \frac{1}{k_2} T_{LS\_ref} \quad (3.2)$$

$$\Omega_{PC\_ref} = k_3 k_4 \Omega_{W\_ref} \quad (3.3)$$

$$\Omega_{W\_ref} = \frac{v_{veh\_ref}}{R_w} \quad (3.4)$$

where  $k_1$ ,  $k_2$  and  $k_3$  represent the gear ratios of the connected gear to EM1, EM2 and planet-carrier of the PSD respectively. The  $k_4$  gain and  $R_w$  shows the differential gear ratio and radius of the wheel for the vehicle. The above relationships from (3.1) to (3.4) can easily be transformed into EMR using a blue parallelogram. As an example, the EMR of the inverted equation (3.1) can be represented as:

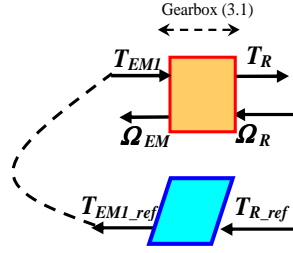


Fig. III. 3 – EMR and Inv.-based Control of the Gearbox

**Inversion of Distribution Elements** – As shown in the EMR of both vehicles, there are three mechanical and one electrical couplings (overlapped parallelograms). The electric coupling which represents the energy distribution from the battery to the electric drives, is not inverted because of no tuning path. The first mechanical coupling element (from right to left) is not inverted because it couples the resistive environmental forces and braking force. The environmental force  $F_{env}$  cannot be measured and is difficult to be estimated but its effect is counted in the velocity controller (see next section “Speed Controller”). The inversion of the second coupling element (from left to right) is just a change of the variable to a vectorial form. In this, the reference speed of ICE ( $\Omega_{ICE\_ref}$ ) is given directly from the strategy. The inversion of the last coupling element (from left to right) is done through inversion of the values of  $T_A$  and  $T_B$  from equation (App.10) (see Appendix C) and shown in equation (3.5) and Fig. III.4.

$$\begin{cases} T_{R\_ref} = \frac{k_{SS} - k_{LS}}{1 - k_{LS}} T_{A\_ref} - \frac{k_{LS}}{1 - k_{LS}} T_{B\_ref} \\ T_{LS\_ref} = \frac{1 - k_{SS}}{1 - k_{LS}} T_{A\_ref} + \frac{1}{1 - k_{LS}} T_{B\_ref} \end{cases} \quad (3.5)$$

where  $T_{R\_ref}$  and  $T_{LS\_ref}$  represents the reference torques of gearboxes attached to electric machines i.e. EM1 and EM2 respectively.

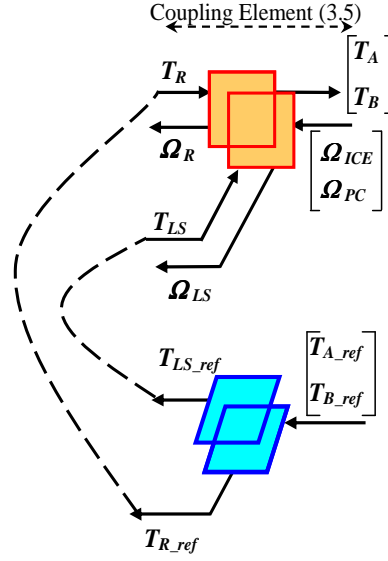


Fig. III. 4 – EMR and Inv.-based Control of Distribution Element

**Speed Controllers** – The subsystem shafts are the vectorial accumulation elements in considered HEVs. To define the reference vector torques from the reference vector speeds and the measured speeds, controllers are required. Therefore, for the inversion-based control of considered HEVs, the accumulation element (rectangle with an oblique bar) is inverted into speed controller (blue parallelogram with an oblique bar) in Fig. III.5. Furthermore, this controller defines the torque vector references  $[T_{A\_ref}, T_{B\_ref}]$  from the speed vector reference  $[\Omega_{ICE\_ref}, \Omega_{PC\_ref}]$ . Furthermore, this controller will also reject the cross effects. The torques  $[T_{C\_ref}, T_{D\_ref}]$  is represented by a dotted line which reflects the compensation or measurement of resistant torques. This element contains the following equation:

$$\begin{bmatrix} T_{A\_ref} \\ T_{B\_ref} \end{bmatrix} = [J] \begin{bmatrix} C_{s1}(t)(\Omega_{ICE\_ref} - \Omega_{ICE\_mea}) \\ C_{s2}(t)(\Omega_{PC\_ref} - \Omega_{PC\_mea}) \end{bmatrix} + [f] \begin{bmatrix} T_{C\_mea} \\ T_{D\_mea} \end{bmatrix} \quad (3.6)$$

The speeds,  $\Omega_{ICE\_mea}$  and  $\Omega_{PC\_mea}$  represent the speed measurements of the ICE and the transmission shaft connected to the planet-carrier of the PSD. The  $C_{s1}(t)$  and  $C_{s2}(t)$  represent the controllers which can be of type PI, IP or other kinds. For the PSD, the output of the vectorial controller  $[T_{A\_ref}, T_{B\_ref}]$  strictly depends on the two reference speeds i.e.  $[\Omega_{ICE\_ref}, \Omega_{PC\_ref}]$ .

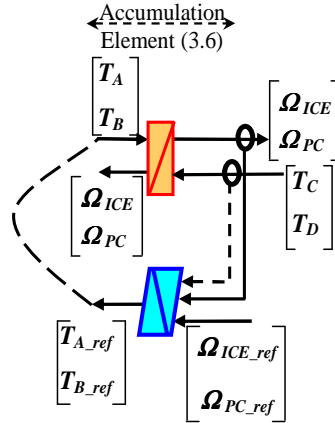


Fig. III. 5 – EMR and Inv.-based Control of Accumulation Element

### III.2.2 Inversion-based Control of Military Truck

The inversion-based control for the military truck is determined by following the EMR inversion philosophy (Fig. III.6). The difference between both vehicles i.e. garbage and military trucks, is the additional clutch assembly in the military truck. The modeling and EMR of this subsystem (clutch assembly) is detailed in section II.2.3 with the determination of the selector switches. The purpose of the selector switches is to ensure the physical energy flow and help the activation of engagement and disengagement of the clutch. For the inversion, when the clutches are engaged and energy is flowing to the system, the EMR of the system can be inverted as shown in Fig. III.6. But when the clutch is in disengaged position, or in other words without energy flow, then the system cannot be inverted. Therefore, in Fig. III.6, only the locked or engaged part of the clutch is inverted and shown.

In Fig. III.6, all control blocks illustrated by blue parallelograms handle only information. Since the accumulation elements (rectangle with an oblique bar) indicate a time-dependence relationship, they cannot be inverted physically. Therefore, a controller is necessary for their inversion. This relationship is determined in (3.6). This is due to the fact that when the clutch is engaged then the modeling and EMR is similar. When disengaged or opened, then chassis of the vehicle shifts to the second accumulation element. This disengagement will lead to no flow of energy within the system. This is the second reason in which the disengaged part of the EMR is not inverted.

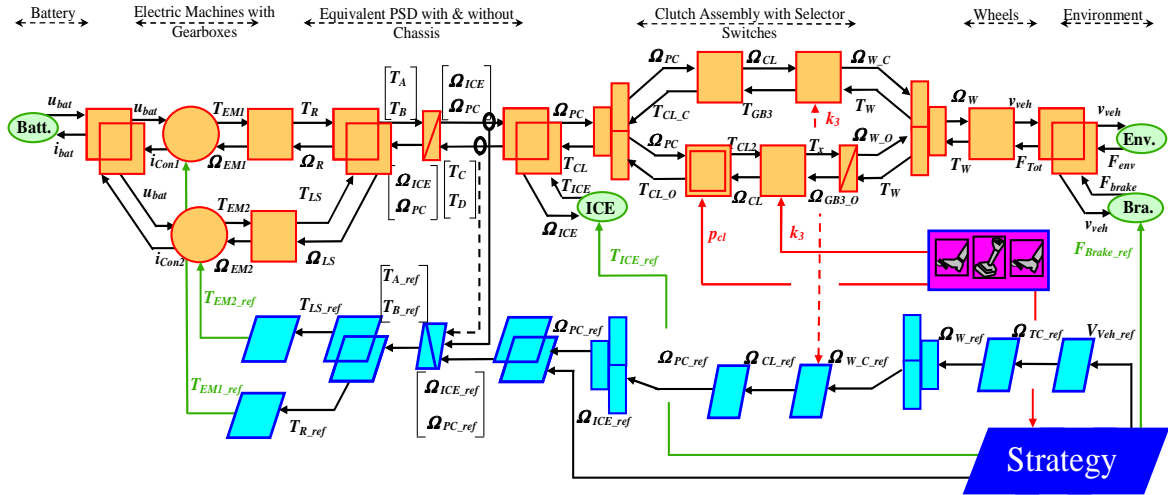


Fig. III. 6 – EMR and Inversion-based Control for Military Truck

The gearboxes and wheels are the conversion elements (square) and are directly inverted through relationships (3.1, 3.2, 3.3 and 3.4). Following maximum control, operations and measurements are obtained under the assumption that all variables can be measured. This leads to a Maximum Control Structure of the studied vehicle and a mirror of EMR is achieved. The control scheme deals with the local energy management as well as simultaneously taking into account the EMS of the system.

### III.2.3 Inversion-based Control of Garbage Truck

The inversion-based control for the garbage truck is established based on the same inversion rules discussed in previous sections (III.1, III.2.1). This inversion (shown in Fig. III.7) is deduced systematically from the EMR of garbage truck.

Similar to the inversion-based control of military trucks, all control blocks are illustrated by blue parallelograms and have a single controller with the same relationship determined in (3.6) but not the same gains or parameter values. Furthermore, as in the military truck, the gearboxes and wheels are the conversion elements and are directly inverted through relationships (3.1, 3.2, 3.3 and 3.4). In conclusion, in a process similar to that of the military truck, a Maximum Control Structure of the studied HEV is achieved which ensures that all variables are calculable. Also, it be concluded that there is only one EMR and Maximum Control Structure for both the

garbage truck and military vehicle (when the clutch is locked only). When the clutch opens (in a military vehicle) then the difference between both the representation and local control structure becomes lucid. This generalization helps in the validation of the control schemes and also in the building of a global energy management strategy.

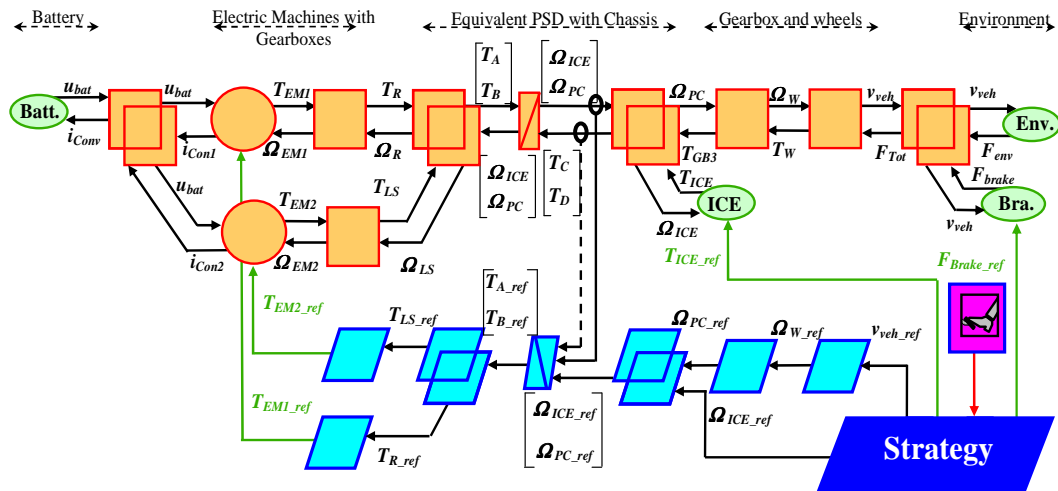


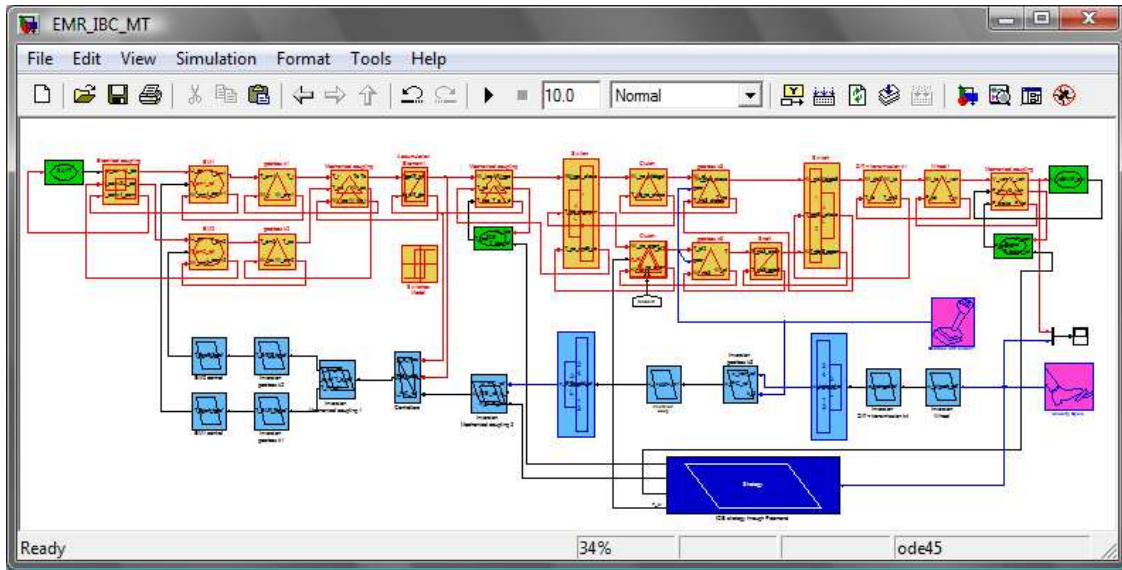
Fig. III. 7 – EMR and inversion-based Control for Garbage Truck

### III.3 Validation of Control Scheme

In this section, the previously discussed EMR and the control scheme of considered HEVs will be validated by simulation. Therefore, for establishing the EMR with its inversion-based control, the simulation software MATLAB-Simulink® is utilized. In the following sections, this validation and simulation result will be discussed.

#### III.3.1 Simulation Validation

The simulation programs have been integrated into MATLAB-Simulink® by using EMR and its inversion-based control for both studied HEVs. Fig. III.8 represents the implementation of EMR and its inversion-based control of military truck and Fig. III.9 represents the implementation of garbage truck. The EMR library in MATLAB-Simulink® has been used [EMR 2012].



**Fig. III. 8 – Simulation Validation in MATLAB-Simulink® for Military Truck**

In both figures (Fig. III.8 and Fig. III.9), the simulation is composed of two parts: the EMR based model, and the inversion-based control. The two parts can run separately and independently. The same model program can be used for the modeling of both HEVs by simply setting different values for certain parameters. Similarly, the same control part can be used to control HEVs using different parameter values. For an example, if the design values of the parameters such as gear ratios, vehicle mass, etc. are changed then the simulation is able to adapt. Therefore, it is possible to use the same program even if different design parameters are set for the same architecture of the HEV. However, to achieve this, the design parameters should be accurate in such a way to get fine results.

In general, the changing of the gear ratio with reference to the vehicle speed is already known through different standardized cycles such as New European Drive Cycle (NEDC), etc. For this, the key challenge is to fulfill the request of a driver through changing these two variables. Therefore, the clutch model's activation position (i.e. Locked or Open) would be the key factor. In chapter II (see section II.2.3), a detailed discussion regarding this activation was addressed for military vehicles through selector switches. For simulation, an observer is defined in such a way that estimates the position of the clutch ( $p_{cl}$ ) through speed and gear change by the driver. This observer in simulation is equivalent to a driver with the clutch pedal in terms of

changing the gear ratio. However, in reality, the driver changes the gear ratios according to his/her comfort i.e slow drive, cruising, etc. To avoid this complexity, a simple cycle of the clutch is taken into consideration as shown in Fig. III.10 below.

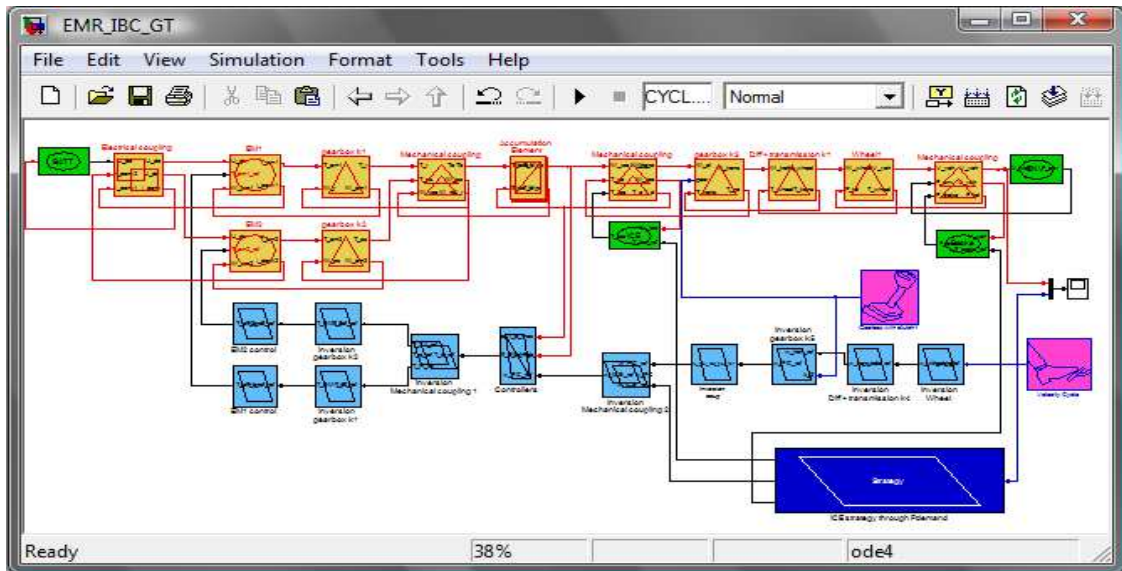


Fig. III. 9 – Simulation Validation in MATLAB-Simulink® for Garbage Truck

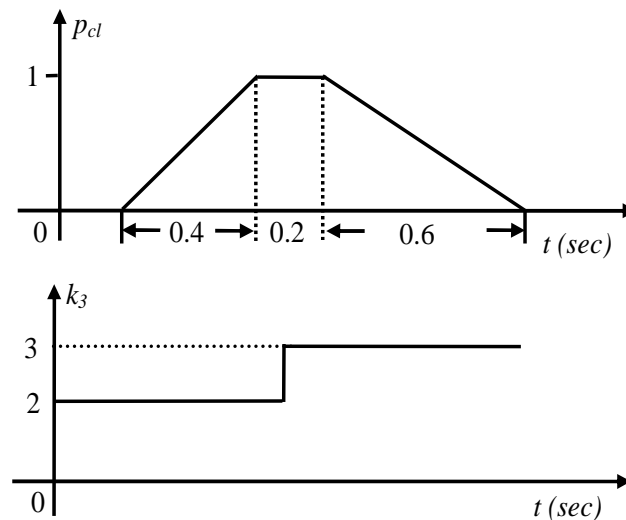


Fig. III. 10 – Clutch Opening and Locking with Gear Change



As illustrated in Fig. III.10, when the clutch completely opens, the clutch position ( $p_{cl}$ ) will be 1 but if it is closed then it would be zero. The entire gear change with the clutch opening and closing lasts for 1.2 seconds with a linear relationship of 0.4 seconds closing to opening, 0.2 seconds for engagement and 0.6 seconds for complete opening to closing. This positioning is defined at a strategy level [Lhomme 2007] which is described in more detail in the following sections (see section III.3.2).

In the validation of EMR and its inversion-based control in simulation program, EMR adheres to its principles, both at the subsystem and whole system levels. Because EMR is a graphical representation, the simulation program using EMR can also be implemented into MATLAB- Simulink®, or other software environments such as SimLab [Berenbrink 2002], AMESim [Bhide 2011], LabView [Gan 2007], VisSim [Panwai 2005], etc. Furthermore, the control schemes deduced from EMR can be implemented into structural modeling software such as Modelica [Fritzson 2004], SimDriveline® [Kapila 2007], PSim [Delarue 2010], Powertrain System Analysis Toolkit (PSAT) [ANL 2012], etc. In the next sections, the simulation results will be described after validating the EMR and its inversion-based control with an initial basic strategy.

### III.3.2 Simulation Results for Military Truck

Before realizing the simulation result, a simple strategy is made to ensure the references for the EMR and inversion-based control. As shown in Fig. III.11 for the military truck, there are five required input reference variables:  $T_{ICE\_ref}$ ,  $\Omega_{ICE\_ref}$ ,  $F_{Brake\_ref}$ ,  $p_{cl}$ ,  $k_3$  and  $v_{veh}$ . The reference torque and speed of ICE ( $T_{ICE\_ref}$  and  $\Omega_{ICE\_ref}$ ) is directly taken from the ICE's static map of its good consumption area while the reference brake force ( $F_{Brake\_ref}$ ) is given directly through strategy. Furthermore, in reality this brake force is given directly by the driver. The positioning of the clutch ( $p_{cl}$ ) will be adjusted through the observer by the strategy with the gear change.

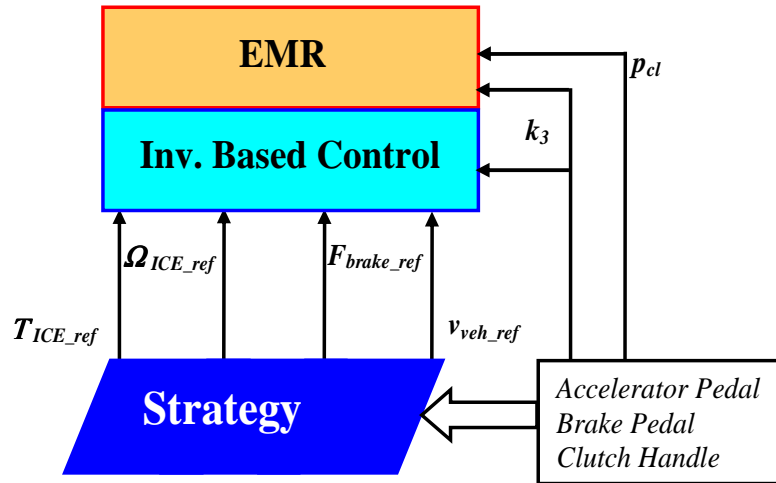


Fig. III. 11 – Strategy building of Military Truck

In reality, the strategy should fulfill the driver's demand for traction power while sustaining the battery's State Of Charge (SOC), optimizing the drivetrain efficiency and reducing fuel consumption and emissions [Salmasi 2007] [Kessels 2008]. Initially, for defining the reference variables at the strategy level, a simple rule-based strategy is considered on the basis of the ICE turning ON and OFF. The implemented strategy is based on the following assumptions:

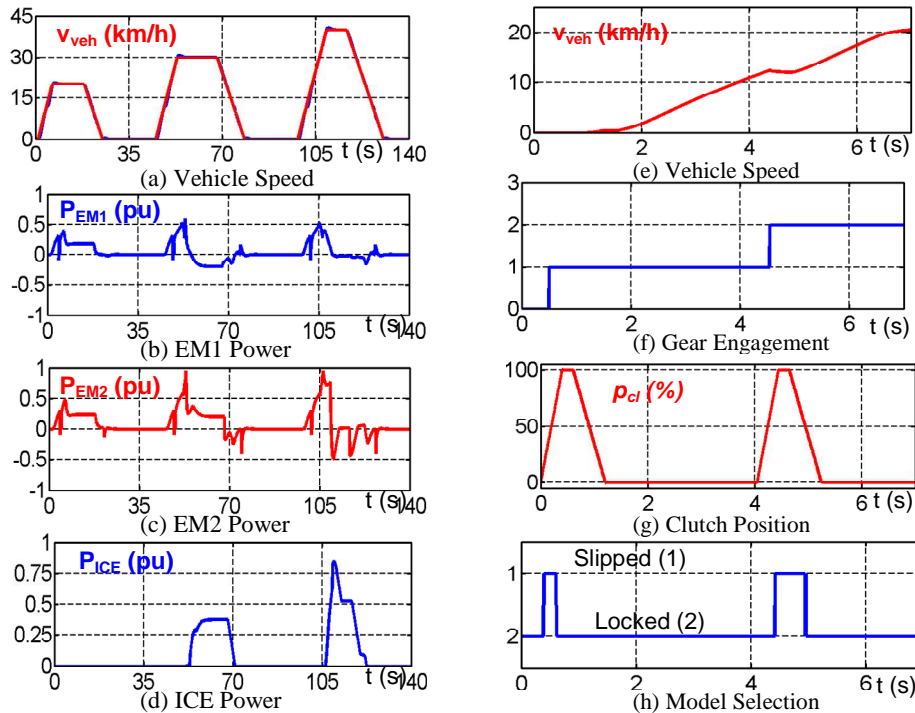
1. The SOC level is constantly maintained between the preset upper and lower limit levels (50%-70%).
2. The ICE will be turned OFF if the SOC level is high and the requested traction power from driver is low. In this case, the batteries will provide the requested power through one EM or both.
3. The ICE will be turned ON if the SOC level is lower than its minimum allowable value. In this case, the ICE will charge the batteries through the EM1, EM2 or both. However, one condition for the ICE in this situation is that it should run in its optimal efficiency zone.
4. The ICE will be ON and provide full traction power if the requested power is beyond the maximum output capacity of batteries.
5. The ICE will always be ON if the driver demand is to cruise the vehicle at high speed.

After the implementation of the basic strategy, the simulation results are shown in Fig. III.12, where Fig. III.12 (a) to III.12 (d) corresponds to the

full urban Standard On-Road Test (SORT) driving cycle [UITP 2001]. The reason the SORT driving cycle is used is because it is a widely used cycle that reflect the speed of heavy-duty class vehicles. The result shown in Fig. III.12 (a) verifies that the simulated speed is the same as the reference speed. The other characteristic curves of electric machines (EM1 and EM2) and ICE are shown in Fig. III.12 (b), III.12 (c) and III.12 (d). Due to the confidentiality of data the results are shown (in Fig. III. 12) in per unit (pu) system. The details for these curves are as follows:

- In this simulation, it is considered that the starting of the vehicle should be solely electric. Therefore, only battery power will accelerate the vehicle through EM1 and EM2, which is verified (see Fig. III.12 (b) and III.12 (c) between the times 0 to 18 seconds).
- Afterwards, when the vehicle speed is constant then the ICE will run alone ( $P_{EM1} = -P_{EM2}$  and  $P_{bat}=0$ ) and directly supply the power through the transmission to the wheels (see Fig. III.12 (d) between the times 53 to 71 seconds).
- For the hybrid traction, when the vehicle accelerates the ICE should then help the vehicle to run. In this case, the EM1 and EM2 will also help to accelerate the vehicle. Therefore, the ICE power and the EM power should both be positive. This is verified in the results shown between the time 106 to 122 seconds (see Fig. III.12 (b), III.12 (c) and III.12 (d)) which shows the traction power is drawn from both the Fuel tank and the batteries.

In this simulation, the clutch characteristics are very important therefore the first seven seconds of the same simulation (which is discussed previously) are taken into account as shown from Fig. III.12 (e) to III.12(h).



**Fig. III. 12 – Simulation Results for Military Truck**

In Fig. III.12 (e), the vehicle speed corresponds to part of the SORT driving cycle. The result verifies that when the gear is engaged or disengaged then the clutch state i.e. slipped (Model 1) or locked (Model 2) will shift accordingly (see Fig. III.12 (h)). Moreover, when the gear shifts, the clutch will be opened and the position of the clutch will be released. This process is shown in Fig. III.12 (g) with the percentage of clutch position ( $p_{cl}$ ) ranging from 0 (close) to 100% (open). The values in-between 0 to 100 correspond to this clutch slipping phenomena.

In conclusion, the simulation results prove that EMR and its inversion-based control are working and interacting with each other properly within MATLAB-Simulink® environment.

### III.3.3 Simulation Results for Garbage Truck

Like the military truck, simulation for garbage truck is carried out on Matlab-Simulink® and the results are taken (Fig. III.14) by imposing the reference torque and speed of the ICE. In this, a similar simple strategy shown in Fig. III.13 is imposed for defining the reference variables through ICE turning ON and OFF. For garbage truck, there are four input reference

variables required:  $T_{ICE\_ref}$ ,  $\Omega_{ICE\_ref}$ ,  $F_{Brake\_ref}$ , and  $v_{veh}$ . as shown in Fig. III.13. Similar to the strategy building in the military truck, the reference torque and speed of ICE ( $T_{ICE\_ref}$  and  $\Omega_{ICE\_ref}$ ) is directly taken from the ICE's static map while the reference brake force ( $F_{Brake\_ref}$ ) is calculated through decrement in traction power with the help of already known reference vehicle speed ( $v_{veh}$ ). For the reference vehicle speed, a real time driving cycle named ARTEMIS (Assessment and Reliability of Transport Emission Models and Inventory Systems) [Peter 2001] is chosen for only first 250 seconds of liaison trip. For this driving cycle, the data was recorded in 1990 over the course of one week in Grenoble (France), when a Renault IV GR191 was instrumented and monitored in normal operation for waste collection truck.

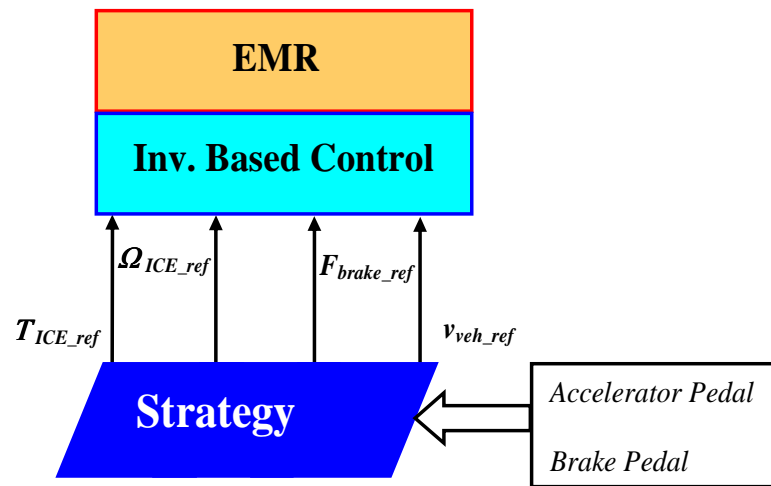
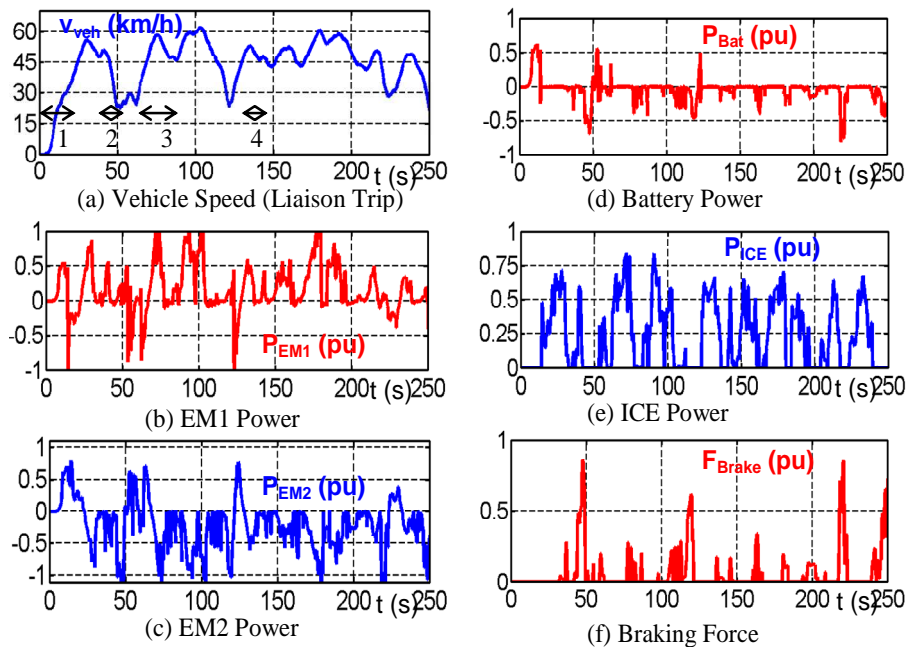


Fig. III. 13 – Strategy building of Garbage Truck

The simulation results shown in Fig. III.14 (a) verifies that the simulated speed is the same as the reference speed. The power of the electric machines' (EM1 and EM2), battery draws off and the ICE in kW are shown in Fig. III.14 (b), III.14 (c), III.14 (d) and III.14 (e). The braking force in kN is shown in Fig. III.14 (f).



**Fig. III. 14 – Simulation Results for Garbage Truck using ARTEMIS**

It is clear from the simulation result (Fig. III.14) that for different operating conditions, the vehicle will function under different modes of operation. The detailed analysis of the simulation results are summarized below:

1. From 0 to 10 seconds – The vehicle starts and the ICE is not running. The EM1 and EM2 power is positive (see Fig. III.14 (b) and III.14 (c)). The powers of both EMs decline after a certain time (see Fig. III.14 (d)) due to a decrease in the power of the batteries. Therefore, during this time, only the battery is working to accelerate the vehicle.
2. From 40 to 50 seconds – The vehicle decelerates and the ICE is not operating. The battery is recharged due to regenerative braking where the EM2 and EM1 act as a generator to give power back to the battery (see Fig. III.14 (f)).
3. From 58 to 73 seconds – Here, the ICE will run alone ( $P_{EM1} = P_{EM2} = 0$  and  $P_{bat} = 0$ ) and directly supply the power through the transmission to the wheels. This is because, at the strategy level, it was defined that at high speeds only ICE will be ON (see Fig. III.14 (b), III.14 (c) and III.14 (d)).

4. From 140 to 146 seconds – Here, the ICE and both EMs (1& 2) provide the traction power to propel the vehicle. In this case, the traction power is drawn from both the fuel tank and the batteries. Therefore the ICE and the EM power are positive (see Fig. III.14 (e), III.14 (b) and III.14 (c)).

## Conclusion

In this chapter, (Chapter III) a detailed description of local control or local energy management through EMR for two considered HEVs i.e. military and garbage truck was completed. This control schemes were deduced through the inversion principles of EMR. Furthermore, these control schemes illustrate the differences and common features related to both HEVs. In both control schemes, a simple rule-based global control or EMS level is defined in such a way to validate the local control in simulation environment of MATLAB-Simulink®.

The first section of this chapter presented the definition of different control structures i.e. local and global with the description of EMR inversion rules. Later, in same section the tuning and control paths for both studied HEVs were defined in order to build the local control scheme for both HEVs.

The second and third sections dealt with the inversion-based control determination for studied HEVs and validation of inverted control scheme in software MATLAB-Simulink®. Furthermore, in the second section, a detailed description of inversion was given for each subsystem and the complete studied HEVs. In the third section, some initial simulation results were shown to validate the local control scheme of studied HEVs. For this validation, a simple strategy was described to find the interaction of each subsystem with each other and as a whole.

In conclusion, this chapter detailed inversion-based local control or local energy management of military and garbage trucks through EMR inversion principles. These local control schemes are a milestone and provide an ease in building a detailed EMS for both HEVs. Therefore, in next chapter (Chapter IV), a thorough EMS is detailed which ensures the energy distribution, consumption and other critical factors in both the military and garbage trucks.



# **Chapter IV**

## **Energy Management Strategy**



## Introduction

The objective of this chapter is to explain global energy management methodologies and propose a new organization for global Energy Management Strategy (EMS) for the studied HEVs i.e. military and garbage trucks. The EMS in vehicles, specifically HEVs, is an important and key issue because it can significantly influence the performance of the overall vehicle. Improving EMS in vehicles can also deliver important benefits such as reduced fuel consumption, decreased emission, lower running cost, reduced noise pollution, and improved driving performance and ease of use. Furthermore, intelligent EMS methods can observe and learn driver behavior, environmental and vehicle conditions, and intelligently control the operation of HEVs.

In this chapter, a new multi-level organization of EMS is proposed and executed for complex systems such as the studied HEVs. The key issue for any EMS is its implementation and this chapter will detail a strategy on how to determine multi-level EMS as well as apply it. Therefore, the objective of this chapter is to detail the organization of a multi-level EMS and validate its possible usage.

The first section encompasses a general discussion on EMS and its classification along with an explanation of key basic concepts needed. In the second section, on the basis of these basic concepts, a multi-level energy management is proposed and realized with the help of State Transition Diagrams (STDs) [Horstmann 2005] [Booch 2009]. Later, in the third and final section, this proposed multi-level energy management is implemented in Stateflow [Mathworks 2011-a] of Matlab-Simulink® environment for both studied HEVs. In the subsections, the simulation results are shown with SORT [UITP 2001] and ARTEMIS [Peter 2001] driving cycles for the military truck and garbage truck respectively.

## IV.1 Energy Management Analysis

### IV.1.1 Overview

Energy management in hybrid vehicles entails deciding the correct amount of power delivered each moment by the available energy sources in a vehicle. Energy management is in stark contrast to the lower-level (subsystem or local) control, which is used to drive single components so that they behave according to the wishes of the driver via the supervisory controller. In Chapter III, local control structures for studied HEVs in application to military and garbage truck was detailed. Building on that idea, in this chapter, a global Energy Management Strategy (EMS) will be described in general and with specific reference to the studied HEVs. The terms EMS and supervisory controller are in fact the same thing. The supervisory controller or EMS is actually a layer above local control and is used to split the power demand between the subsystems. Furthermore, the EMS decides when such power split can or should be applied in normal or sometimes critical situations during different driving conditions.

In Fig. IV.1, a series-parallel HEV layout of considered studied HEVs with an energy management controller is shown. The possible inputs to the energy management controller can be the driver's power demand, vehicle speed or acceleration, batteries SOC level, present road load or even, in certain cases, information predicting traffic conditions from the Global Positioning System (GPS), etc. There are also other limitations of the overall system and its subsystems e.g. for an EM or Electric Drive (ED) the limitations are current, temperatures, etc. In Fig.IV.1 (for EM1, EM2, ICE, etc.), all of the dotted lines going back to EMS represent the information of the component. Through manipulating this recent information of the subsystem, EMS will provide the references, shown by the dark black line. Furthermore, the outputs of EMS are decisions which include turning the drivetrain components on and off and transitioning their operating points by commanding subsystem controllers to achieve best overall performance and system efficiency.

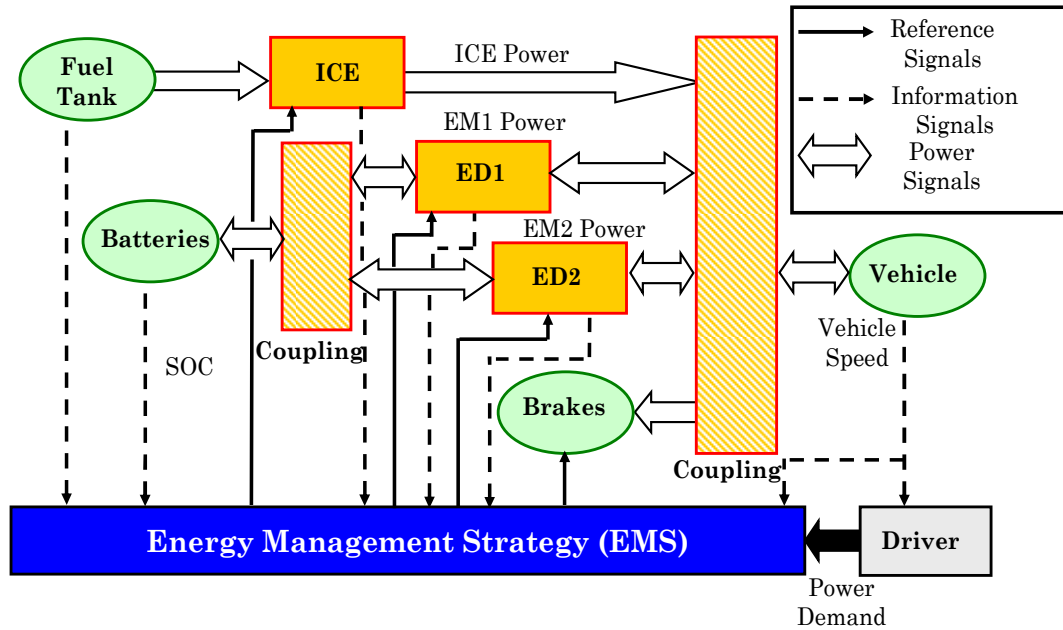


Fig. IV.1 – Energy Management Layout

When comparing a conventional vehicle with ICE to an HEV, the conventional vehicle has no need for an EMS. This is because the driver decides the instant speed and the power delivery using the brake and accelerator pedals. Also, in manual transmission vehicles, the driver can decide which gear is engaged at a certain time. The driver's desires are translated into action by local controllers. For example, the Electronic Control Unit (ECU) determines the amount of fuel to be injected given the accelerator input and the automatic transmission controller decides when to shift gear based on engine conditions and vehicle speed, etc. [Serrao 2009]. Contrarily, in HEVs, there is an additional choice that must be taken. This decision is how much power is sent by each of the available energy sources on the vehicle. This leaves the driver to decide only on how much total power is needed. This is the reason why all HEVs contain an energy management controller, which can be seen as an additional tier between the driver and the component controllers. The choice on what is indeed optimal depends on the specific application. In practice, the strategies generally minimize fuel consumption, emissions and the maximize power delivery and performances.

### IV.1.2 Classification

Several different groups of energy management strategies have been put forward in literature; each with different characteristics and possible implementations. Energy management strategies can be classified by focusing on some of the important characteristics specific to HEVs. In [Salmasi 2007] and [Wirasingha 2011], they propose that there are two main categories—rule-based and optimization-based energy management strategies (see Fig. IV.2). These two categories are further divided based on their implementation. A precise overview of these strategies is detailed in the following.

1. Deterministic rule-based are based on heuristics and operate according to a set of pre-defined rules that have been implemented prior to actual operation. Furthermore, human experiences are used in the design of deterministic rules. These are generally implemented through mediums such as lookup tables, flow charts or control parameter tables. This strategy consists of types such as state machines, [Phillips 2000] power follower, and thermostat.
2. Fuzzy rule-based are also heuristic based and ideal for nonlinear time-varying systems. In addition, these strategies are very robust and are able to tolerate inexact measurements and component variations. It consists of conventional, adaptive [Johnson 2000] and predictive [Rajagopalan 2003] fuzzy-rule based methods.
3. Global optimization methods, take the complete optimization problem into consideration as a whole. The cost function is expressed using previous data and is minimized depending on future expectations and results. Many times, these are optimized offline and applied later. Furthermore, these methods are acausal and used for non-causal systems (because the system relies on future values). This strategy is comprised of such methods as Simulated Annealing [Delprat 1999] [Delprat 2004], Game Theory [Gielniak 2004], Linear Programming [Tate 1998], Optimal Control Theory [Delprat 2004], Dynamic and Stochastic programming [Lin 2003], and Genetic algorithms [Piccolo 2001].
4. Real-time optimization has the ability to optimize itself in real time using a simplified problem. Thus the solution for it is suboptimal optimization. Similar to global optimization, real-time optimization using a simplified problem attempts to improve a cost function that was based

on previous information [Kermani 2009]. Therefore, these can be termed as causal and used for casual systems. They consist of Equivalent Fuel Consumption [Paganelli 2001], [Sciarretta 2004] [Kessels 2007], Dynamic Control [Pisu 2005], Robust Control Approach [Pisu 2003], Optimal Predictive Control [Salman 2005].

The above discussion is summarized in Fig.IV.2. All of the remaining strategies are subcategories of these two main categories. In this research work, only deterministic rule based-power follower control strategy is utilized because it is an interesting approach for first development of the new organization of multi-level EMS. In the following, a detailed overview is explained about the rule-based strategies.

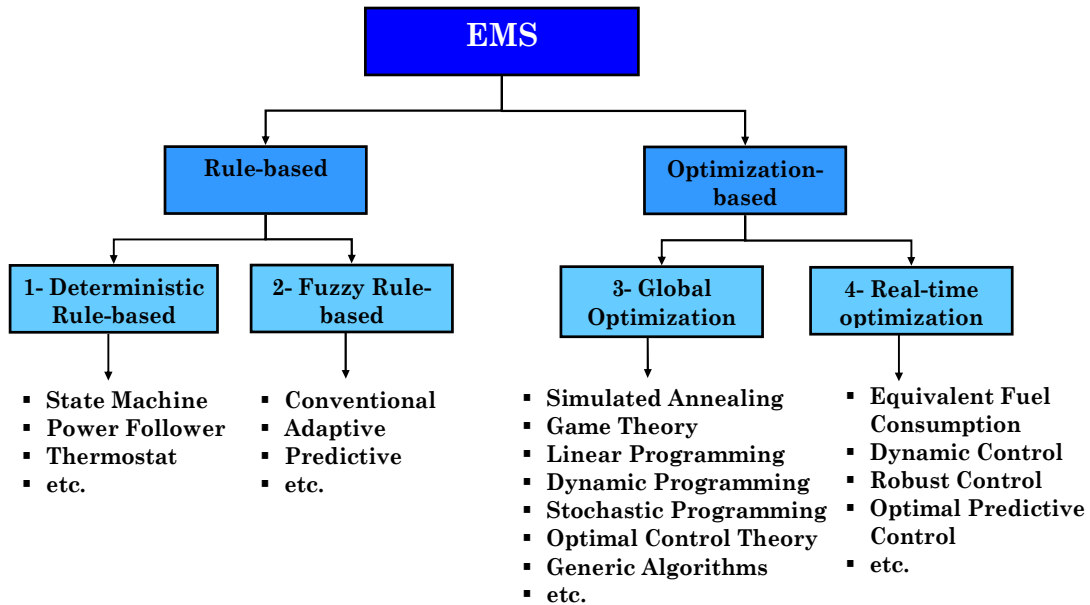


Fig. IV. 2 – Energy Management methods

**Rule-based Energy Management** – Rule-based energy management strategies are the most commonly utilized way to apply a supervisory control in HEVs [Schouten 2002] [Lin 2003] [Hofman 2007] [Salmasi 2007]. It is common use in HEVs is due to its simplicity in implementation. In its implementation, a set of rules is introduced which presents some observed values with meaningful parameters that later decide the power split between the different energy sources. Furthermore, like other strategies, this kind of

strategy does not rely on formal ordinary differential equations models and a formal description of the problem. Instead, the rules are based on engineering intuition. The deterministic way typically has main three approaches for its implementation. But, in this research work, a new way is explained to impose all of the State Machine approaches (see IV.2 and IV.3).

All rule-based strategies have instant conditions that make it easier to take into account local constraints such as limitations on power, torque, speed etc of the different energy sources. On the other hand, this makes it impossible to guarantee the optimality of the solution and the respect of the integral constraints such as charge sustainability. Therefore, the rules of these strategies can only force a given integral measure (like SOC) to remain between the bands i.e. upper and lower. Furthermore, parameters such as threshold values decide when to switch from one mode to another, which is usually obtained through calibration. To obtain better control results, dynamic programming can be used to benchmark, to test the effectiveness of the strategy [Sciarretta 2004] [Pissu 2007] or as a guideline in fixing the control rules [Lin 2003], [Hofman 2007] [Trigui 2011].

In conclusion, deterministic rule-based strategy is advantageous to implement because of its conceptual straightforwardness and its ease of implementation on complex HEVs. The main disadvantages of this approach are lack of optimality and that there is no regular procedure for synthesizing the rules. Also, the fact that there are many thresholds and parameters makes it hard to find an appropriate calibration that can function for a wide scope of driving conditions. Nevertheless, rule-based strategies are still commonly used and possibly used with other algorithms based on optimal control. For example, it is feasible to apply an effective equivalent consumption minimization strategy to only in one part of a vehicle operating range and use the rule-based strategy for the remaining conditions [Hofman 2007].

### **IV.1.3 Basic Concepts of Energy Management**

Most HEVs contain two or more onboard energy sources such as electrical, mechanical, etc. This integration of different energy sources or components makes the system complex. For the energy management of these HEVs, specifically those with a Power Split Device (PSD), the constraints and limitations of the vehicles and PSDs become important and should be taken



into account. These constraints and limitations define the local control on the basis of the operating modes and power flows of the vehicle. Furthermore, to corral these issues a multi-level energy management strategy is needed to control all of the operating modes and flows of power between the different sources and components of the system. The operating modes and power flows are critical factors because they are highly interconnected. Previously, in [Eshani 2005], [Shumei 2006], [Kessels 2008], [Rahman 2008] and [Wirasingha 2011] the operating modes and power flows for a control strategy are described. However, the definitions of these factors and a clear idea for the PSD were not explained. In this research work, these factors are determined and explained by proposing a new energy management for the considered HEV. The following concepts are defined for building the energy management for considered HEV.

**Functions** – *A function is a specific process, action or task that a system is able to perform.* In HEVs, the possible basic functions are propulsion, braking and charging. From these basic functions other two combined functions can also be found such as propulsion with charging and charging with braking.

**Operating Modes (OM)** – *The operating modes are the routes determined by the interaction of all possible functions and on-board energy sources in a system.* The operating modes strictly depend on the number of energy sources and considered functions.

**Power flows (PF)** – *The power flows are the paths utilized to achieve operating modes by taking into account the architecture of the system.* They strictly depend on the architecture of the system and are arranged under the concerning operating modes. The same operating mode can be achieved by several different power flows.

The above definitions or basic concepts for energy management will help to provide an ease in the understanding and building of a multi-level energy management for any kind of HEVs. In the next sections, on the basis of above basic concepts, a detailed analysis of a proposed energy management for considered studied HEVs are discussed. Furthermore, for developing this multi-level energy management, key concerns are also taken into consideration such as stability of the system, correctly interfacing with the local control structure, distribution criteria between regenerative and mechanical braking, etc.

## IV.2 Proposed Global Energy Management

In this section, a new multi-level management is proposed for the considered HEVs. Furthermore, it is explained how and through which critical factors multi-level energy management can be achieved.

### IV.2.1 Proposed Multi-level Energy Management

The systematic flow of the multi-level EMS on the basis of the above discussion (in section IV.1.3) is concluded in Fig. IV.3 below. The arrangement is done in such a way that the driver can demand a function that the system should perform like propulsion, braking, etc. These functions then interact with the energy sources to determine the operating modes. Afterwards, these operating modes find the specific path through which the power should be delivered by keeping the architecture of the system in account.

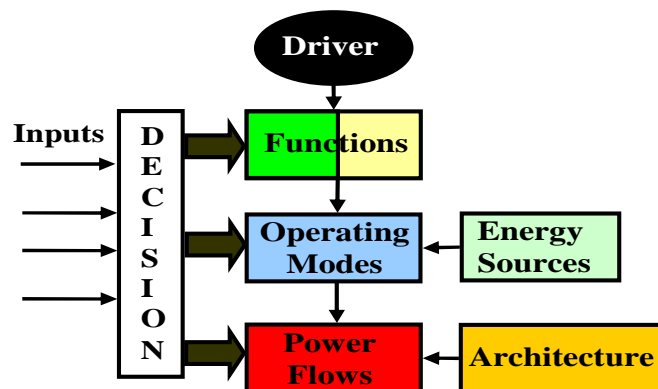


Fig. IV. 3 - Concepts for multi-level EMS

From Fig. IV.3, it is clear that for building a multi-level EMS it is essential to find the operating modes and power flows of the system in line with the driver's demand. Therefore, to begin, the operating modes of the vehicles are determined for the studied HEVs and discussed in the following sections. It is also noted that these operating modes are not only applicable to the studied HEVs but also for other kinds of HEVs. Later, the paths for power flows are determined according to specific operating modes and keeping in consideration the architecture of the studied HEVs.

### IV.2.1.1 Modes of Operation or Operating Modes (OM)

This section deals with the determination of the OMs in the considered HEV. As described previously (section IV.1.3), OMs are the routes determined by the interaction of all possible functions and on-board energy sources in a system. In other words, they can be determined by considering the relationship between the containing energy sources with the functions in the vehicle. Using that same principle, for the considered HEV, the operating modes are determined (Fig. IV.4). Furthermore, in this determination, plug-in and braking for the ICE are not taken into consideration. The four sources in the considered HEVs are the fuel tank (FT), batteries (BAT), vehicle chassis with wheels and drag forces of environment (VEH) and mechanical brakes (BRAKE).

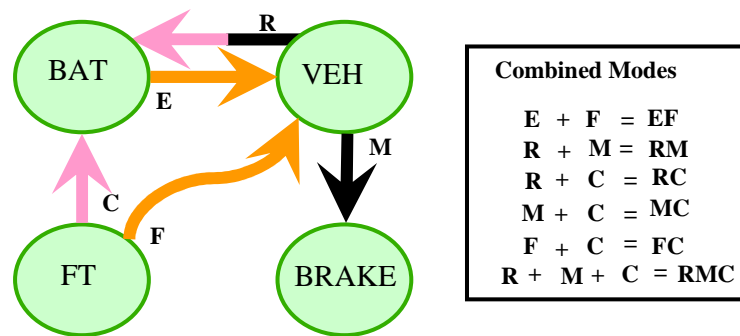


Fig. IV. 4 - Operating Modes

The Fig. IV.4 clearly shows all of the possibilities for the OMs in the considered HEV. In addition, the operating modes are explained and arranged under their three basic functions i.e. propulsion, braking and charging as well as two combined functions i.e. propulsion-charging and braking-charging. Also, Fig. IV.4 shows that there are 5 OMs under basic functions and the remaining 6 are combinations of the 3 basic functions. In the above determination for OMs, the power supplied to the auxiliaries is not considered. This is because the auxiliary power is not significant when compared to the traction power. Also, in this study the dynamic relationship between the ICE and fuel tank is not taken into consideration and is considered as one unit. Therefore this complete assembly i.e. the FT with ICE is referred to as ICE in this study. The determined OMs are defined in the following:

### ***Operating Modes under Basic Functions***

1- *Electric Propulsion (E)* – In this mode of operation, only electrical energy is supplied for the propulsion. For this, batteries are used to supply the power for propulsion. There is no energy taken from the fuel tank.

2- *ICE Propulsion (F)* – The traction power is only supplied by fuel tank by burning of fuel in ICE. In this, batteries neither draw nor deliver power to the wheels.

3- *ICE Charging (C)* – In this OM, batteries are being charged only by the fuel tank. No traction power is supplied to the wheels by the batteries or fuel tank.

4- *Mechanical Braking (M)* – In this OM, the mechanical brakes are being utilized to decelerate the car without any charging of the batteries through the brake pedal.

5- *Electric and ICE propulsion (EF)* – This OM is also called hybrid traction and in this the traction power is drawn from both the energy sources i.e. batteries and fuel tank.

### ***Operating Modes under Combined Functions***

6- *Charging by Regenerative Braking (R)* – This OM is the combination of the basic functions of braking and charging. In this, the power is given to charge the batteries only by the braking of vehicle instead of using any energy from the fuel tank.

7- *Regenerative and Mechanical Braking (RM)* – In this, both brakes through the EM and brake decelerate the vehicle. But by consequence of regenerative braking, the batteries are being charged at the same time.

8- *Regenerative Braking and ICE Charging (RC)* – In this, both the fuel tank and the braking energy charge the batteries.

9- *Mechanical Braking and ICE Charging (MC)* – In this, the vehicle will decelerate with mechanical braking and at the same time the fuel tank will charge the batteries. From an energetic point of view, this mode has low interest but is still possible.

10- *ICE Propulsion and Charging (FC)* – In this OM, the fuel tank charges the batteries and also provides the traction power.

11- *Regenerative and Mechanical Braking with ICE Charging (RMC)* – This OM is the combination of the mode of operation discussed in 8 and 9. In this, the vehicle is being decelerated through both electric and mechanical

braking and as well as charging the batteries through fuel tank and regenerative energy during braking. This mode also is of low interest from an energetic point of view.

#### IV.2.1.2 Power Path Flows or Power Flows (PF)

This section details the description and determination of power flows for the considered HEVs. To reiterate, power flows are the paths utilized to achieve operating modes by taking into account the architecture of the system. From the above discussion (section IV.2.1.1), it is clear that there are 11 OMs, each of which can take any path to deliver and/or absorb energy from the sources. The path taken is dependent on the chosen mode of operation. It is possible to find the power flows directly, but then to understand the system or to arrange for the control strategy proves difficult. This difficulty arises because of the complexity of the system. Therefore, it is easier to arrange these power flows on the basis of the operating modes. The total number of power flows determined for HEVs in application to garbage and military trucks is 39. In the following, the power flows are discussed only for two operating mode under basic and combined functions i.e. electric propulsion (E) and regenerative braking (R) to demonstrate the differences between the OMs and PFs. The remaining power flows for the other operating modes are explained and shown in Appendix D and shown in Table IV.1.

*A) Power flows in Electric Propulsion OM* – This power flow is determined when only the electrical power of the batteries propels the vehicle through the PSD. The possible power flows during electric propulsion in the considered HEV are:

- a)  $BATT \longrightarrow EM1 \longrightarrow Vehicle$
- b)  $BATT \longrightarrow EM2 \longrightarrow Vehicle$
- c)  $BATT \longrightarrow EM1 \ \& \ EM2 \longrightarrow Vehicle$

In these power flows, the ICE is turned off and all power flows are taken from the batteries.

*B) Power flows in Charging by Regenerative Braking OM* – This and the previous path flow are the same just opposite in the direction of the operating mode. In the previous power flow, the operating mode of the chosen path was from batteries to wheels, but in this case, the chosen path is from

the wheels to batteries. Therefore, the possible power flows for this operating mode are:

- a)  $Vehicle \longrightarrow EM1 \longrightarrow BATT$
- b)  $Vehicle \longrightarrow EM2 \longrightarrow BATT$
- c)  $Vehicle \longrightarrow EM1 \ \& \ EM2 \longrightarrow BATT$

## IV.2.2 Proposed Energy Management Realization

In the previous section (IV.2.1), a detailed analysis was given describing critical factors such as functions, operating modes and power flows in multi-level energy management. Now, the main problem remaining is the realization and arrangement of the given factors. This arrangement is difficult because it consists of three distinct levels. Therefore, to resolve this issue, State Transition Diagrams (STD) are utilized. STDs are the graphical representation of a finite state machine and are used from the beginning in the object-oriented modeling [Olivé 2007] [Decon 2004] [Ao 2008].

In STDs, by definition, a state machine exists in exactly one state at any given time, and transitions to other states are done entirely on combinatorial logic that takes the states and inputs into account [Babers 2006]. In other words, it illustrates the flow of control using the states and transitions of a given system. The state of the system is the conditions in the life of an object that satisfies certain conditions and the transitions are the relationship between any 2 states [Magyar 2007].

Initially, in considered multi-level energy management, a flow diagram of the strategy is plotted to find the exact total number of states. For this, the energy-management is arranged into three levels i.e. Functions, Operating Modes and Power Flows (Fig. IV.5 and Table IV.1).

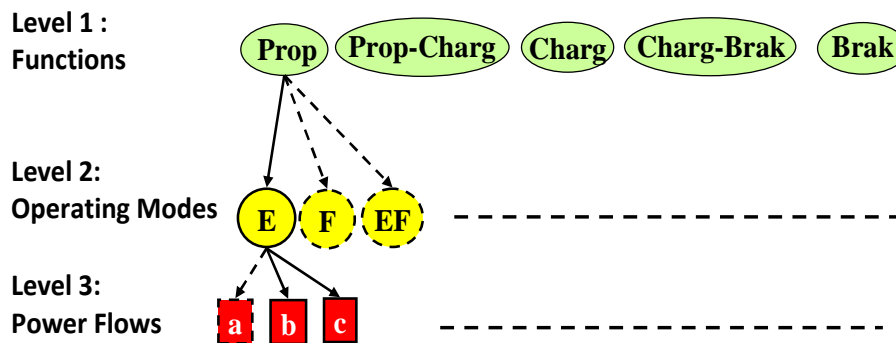


Fig. IV. 5 - Multi-Level Energy Management Arrangement

**Table IV.1 Arrangement of Functions, OMs and PFs**

Functions	Operating Modes	Power Flows
Prop	E	a) <i>Vehicle</i> → <i>EM1</i> → <i>BATT</i> b) <i>Vehicle</i> → <i>EM2</i> → <i>BATT</i> c) <i>Vehicle</i> → <i>EM1 &amp; EM2</i> → <i>BATT</i>
	F	a) <i>ICE</i> → <i>Vehicle</i> b) <i>ICE</i> → <i>Vehicle</i> ↓ <i>EM1</i> → <i>EM2</i> → <i>Vehicle</i> c) <i>ICE</i> → <i>Vehicle</i> ↓ <i>EM2</i> → <i>EM1</i> → <i>Vehicle</i>
	EF	a) <i>ICE</i> → <i>Vehicle</i> <i>BATT</i> → <i>EM1</i> → <i>Vehicle</i> b) <i>ICE</i> → <i>Vehicle</i> <i>BATT</i> → <i>EM2</i> → <i>Vehicle</i> c) <i>ICE</i> → <i>Vehicle</i> <i>BATT</i> → <i>EM1 &amp; EM2</i> → <i>Vehicle</i> d) <i>ICE</i> → <i>Vehicle</i> ↓ <i>EM1</i> → <i>BATT</i> → <i>EM2</i> → <i>Vehicle</i> e) <i>ICE</i> → <i>Vehicle</i> ↓ <i>EM2</i> → <i>BATT</i> → <i>EM1</i> → <i>Vehicle</i>
Charg	C	a) <i>ICE</i> → <i>EM1</i> → <i>BATT</i> b) <i>ICE</i> → <i>EM2</i> → <i>BATT</i> c) <i>ICE</i> → <i>EM1 &amp; EM2</i> → <i>BATT</i>
Brak	M	a) <i>Vehicle</i> → <i>Brake</i>
Prop-Charg	FC	a) <i>ICE</i> → <i>Vehicle</i> ↓ <i>EM1</i> → <i>BATT</i> b) <i>ICE</i> → <i>Vehicle</i> ↓ <i>EM2</i> → <i>BATT</i> c) <i>ICE</i> → <i>Vehicle</i> ↓ <i>EM1 &amp; EM2</i> → <i>BATT</i> d) <i>ICE</i> → <i>EM1</i> → <i>BATT</i> ↓ <i>EM2</i> → <i>Vehicle</i> e) <i>ICE</i> → <i>EM2</i> → <i>BATT</i> ↓ <i>EM1</i> → <i>Vehicle</i>

Brak-Charg	R	a) <i>Vehicle</i> → <i>EM1</i> → <i>BATT</i> b) <i>Vehicle</i> → <i>EM2</i> → <i>BATT</i> c) <i>Vehicle</i> → <i>EM1 &amp; EM2</i> → <i>BATT</i>
	RM	a) <i>Vehicle</i> → <i>EM1</i> → <i>BATT</i> ↳ <i>Brake</i> b) <i>Vehicle</i> → <i>EM2</i> → <i>BATT</i> ↳ <i>Brake</i> c) <i>Vehicle</i> → <i>EM1 &amp; EM2</i> → <i>BATT</i> ↳ <i>Brake</i>
	RC	a) <i>ICE</i> → <i>EM1</i> → <i>BATT</i> <i>Vehicle</i> → ↑ b) <i>ICE</i> → <i>EM2</i> → <i>BATT</i> <i>Vehicle</i> → ↑ c) <i>ICE</i> → <i>EM1 &amp; EM2</i> → <i>BATT</i> <i>Vehicle</i> → ↑ d) <i>ICE</i> → <i>EM1</i> → <i>BATT</i> <i>Vehicle</i> → <i>EM2</i> → ↑ e) <i>ICE</i> → <i>EM2</i> → <i>BATT</i> <i>Vehicle</i> → <i>EM1</i> → ↑
	MC	a) <i>ICE</i> → <i>EM1</i> → <i>BATT</i> <i>Vehicle</i> → <i>Brake</i> b) <i>ICE</i> → <i>EM2</i> → <i>BATT</i> <i>Vehicle</i> → <i>Brake</i> c) <i>ICE</i> → <i>EM1 &amp; EM2</i> → <i>BATT</i> <i>Vehicle</i> → <i>Brake</i>
	RMC	a) <i>ICE</i> → <i>EM1</i> → <i>BATT</i> <i>Vehicle</i> → ↑ → <i>Brake</i> b) <i>ICE</i> → <i>EM2</i> → <i>BATT</i> <i>Vehicle</i> → ↑ → <i>Brake</i> c) <i>ICE</i> → <i>EM1 &amp; EM2</i> → <i>BATT</i> <i>Vehicle</i> → ↑ → <i>Brake</i> d) <i>ICE</i> → <i>EM1</i> → <i>BATT</i> <i>Vehicle</i> → <i>Brake</i> ↳ <i>EM2</i> → <i>BATT</i> e) <i>ICE</i> → <i>EM2</i> → <i>BATT</i> <i>Vehicle</i> → <i>Brake</i> ↳ <i>EM1</i> → <i>BATT</i>



In the first level, propulsion, charging, braking, propulsion-charging and braking-charging functions are represented by Prop, Charg, Brak, Prop-Charg and Brak-Charg, respectively. In the next level of operating modes, e.g. under the Prop function, three connected OMs such as electric (E), ICE (F) and hybrid propulsion (EF) are arranged. In the last level of power flows, the three options are given to achieve the electric propulsion of the vehicle (see section IV.2.1.2). In the similar way for all other OMs and PFs are determined and arranged under their concerned function. In the following, the Table IV.1 represents all that arrangement of function, operating mode and power flow in a summarized way. Descriptions of each power flow are given in Appendix D.

Fig.IV.5 and Table IV.1 give the idea of the flow of the system within a hierarchical order. This figure and table give no information about the transitions with its conditions between any states. Therefore, it is necessary to build an STD of the studied multi-level EMS with the same hierarchical order shown in Fig. IV.5 for all of OMs and PFs. This is taken separately to avoid complexity and confusion between any two states. Furthermore, this will aid in easily locating the transitions and its conditions. For this reason, in the following section (IV.2.3) an example is elaborated on the base of the flow diagram shown in Fig. IV.5. The example illustrates the sequence from Driver to level 1 of propulsion later through passing electric propulsion (level 2) and its power flow at level 3.

### **IV.2.3 Organization of multi-level EMS**

In this section, a description is given on how to achieve multi-level energy management with the help of State Transition Diagrams (STDs). The basic details of the STD charts are given in Appendix E but this section details the methodology for developing EMS through these STD charts. The proposed EMS becomes intricate when there are existences of multi states in a same level and/or states within a state. To address this issue, the STD is first built from the driver until the function level. To realize EMS, in all of the STD charts there is a rule that each STD must have a start state in every chart and one stop in the main level i.e. function. The start state in each chart ensures the validation of that level and the stop ensures the turning off the strategy (shown in Fig. IV.6 for idling only).

For developing STDs, contact between the states or within a state, called a physical phenomenon, is also taken into consideration. As an example, after the driver starts the vehicle, he/she cannot demand the brake as the vehicle is already in a stationary position. Therefore, after the vehicle starts the driver can only choose to propel or do nothing in normal conditions. While including these physical possibilities, the proposed energy management will also decide what could be the best solution for fulfilling the driver's demand while keeping in consideration the other requirements of the vehicle such as SOC, different subsystems limitation, etc.

Below in Fig. IV.6, an STD is shown which demonstrates a vehicle being started then going directly to an idling state. It should be noted that during idling the vehicle is in rest position and this is considered a function of the vehicle. However, to simplify, idling is not considered as a function in Section IV.2.2 function levels. But for the final implementation of EMS, idling is taken into account as a function.

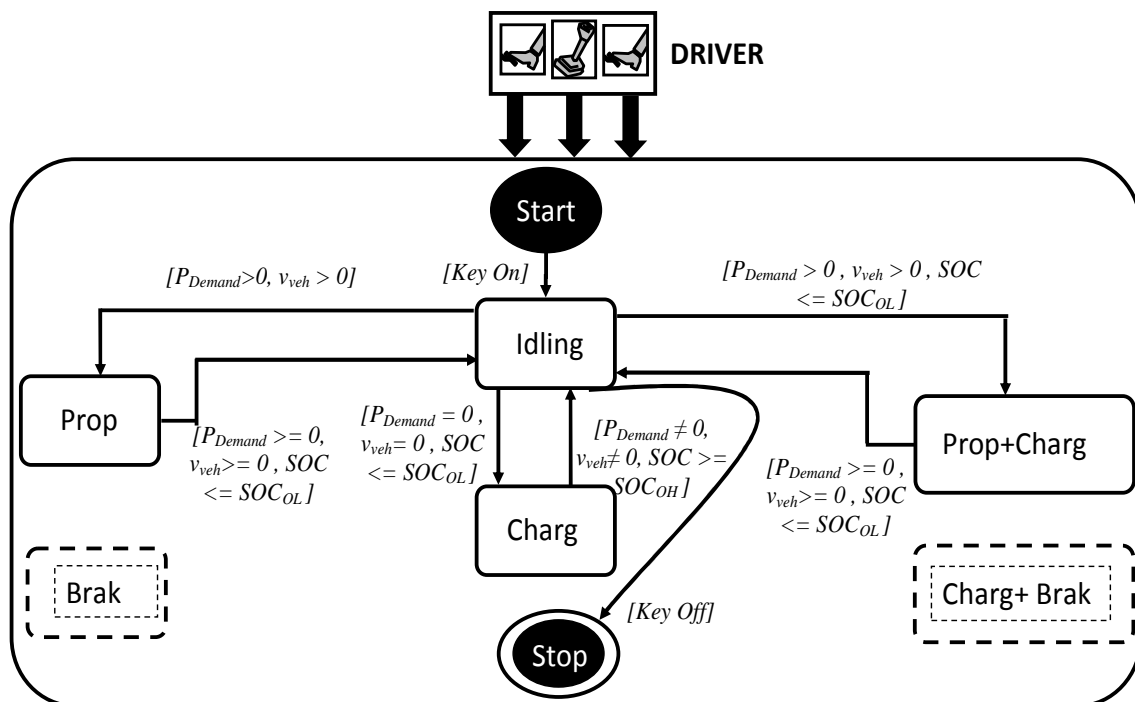


Fig. IV. 6 - State Transition Diagram – Level 1 (Idling Function)

Two factors i.e. the driver's demand and physical phenomenon help to determine the transition and its conditions easily. As an example, when the

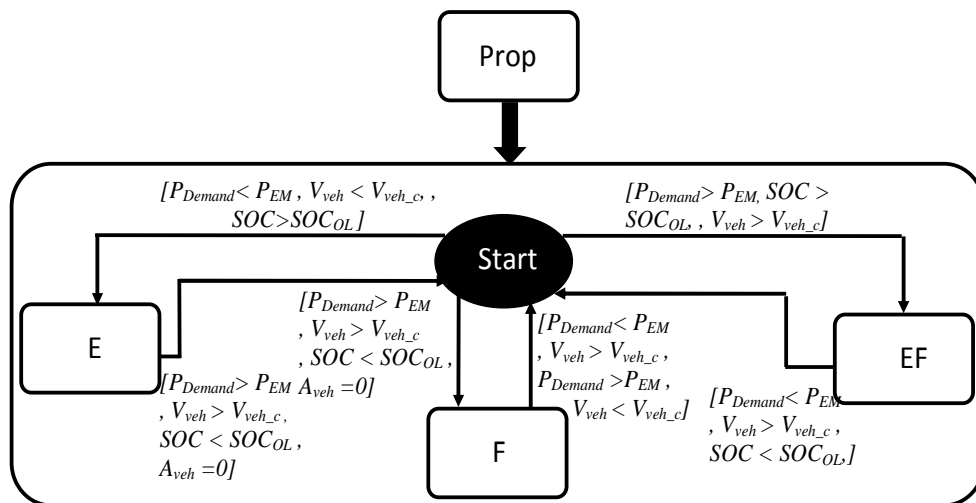
vehicle speed ( $v_{veh}$ ) exceeds 0 m/s then from the idling state it will pass to neighboring states such as Prop or Prop-Charg. But if the SOC is lower than the optimal limit ( $SOC_{OL}$ ) then the strategy directs it Prop-Charg to keep the SOC level high while still fulfilling the driver request. If due to some special circumstance, the driver's request cannot be met, it will go directly to Prop only.

Similarly, in other situations, if the vehicle is started and in an idling state but the SOC level of the batteries is low, then the strategy ensures that the ICE will charge the batteries until its upper or optimal limits ( $SOC_{OH}$ ). This function i.e. charging (Charg) may not have any importance for civil applications such as a garbage truck but for the military vehicle it may be beneficial in their sniper or silent actions in the battle field. Furthermore, in Fig IV.6 a condition for the return path is also given. These return path conditions will help in final implementation to switch from one state to another state (see IV.3).

The above description about Fig.IV.6 explains the transitions and their condition to travel from idling to neighboring states only. Through a similar process, each state of function level i.e. Prop, Brak, Charg, Prop-Charg, Brak-Charg is analyzed and a separate STD was built. Furthermore, by applying the same method to the daughter states of levels 2 and 3, their STD charts were also built. This multi-level energy management for levels 2 and 3, the method shown in the following paragraphs are only from the start state to its neighboring daughter states. Here, it is obvious that the final STD will be very complex because of the many states, transitions and conditions at each level. However, the advantage of this method is that provides an ease in building the strategy step by step through thoroughly analyzing each state. During this analysis and building of each state's STD, the transition and its subsequent conditions can be determined easily. To illustrate, in level 1, after any state is reached, for example Prop, the signal then tries to shift to a suitable daughter state after fulfilling the transition conditions. This situation is called state within a state. The level 2 daughter states for Prop are the operating modes electric (E), ICE (F) and hybrid (EF), shown in Fig. IV.7.

In level 2, the design values of the machine, along with other parameters, are used. Furthermore, it is assumed that all of the lower speeds of the vehicle are all electric. The electric mode (E), shown in Fig. IV.7, illustrates that if the  $P_{Demand}$  by the driver is lower than the design power of the electric

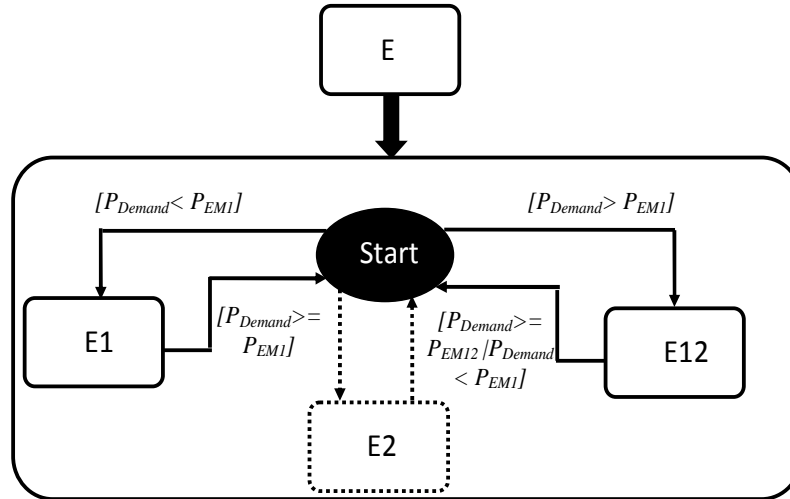
machines ( $P_{EM}$ ) then all of the energy will be given by the EMs exclusively at lower speeds. But to achieve this mode, the SOC level should be above its lower limit. Similarly, for the ICE mode, it is assumed that it will function on two possibilities: 1) when the  $v_{veh}$  is higher than certain limits ( $v_{veh\_c}$ ) and  $P_{Demand}$  is greater than the  $P_{EM}$  with constant acceleration ( $A_{veh}$ ); or 2) the driver need propulsion and the SOC level is low. For hybrid mode (EF), to avoid conflict between the ICE propulsion, it is assumed that the acceleration of vehicle is not constant and the SOC is above its lower limit. Furthermore, it is also noted that here there is no stop state because it is a state within a state and therefore not needed for this and the next level of power flows shown below in Fig. IV.8.



**Fig. IV. 7 - State Transition Diagram – Level 2 (OM in Prop-Function)**

For the last level, i.e. (level 3), the power flows of the concerned operating modes are also states within a state. Therefore, to understand this level, the power flows for the operating mode of electric propulsion (E) is chosen and shown in Fig. IV.8. In this (Fig. IV.8), the transition conditions are defined according to the design value of the EMs. In strategy, to use only one EM, then two options are available, EM1 (E1) or EM2 (E2). Therefore, a conflict in conditions will arise but it can be settled with the variation and addition of other parameters such as temperatures, etc. Here, only one machine (E1) is taken if the power demand by the driver is less than the design power. When the power demand for electric traction exceeds its design value but is less than power rating of both EMs together, the power flow will switch from

E1 to both EMs (E12) after passing through the idling state. The dotted state and transition in Fig. IV.8 presents the unconsidered power flow of the system.



**Fig. IV. 8 - State Transition Diagram – Level 3 (PFs in Electric OM)**

The same process shown and discussed above is tried for the remaining 5 functions at level 1, all of the operating modes (11) in level 2 and power flows in level 3 (39 in total for both trucks). This procedure for EMS is quite lengthy and time consuming but covers every aspect of the system. Furthermore, this procedure for EMS minimizes the possibility of errors and eliminates the overlooking of any state in different levels of the studied HEVs. Also, this strategy helps to improve the robustness of the vehicle controllers.

### **IV.3 Validation and Simulation Results**

The objective of this section is to demonstrate the validation of organization of multi-level EMS and its implementation in Matlab-Simulink® and Stateflow.

#### **IV.3.1 Validation in Stateflow**

For building a multi-level EMS based on the STD charts, Stateflow is taken into consideration. The Stateflow chart founded by Harel [Mathworks 2011-a] is a graphical design tool that works with Matlab-Simulink®, to simulate event-driven or reactive systems. Stateflow provides clear and concise descriptions of complex system behavior, using finite state machine theory,

flow diagram notations, and state-transition diagrams. Furthermore, this tool is good for constructing hierarchical states or events and can easily be connected with continuous-state blocks in Simulink [Colgren 2006] [Karris 2007]. The main advantages in using this technique in conjunction with Simulink are:

- ease in implementing STD charts for proposed rule-based multi-level energy management
- visual simulation of complex proposed energy management
- ease in alteration, evaluating the results, and validating system performance at any stage
- ability to send references directly after the choice of a specific power flow to local control of the system in a Simulink environment.
- the strategy easily downloadable to the electric control unit (ECU) of an actual vehicle.

In the previous section (IV.2.3), the background theory of implementation is already detailed. Therefore these STDs are directly implemented in Stateflow after the STD chart is found for each state at every level. It should be noted that in Stateflow diagrams, the transition conditions for the reverse path for any state should be given (as shown in Fig IV.9). This is to avoid an error in simulation runtime. This simulation error is due to a state being invalid but having no path to go back to its parent or switch to the next state(s). Therefore, in the final implementation in Stateflow, the reverse path from a state to the next state(s) of functions, operating modes and power flows is given in such a way that it can shift without any conflict. Furthermore, an additional state is also included at each level called the Decision state. This additional state i.e. Decision state is added because it 1) makes the strategy easier to handle, 2) allows for easier implementation of the final strategy, 3) makes access and location of simulation errors quicker and, 4) allows for less complicated switching from one state to another state at the same level (see Fig. IV.9, 10 and 11).

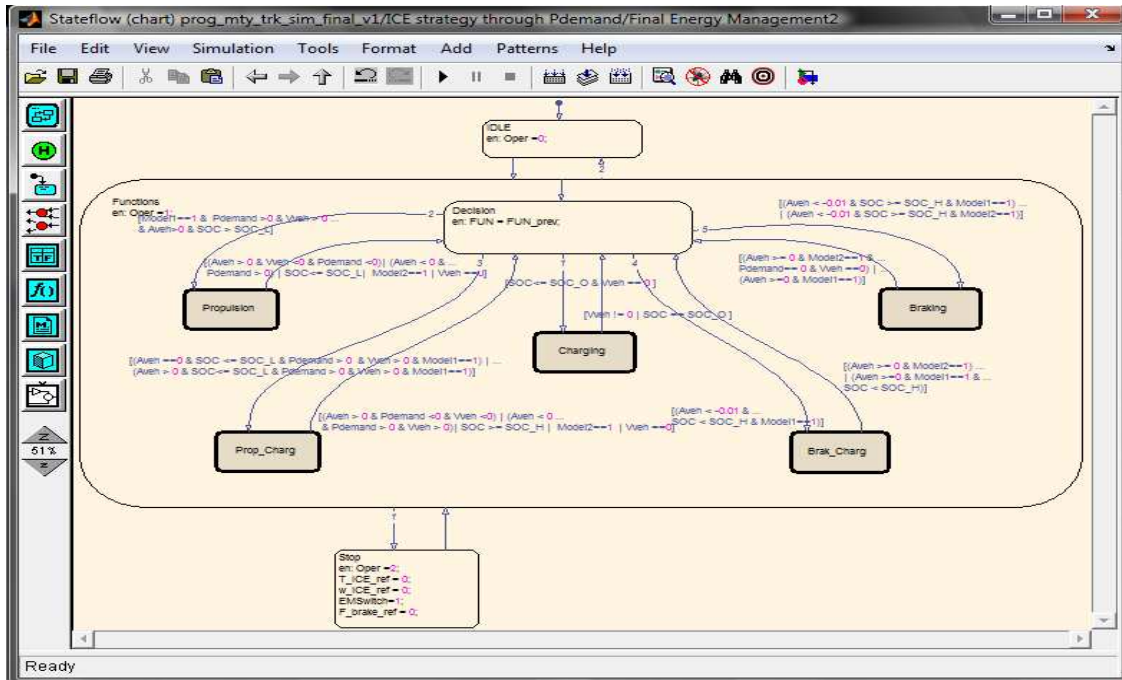
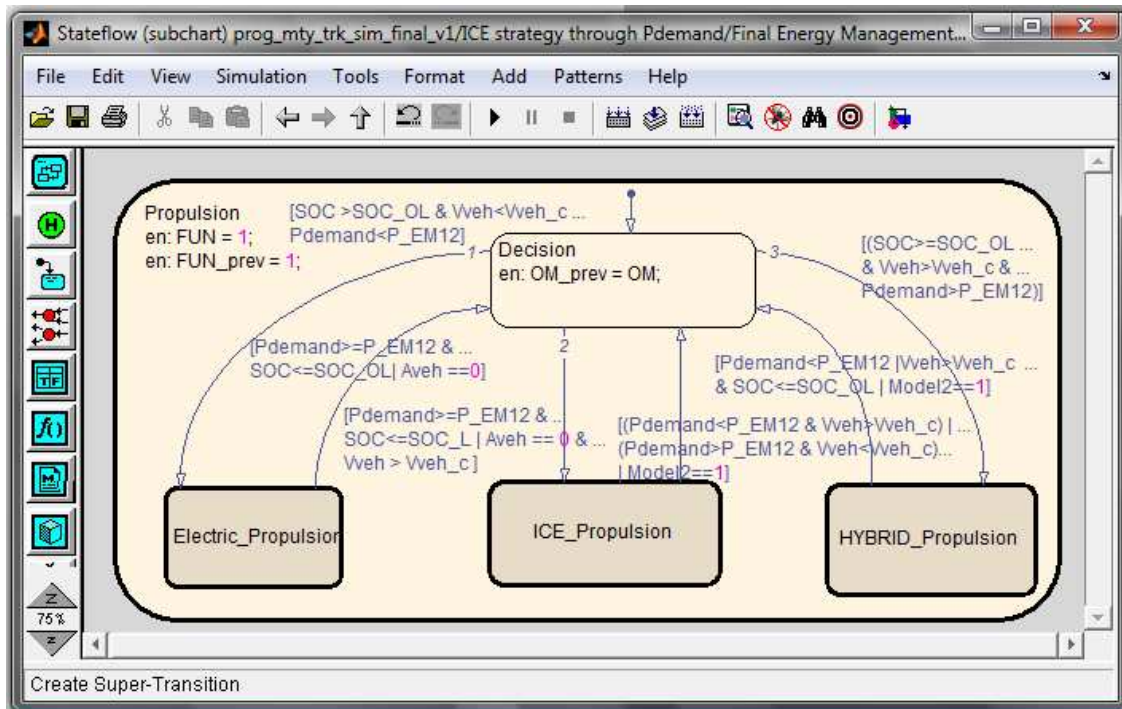


Fig. IV. 9 - Stateflow – Level 1 (Functions)

After the implementation of the first level (i.e. function) of multi-level EMS, a sub-chart of each function is created. As an example, shown in Fig. IV.10, the propulsion function containing electric, ICE and hybrid propulsion operating modes is built. Here, also the transition is drawn and its conditions are given.

The Fig. IV.9 represents the implementation of level 1 i.e. functions of proposed multi-level energy management in Stateflow for both HEVs. Although the same implementation is done for both HEVs, there are differences in the transition condition values such as vehicle speed, SOC, power demand, etc. This difference in values is due to the different requirements of both HEVs and the driving cycles.

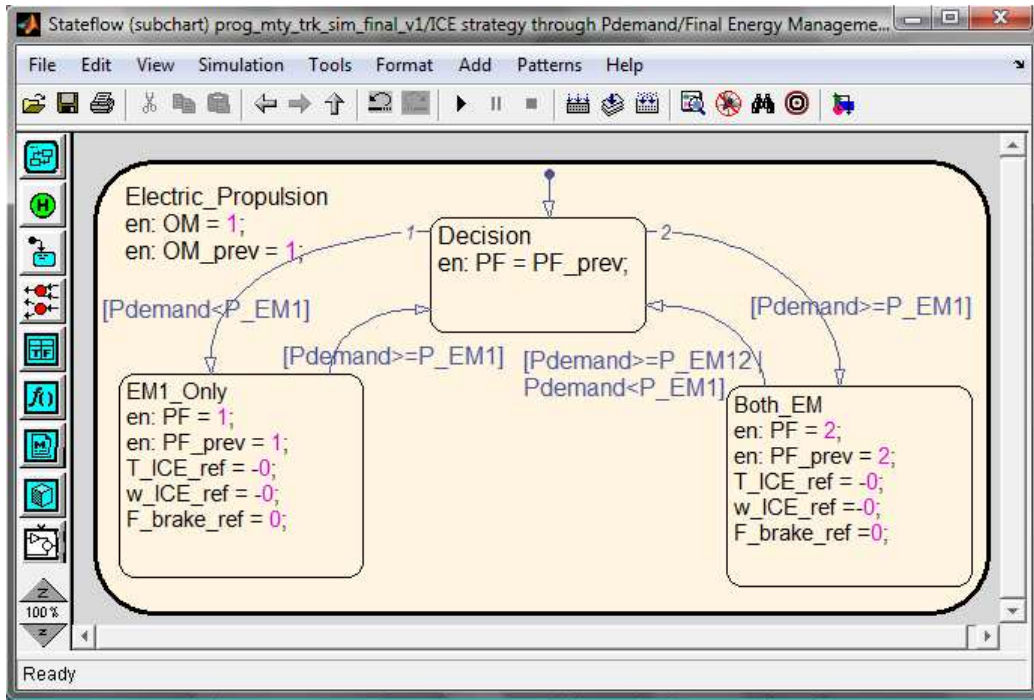
After the implementation of first level (i.e. function) of multi-level energy management, a sub-chart of each function is created. Fig. IV.10 shows an example containing the propulsion function containing the operating modes of electric, ICE and hybrid propulsion. Here, also the transition is drawn and its conditions are given.



**Fig. IV. 10 - Stateflow – Level 2 (Operating Modes for Propulsion)**

In the end, the STD charts for power flows are also implemented into Stateflow. In this study, due to simplification, only one power flow for each operating mode is taken into consideration except for electric propulsion and regenerative braking. This is done to avoid conflicts between different power flows due to a limited number of inputs. But if the complete dynamics of the system are taken into account, including the temperatures and limitations of each subsystem such as EM, ICE, etc., then all power flows can be easily accommodated and simulated. In Fig. IV.11, the third level of power flows for the electric propulsion of energy management is shown. It can be easily seen that when the power demand by the driver exceeds the design limit of one EM then it shifts to both EMs. Similarly when the power demand exceeds the design power limit of both EMs, it will shift to the previous level and take another operating mode's power flow to fulfill the power requirement of the driver. Also, the necessary inputs needed for local control are defined as the mechanical brake force ( $F_{brake\_ref}$ ), torque and speeds of ICE ( $T_{ICE\_ref}$ ,  $\Omega_{ICE\_ref}$ ). Furthermore, in electric mode, the ICE is turned off therefore in Fig. IV.11, the speed and torque for ICE is 0.





**Fig. IV. 11 - Stateflow – Level 3 (Power Flows in Electric)**

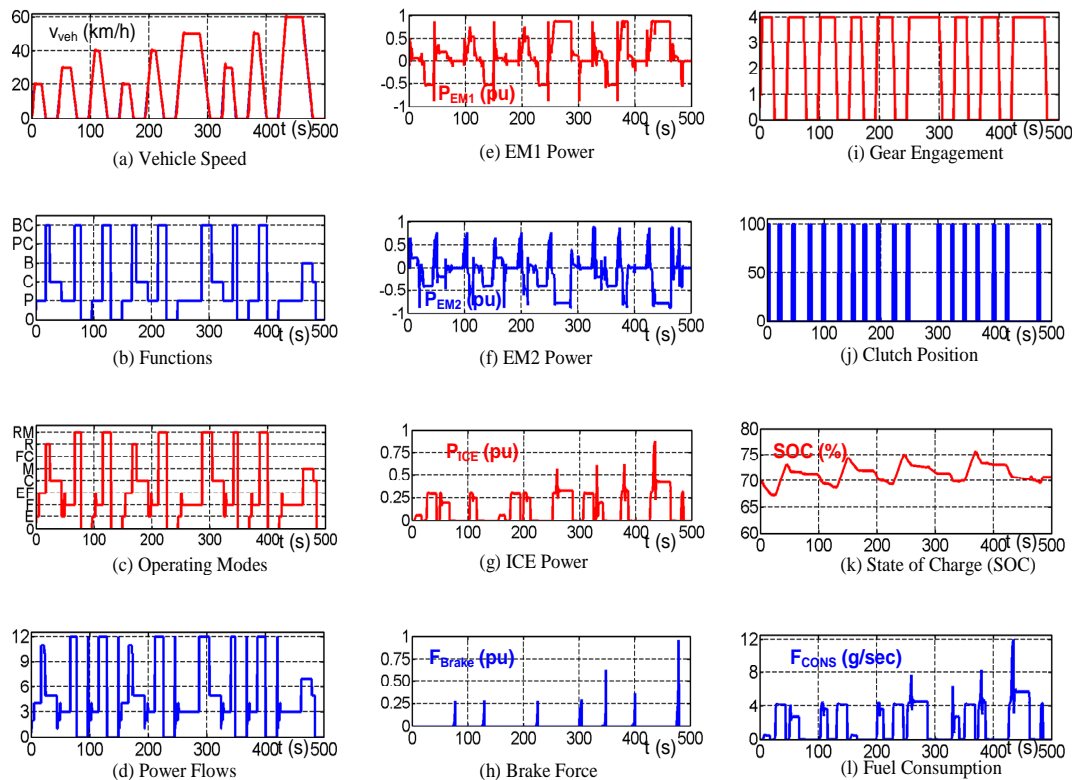
In the above discussion, the implementation of proposed multi-level EMS was detailed in Stateflow for the Matlab-Simulink® environment. After implementation, the results for both considered HEVs application to military and civil application are discussed in the next sections IV.3.2 and IV.3.3 respectively.

### **IV.3.2 Simulation Results for Military Truck**

Simulation is carried out on Matlab-Simulink® and shown in Fig. 12. In this simulation, the full Standard On-Road Test (SORT) driving cycle i.e. urban and suburban has been used as a reference to reflect the speed of the wheels [UITP 2001]. Due to system limitations some assumptions must be taken into account before realizing the simulation result. First, it must be assumed that the two gear ratios for high speeds in dual-range gearboxes are considered for medium speeds. The second choice is that the SOC will remain between 65 to 75% to validate the other operating modes and power flows.

The proposed multi-level EMS is implemented into Stateflow® of the Matlab-Simulink® platform. This implementation in simulation has been done on the basis of above discussion (see IV.2 and IV.3.1). The simulation

result verifies that the simulated speed is the same as the reference speed (Fig. 12.a). The other features or responses of subsystems such as EMs, ICE, gear change, etc. with the corresponding functions, operating modes and power flows of multi-level EMS are shown in Fig. 12(b) to 12(l). In these results the numerical values are not presented to keep the data confidential. Therefore the results are presented in per-unit (pu) system.

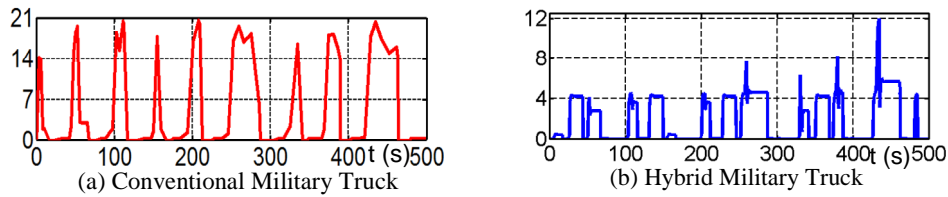


**Fig. IV. 12 – Simulation Results for Military Truck**

In Fig. 12(e), 12(f) and 12(g) the powers of EMs and ICE are shown under their design limits. To reiterate, in this implementation, initially, only 8 OMs are considered with one power flow each except for the electric and regenerative operating modes. In the electric mode two power flows are chosen i.e. EM1 only and both EM.

In Fig. IV.13 (a) and (b) the instantaneous fuel consumption of the military vehicle with and without hybridization in grams per second (g/s) is shown. The estimated fuel consumption for military truck for 100 km with

hybridization is 40 liters. In addition, the same vehicle is simulated but uses only 2 OMs (i.e. ICE propulsion (F) and mechanical braking (M)) of multi-level EMS the cumulative fuel consumption is 64 liters. Furthermore, for heavy-duty vehicles in the same class i.e. 8 equipped only with ICE, the estimated fuel consumption is about 60 liters [Yanowitz 2000] [Zachariadis 2001] [MfE 2011] [Stanley 2011]. Therefore, here it becomes obvious that the hybridization of heavy-duty vehicles is beneficial in terms of fuel economy and emission reductions.

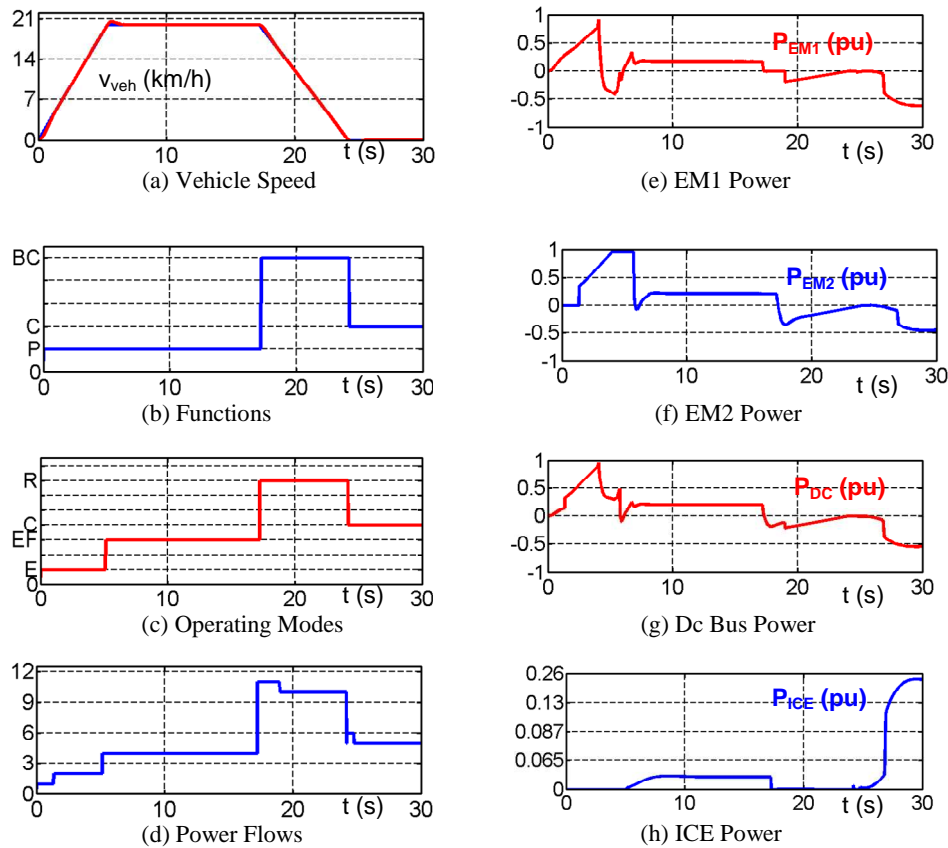


**Fig. IV. 13 – Instantaneous Fuel Consumption in g/s**

To illustrate the above figure (Fig. IV.12) and closely see the behavior of the proposed multi-level energy management the first 30 seconds of the cycle is detailed and shown in Fig. IV.14. Furthermore, in this, to avoid complexities, the behavior of clutch and gear change is taken separately and shown in Fig. IV.15. Fig. IV. 14(a) shows that the simulated speed follows the reference speed. To reiterate, in this study, the startup of the vehicle is considered all electric. Therefore as shown in Fig. 14(b) when the function propulsion (P) is active during start-up, then it takes the operating mode of all electric (E) in Fig.14(c). In the electric mode, two options are available: EM1 only or both EMs. Therefore the strategy decides the first power flows from 0 to 2 seconds and later as the speed or power demand by the driver increase it takes power flow 2 (from 2 to 5 seconds see Fig. IV.14(d)). At the same time if the behavior of EMs and DC bus power shown in Fig IV.14(e),(f) and (g) can be seen which respects the same rule.

Similarly, when the speed becomes 20 km/h then the strategy decides to switch the operating mode E to hybrid propulsion EF between 5 to 18 seconds (see Fig. IV. 14(b) and (c)). In this mode, the power is taken from both EMs and as well from ICE (see Fig. IV. 14(h)). After taking the respective power flow 4 as shown in Fig. IV.14(d), it can be easily seen in Fig. IV. 14(e)

to (h) that for fulfilling the driver's request the power is drawn from both sources.



**Fig. IV. 14 – Simulation Results for 30 seconds**

Later for the braking of the vehicle, it is assumed that low speed braking is always regenerative (R), medium speed braking regenerative with mechanical (RM) and higher speed braking only mechanical (M). Furthermore, for the power flow with one EM during regenerative braking (R), instead of EM1, the other electric machine i.e. EM2 being utilized. From the Fig. IV. 14(b), (c) and (d), it can be seen that when the function braking-charging (BC) is active then it follows regenerative braking OM with its respective power flows 10 and 11. The power flow 10 is active for only EM2 and power flow 11 for the both EMs. Fig. IV. 14(e) to (h) between 17 to 19 seconds verifies that when there is single power flow i.e. 10 then the braking energy is recovered by the EM2. Later (between 19 to 23 seconds) the power flow switches from 10 to 11 and in this both EMs recover the energy. Here, it should be noted

that EM1 is recovering less power compare to EM2. This is because the EM2 can recover all the energy but to show the effectiveness or workability of this energy management this power flow is taken into account.

Finally, between 24 to 30 seconds the vehicle speed is 0 and in the stop state. Here in the strategy, the assumption is taken that when the vehicle is in the rest position and SOC is below 70%, then the ICE should charge the batteries until its maximum limit of 75%. Therefore, in Fig. IV. 14(b) when the function charging (C) is active then it takes its alone operating mode i.e. charging with ICE (C) (see Fig. IV.14(c)). In this due to the clutch position it can follow two states of same power flow i.e. one with open position of the clutch (power flow 6) and the other with locked position (power flow 5) (see Fig. IV.14(d)). In Fig. IV.14 (e) to (h) and Fig. IV.12(k) it can be seen that the ICE is powering the batteries through both machines EM1 and EM2.

In this simulation, the clutch characteristics are very important. Therefore the first five seconds of the same simulation (which is discussed previously) are taken into account as shown from Fig. IV.15 (e) to IV.15(h).

In Fig. IV.15 (a), the vehicle speed corresponds to part of the SORT driving cycle. The result verifies that when the gear is engaged or disengaged then the clutch state i.e. slipped (Model 1) or locked (Model 2), will shift accordingly (see Fig. III.15 (d)). Moreover, when the gear shifts, the clutch will be opened and the position of the clutch will be released. This process is shown in Fig. III.15 (c) with the percentage of clutch position ( $p_{cl}$ ) ranging from 0 (close) to 100% (open). The values in-between 0 to 100 correspond to this clutch slipping phenomena.

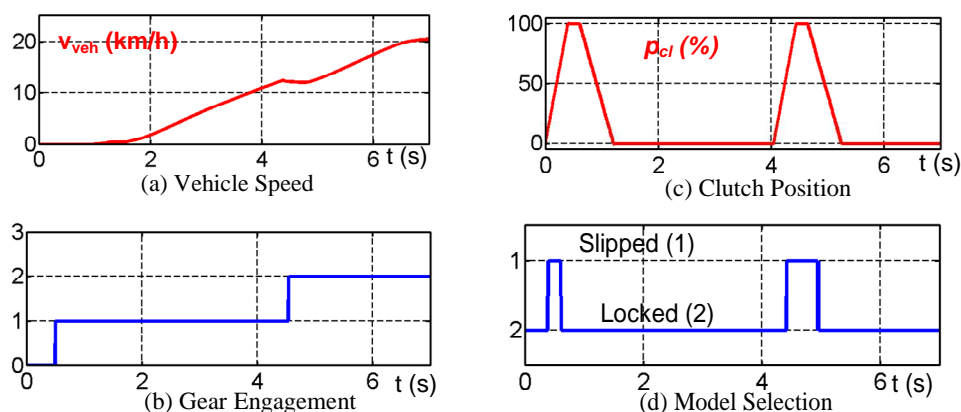


Fig. IV. 15 – Behavior of Clutch and Gear Change

In conclusion, these simulations results verify the validity of this organization of energy management and prove that it works and interact with EMR and its inversion-based control within MATLAB-Simulink® environment. Furthermore, the same method can be applied to other HEVs to find the similar type of energy management with detailed overview.

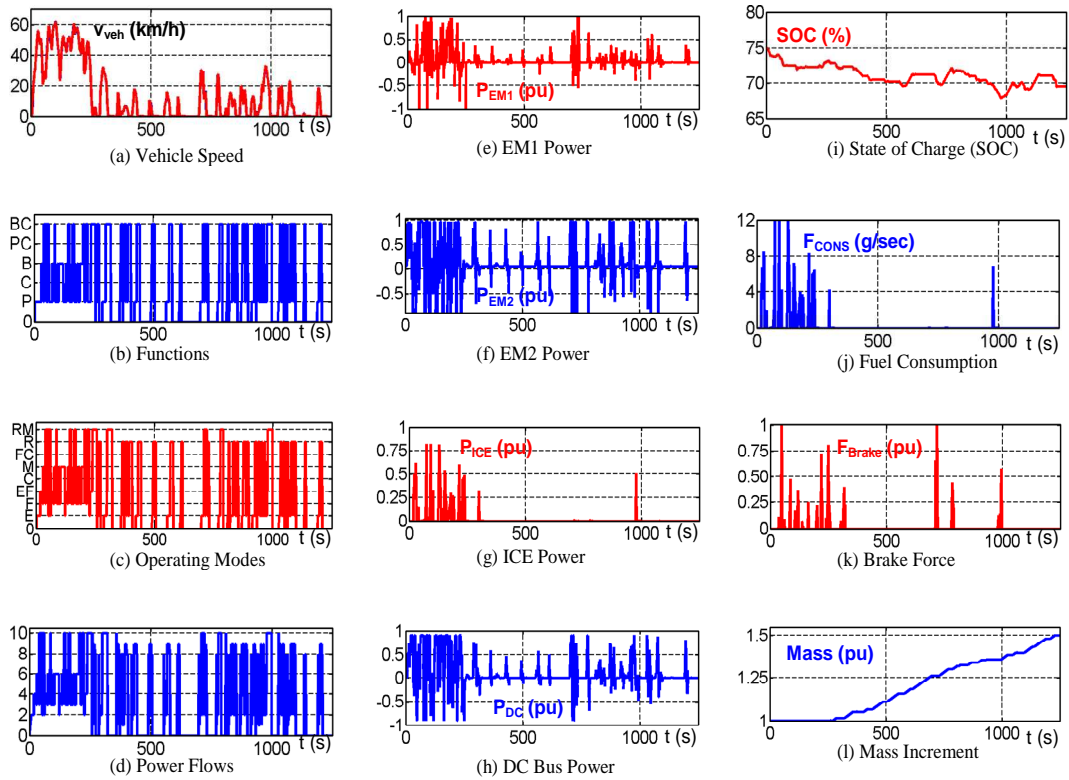
### **IV.3.3 Simulation Results for Garbage Truck**

For the garbage truck, similar to the military truck, the simulation is carried out on Matlab-Simulink® (Fig. IV.16). In this simulation, a full real time the ARTEMIS driving cycle is used as a reference (Figure IV. 16(a)).

The same proposed multi-level EMS is utilized for the garbage truck (see section IV.2 and IV.3.1) but implemented with some additional assumptions such as: 1) the start of the vehicle should be all electric, 2) at high speeds or liaison trips the ICE should work primarily, and 3) during collector phases the vehicle should propel itself primarily in the electric mode and the braking should be mainly regenerative. However, when the speed exceeds 31 km/h or the SOC is on its upper limit, the braking should be mechanical. The reason these assumptions are taken is that the goal of this EMS is to allow for the garbage truck to run as close as possible to a pure electric vehicle.

The simulation result verifies that the simulated speed is the same as the reference speed (Fig. 16(a)). The other features or responses of subsystems such as EMs, ICE, DC bus, etc. with the corresponding functions, operating modes and power flows of multi-level energy management are shown in Fig. 15(b) to 15(l). Similar to military truck, the results are presented in per-unit (pu) system due to the confidentiality of the data.

In this simulation, for the collector phase, the increases in mass increment while the vehicle is in rest position are also taken into account. In other words, the total mass of the vehicle during the collector phase will increase due to the collection of waste (Fig. IV. 16(l)). This i.e. mass increment makes the simulation more intricate but it is taken into account to make simulation closer to real world.



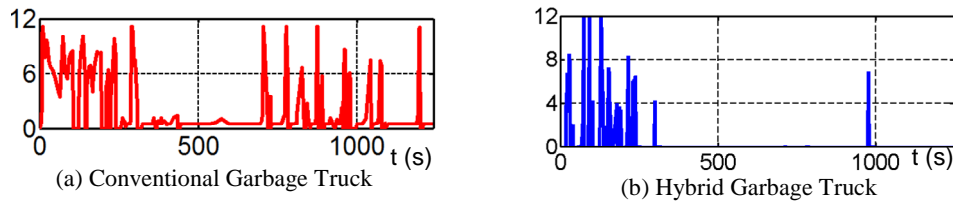
**Fig. IV. 16 – Simulation Results for Garbage Truck**

Here, similarly to the military truck, only 8 OMs are considered with one power flow each except for the electric and regenerative operating modes. In the electric mode two power flows are chosen i.e. EM1 only and both EMs. In Fig. 16(e), 16(f) and 16(g) the powers of EMs and ICE are shown under their design limits.

In Fig. IV.17(a) and (b) the instantaneous fuel consumption of the garbage truck with and without hybridization is shown in grams per second (g/s). The estimated fuel consumption for a hybrid garbage truck for 100 km is 12 litres and for a conventional truck is 68 litres<sup>2</sup>. The fuel consumption for hybrid garbage trucks is less to keep in line with the assumption that the propulsion and braking of the vehicle will be primarily all electric. Also, this assumption can be verified by the power of ICE in Fig. IV.16(g) in that the ICE is only working only at high speeds but at lower speeds it is just turned off. Furthermore, Fig. IV.16(k) verifies the assumption that the mechanical brak-

<sup>2</sup> This difference is due to large battery size and its capacity.

ing alone or together with regenerative braking works only at high speeds. However, at lower speeds only the regenerative braking is utilized to charge the batteries.



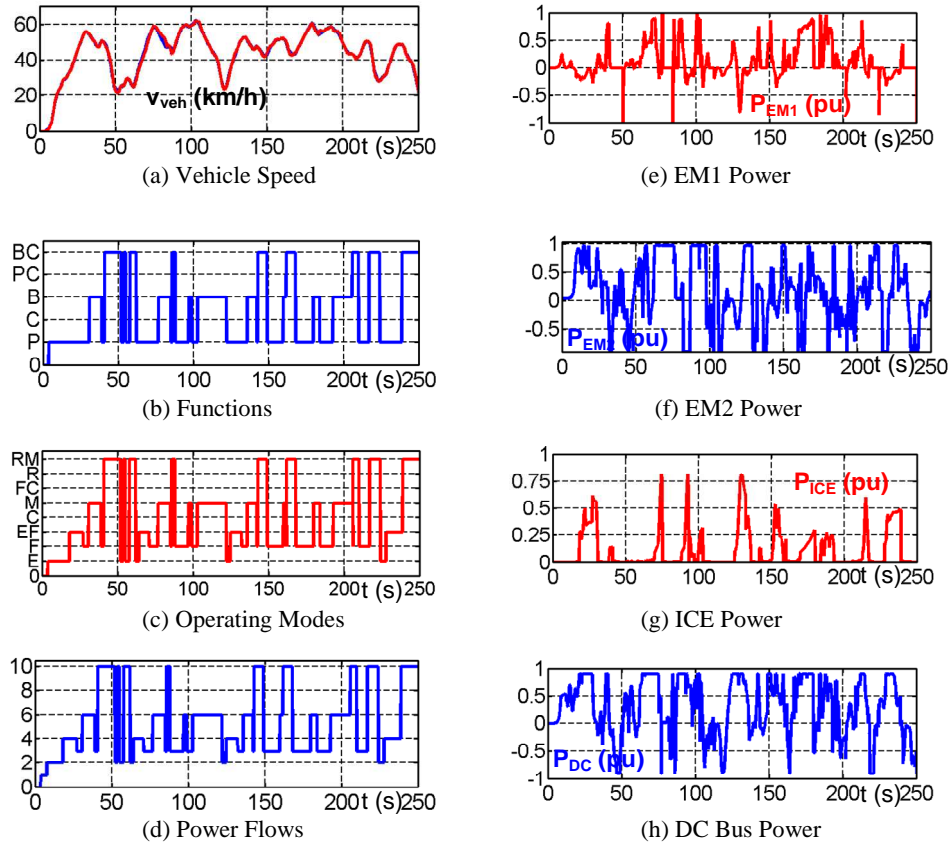
**Fig. IV. 17 – Instantaneous Fuel Consumption in g/s**

To illustrate the above figure (Fig. IV.16) and closely see the behavior of the proposed multi-level energy management, the first 250 seconds of the liaison trip is detailed and shown in Fig. IV.18. Fig. IV. 18(a) shows that the simulated speed follows the reference speed. As considered the startup of the vehicle is all electric, therefore, shown in Fig. 18(b) when the function, propulsion (P) during startup is active then it takes the operating mode of all electric (E) in Fig.18(c). In the electric mode, two options are available: EM1 only or both EMs. Therefore the strategy decides the first power flows from 4 to 8 seconds and later as the speed or power demand by the driver increase it takes power flow 2 (from 8 to 18 seconds see Fig. IV.18(d)). At the same time if the behavior of EMs and DC bus power shown in Fig IV.18(e),(f) and (g) can be seen which respects the same rule.

Similarly, when the speed becomes 31 km/h then the strategy decides to switch the operating mode (E) to hybrid propulsion (EF) between 18 to 27 seconds (see Fig. IV. 18(b) and (c)). In this mode, the power is taken from both EMs and as well from the ICE (see Fig. IV. 18(g) and (h)). After taking the respective power flow 4 as shown in Fig. IV.18(d), it can be easily seen in Fig. IV. 18 (e) to (h) that to fulfill the driver's request the power is drawn from both sources. Furthermore, when the speed of the vehicle exceeds 50 km/h then the strategy decides to propel the vehicle using only the ICE. Therefore the operating mode switches from hybrid propulsion (EF) to ICE only (F). After taking the respective power flow 3 between 78 to 93 seconds, the power is supplied only by ICE. In the first 250 seconds of the ARTEMIS driving cycle, the braking of the vehicle is considered mechanical (M) alone of



power flow 6 or mechanical with regenerative braking (RM) of power flow 10 (see Fig. IV. 18(b), (c) and (d)).



**Fig. IV. 18 – Simulation Results for Liaison Trip**

In conclusion, the above simulation results for garbage truck verifies that the hybridization of these heavy-duty vehicles is indeed beneficial. Furthermore, the results confirm that the organization of proposed multi-level EMS works and interact with EMR and its inversion-based control within MATLAB-Simulink® environment. Of course more advanced strategies have to be developed by taking into account all OMs and its PFs.

## Conclusion

In this chapter, (Chapter IV) a detailed strategy for global energy management for two considered HEVs i.e. military and garbage truck was proposed and realized. This energy management strategy provides the references needed for the local control structure of the system while managing or controlling the energy between different energy sources. Furthermore, through the simulation results, this strategy proved that it can easily hold all of the information needed for the system and react quickly to fulfill the driver's demand while increasing performances of the system.

The first section of this chapter gave an overview of the energy management strategies while defining its basic concepts such as functions, operating modes and power flows. On the basis of these key concepts, the second section proposed and arranged the strategy through State Transition Diagrams (STDs). The STDs proved effective for helping to ease the understanding and build the proposed strategy. In the third section, this proposed strategy was realized in Stateflow of Matlab-Simulink® environment and shown the simulation results.

In conclusion, this chapter proposed a new arrangement of global energy management in application to studied HEVs i.e. military and garbage trucks. This arrangement was realized in different levels i.e. level-1 (functions), level-2 (operating modes) and level-3 (power flows). This multi-level EMS gives a great overview on how to handle the system in different situations of vehicle's driving life. Also, it gives an in depth view of the actual system's performances. First, a simple and rule-based strategy has been developed using this multi-level frame. This proposed multi-level strategy proved its effectiveness through the simulation results. This strategy gives a detailed picture of the vehicle and assures that nothing is missing resulting in increased vehicle performance. Similar methodology could be implemented into other types of HEVs such as parallel, double parallel, series, etc. On the down side, this strategy is labor intensive as it takes many charts to build and analyze each phase of the system. Of course more advanced strategies could be developed using this decomposition in 3 levels for the EMS.

# **Final Conclusion**



# Final Conclusion

The objective of this research work is to provide a model-based control and proposed an organization for multi-level Energy Management Strategy (EMS) of the studied HEVs for application to military and garbage trucks. This model-based control was realized by a means of formalism called Energetic Macroscopic Representation (EMR) which leads to local control structure (or local energy management) and global energy management called EMS of the system. This research focused on two studied HEVs that contain a complex device called the double planetary geartrain. Through this research work, EMR proved its capability by representing this complex system as well deducing local control structures. The same EMR and local control structure were deduced for both studied HEVs. Later, organization of multi-level EMS was proposed to respect the constraints and energetic properties of the overall system and its subsystems.

Detailing this objective, Chapter I revealed the intention behind this research work through highlighting the main concerns and difficulties for developing an HEV for heavy-duty class vehicles. Furthermore, this chapter explained why a compound planetary gear was used for this study and elaborated on its benefits such as compactness, increased number of connectable sources, ability to fulfill the high power requirement of the systems, etc. In its subsection (Chapter I) kinematic and energetic studies were done for the power split device to assure easier final modeling of the whole HEVs.

The detailed modeling and EMR graphical description for the studied HEVs was given in Chapter II. In this, the similarities and differences between both vehicles' architecture and their subsystems were discussed from the modeling perspective and its representation. Here, in both HEVs, a specific complex device, i.e. double planetary geartrain is utilized to achieve series-parallel architecture. This geartrain can connect 4 shafts leading to 4 total torques and speeds. However, by using the Willis relationship 2 rotation speeds are enough to represent its state variables. Thus, a detailed modeling of this geartrain has been reorganized with the equivalent torques (sum of all

sources torques) as input and 2 rotation speeds as output. A vectorial element has thus been used in EMR to represent these state variables by accumulating the total mass and moment of inertias. Furthermore, after a detailed modeling and representation of each subsystem in both HEVs, the final EMR was presented to resolve the association problems for functional representation. Thanks to the EMR merging and permutation rules these association problems for the studied HEVs were easily resolved. EMR demonstrated that it had the global capabilities to depict the energetic properties of the complex system as a whole or through each part of the system. Through EMR, the similarities and differences in both HEVs were more easily recognizable.

The modeling and EMR presented in Chapter II easily lead to finding the local and global control schemes for both vehicles. This local control structure or local energy management in EMR is called inversion-based control and is detailed in Chapter III. In this chapter, a detailed description of local control or local energy management through EMR for two considered HEVs i.e. military and garbage truck was completed. This control schemes were deduced through the inversion principles of EMR. Furthermore, these control schemes illustrated the differences and common features related to both HEVs. For the validation of these control schemes, primarily results are shown after implementing a simple rule-based strategy in MATLAB-Simulink® environment.

Later, in Chapter IV, to accomplish the objective of this thesis, an organization of multi-level energy management i.e. EMS was proposed and detailed for both considered HEVs. The EMS provided the references needed for the local control structure of the system while managing or controlling the energy between different sources. Through the simulation results, this strategy proved that it could easily hold all of the information needed for the system and react quickly to fulfill the driver's demand while increasing performances of the system.

In the subsections of Chapter IV, basic concepts such as functions, operating modes and power flows for energy management were defined. Later, they were arranged into 3 levels with the help of State Transition Diagrams (STDs). The STDs proved effective in handling these multi-levels and provided an easier method to implement into the simulation software i.e. Stateflow of Matlab-Simulink® environment. Later, in the last section, the simulation results are provided which verify that the hybridization of these heavy-duty

vehicles is indeed beneficial. Furthermore, the results confirm that the organization of the proposed multi-level EMS works and interacts with EMR and its inversion-based control within MATLAB-Simulink®.

In conclusion, this thesis, with modeling, graphical representation through EMR proposed and realized a new arrangement of multi-level EMS with application to both studied HEVs. This multi-level energy management consisted of 5 functions and 11 operating modes for both HEVs. However, in level-3, there are 39 power flows for the military and garbage truck. This proposed organization of energy management allowed for a great overview on how to handle the system in different situations of the vehicle's driving life. It also gave an in-depth view of the actual system's performances. This proposed strategy proved its effectiveness through the simulation results.

For the future work, this multi-level energy management should be extended to implement all of the functions, operating modes and power flows to the studied HEVs. Furthermore, in this research work, the heuristic control strategy that was discussed and implemented could be extended to implement more advanced optimized and complex strategies with comparing simulation results.

The studied HEVs have not been validated experimentally and it would be of great interest to see the actual performance of the strategy implemented in the reference vehicle and the results compared to the simulation results. Also, extending the simulation model presented in the thesis with an emission model would be one of the main goals for future work. Experimental investigations of these emissions such as carbon dioxide (CO<sub>2</sub>), oxides of nitrogen (NO<sub>x</sub>) and so on would be of great interest.

For long term gains, this research can be extended to implement the same strategy to other HEV types such as series, parallel, double parallel, etc. Also, not limited to HEVs, this methodology of multi-level organization can be extended to other engineering applications. The relevance of this multi-level EMS is significant at a time when energy optimization and reduction of oil consumption make headlines almost every day.





# Appendixes



# Appendix A:

## EMR and Inversion-based control

Energetic Macroscopic Representation (EMR) was developed by the Laboratory of Electrical Engineering and Power Electronics (L2EP), Lille, France in the 2000s. EMR is a synthetic graphical tool based on the principle of action and reaction, which is used to organize the interconnection of sub-systems according to physical causality i.e. integral causality. This graphical tool is helpful to represent complex systems, in accordance with a functional description [Bouscayrol 2003-a].

**Basics of EMR** -EMR is based on 4 kinds of elements that describe the physical state of a component (see Table App.1).

*Source elements* (green oval pictograms) produce variables (outputs). They can be either generators or receptors. They are disturbed by reactions of other elements.

*Conversion elements* ensure energy conversion without energy storage. They have tuning inputs to define the conversion between variables. They can hold multi-physical or mono-physical elements. The mono-physical elements are depicted by orange square pictograms whereas multi-physical converters are represented by orange circular pictograms.


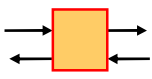
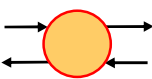
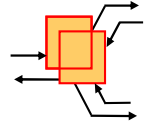
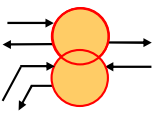
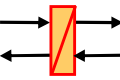
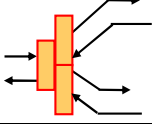
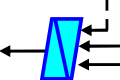
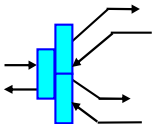
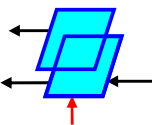
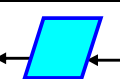

*Accumulation elements* (orange rectangular pictograms with an oblique bar) connect other elements, thanks to energy storage, which induces at least one state variable. All these elements are connected through exchange vectors according to the principle of action and reaction. For energy conversion systems, specific association rules have been defined to build their EMR.

*Distribution elements* (overlapped orange pictograms) ensure an energy distribution between several chains of conversion.

*Switches* are used to switch from one model to another. These switches are helpful to represent models with nonlinear behavioral subsystem such as clutch [Lhomme 2007].

All these elements are interconnected according to the principle of action and reaction. The product variables action-reaction between two elements gives the instantaneous power exchanged between any two elements [Bouscayrol 2003-a].

**Table App.3 - Summary of Elements of EMR formalism**

Element	Symbol	Description
Source		Source of energy
Converters		Mono Physical (without energy accumulation)
		Multi-Physical converter (without energy accumulation)
Distribution		Mono-Physical distribution (without energy accumulation)
		Multi-Physical distribution (without energy accumulation)
Accumulation		Element with energy accumulation
Switch		Switching of Models related to any kind of energy type
Controller		Inversion of Accumulation element with closed-loop control
Control Blocks		Inversion of Switch (switching energy in a way to choose two different models)
		Inversion of Mono or Multi-physical couplings
		Inversion of Mono or Multi-physical converter
Strategy		determines the criteria and references for the local control

## **Appendix B:     Static Maps**

## Appendix C: Equivalent Shafts

In this Appendix, the modeling of the equivalent shaft with the chassis will be discussed. In this modeling, for the sake of simplification, whole clutch modeling in the dual-range gearbox is ignored. Due to this assumption, the modeling is simplified and a similar kind of EMR that will be used for the other application (waste collection) without clutch can be easily found.

The studied system consists of many shafts containing their state variables and torques as shown in the following in Fig. App.2.

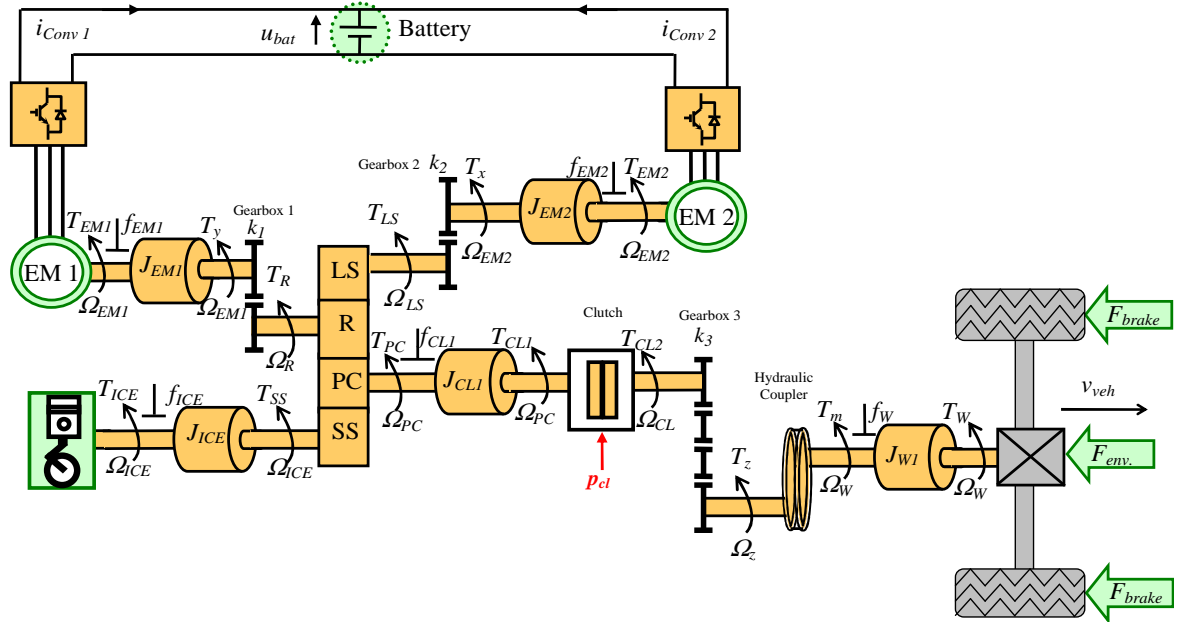


Fig. App. 1 – Military Truck Layout

The equation of the shafts by including gearboxes are:

$$T_{EM1} - \frac{T_R}{k_1} = J_{EM1} \frac{d}{dt} \Omega_{EM1} + f_{EM1} \Omega_{EM1} \quad (\text{App.1})$$

$$T_{ICE} - T_{SS} = J_{ICE} \frac{d}{dt} \Omega_{ICE} + f_{ICE} \Omega_{ICE} \quad (\text{App.2})$$

$$T_{EM2} - \frac{T_{LS}}{k_2} = J_{EM2} \frac{d}{dt} \Omega_{EM2} + f_{EM2} \Omega_{EM2} \quad (\text{App.3})$$

$$T_W - k_3 k_4 T_{PC} = k_3 k_4 \left[ J_{W1} \frac{d}{dt} \Omega_{PC} + f_W \Omega_{PC} \right] \quad (\text{App.4})$$

It is tried to build an equivalent shaft through modeling which should take all of the shaft dynamics and the chassis and represent them with a single accumulation element of an EMR as presented in [Chen 2010] and [Lhomme 2007]. Therefore, for modeling in equation (App.4),  $\Omega_W$  is replaced by the speed  $\Omega_{PC}$  to avoid the multiplication of two gains ( $k_3$  and  $k_4$ ) and to get the same speed variable as the PSD equation. Furthermore, due to the association problems, the mass of the vehicle is added to the moment of inertia of  $J_{W1}$  through relationships (2.19) – (2.23), (2.29) and (2.30) such that:

$$J_W = J_{W1} + M_{veh} \left( \frac{R_W}{k_3 k_4} \right)^2 \quad (\text{App.5})$$

The speed equations for the PSD have already been derived in equations (1.9) and (1.10) (Chapter I). Therefore by inserting the values of corresponding speeds, the following relationship will be realized:

$$\frac{\Omega_{EM2}}{k_2} - k_{LS} \frac{\Omega_{EM1}}{k_1} + (k_{LS} - 1) \Omega_{PC} = 0 \quad (\text{App.6})$$

$$\Omega_{ICE} - k_{SS} \frac{\Omega_{EM1}}{k_1} + (k_{SS} - 1) \Omega_{PC} = 0 \quad (\text{App.7})$$

As discussed in section II.2.1, for resolving the system to achieve two state variables, the equation (App.1) to (App.3) with (App.6) and (App.7) are solved and the following expression is determined:

$$T_1' = J_1 \frac{d}{dt} \Omega_{ICE} + f_1 \Omega_{ICE} - J_2 \frac{d}{dt} \Omega_{PC} - f_2 \Omega_{PC}, \quad (\text{App.8})$$

$$\text{with } T_1' = T_{ICE} + \frac{k_1}{k_{SS}} T_{EM1} + k_2 \frac{k_{LS}}{k_{SS}} T_{EM2},$$

$$\left\{ \begin{array}{l} J_1 = J_{ICE} + \frac{k_1^2}{k_{SS}^2} J_{EM1} + k_2^2 \left( \frac{k_{LS}}{k_{SS}} \right)^2 J_{EM2} \\ J_2 = -k_1^2 \frac{(k_{SS} - 1)}{k_{SS}^2} J_{EM1} + k_2^2 \frac{k_{LS}(k_{LS} - k_{SS})}{k_{SS}^2} J_{EM2} \\ f_1 = f_{ICE} + \frac{k_1^2}{k_{SS}^2} f_{EM1} + k_2^2 \left( \frac{k_{LS}}{k_{SS}} \right)^2 f_{EM2} \\ f_2 = -k_1^2 \frac{(k_{SS} - 1)}{k_{SS}^2} f_{EM1} + k_2^2 \frac{k_{LS}(k_{LS} - k_{SS})}{k_{SS}^2} f_{EM2} \end{array} \right.$$

It is shown in equation (App.8) that the torque  $T_1'$  is made up of the torques  $T_{ICE}$ ,  $T_{EM1}$  and  $T_{EM2}$ ; with their respective moment of inertias of the connected shafts ( $J_{ICE}$ ,  $J_{EM1}$  and  $J_{EM2}$ ) and viscous frictions ( $f_{ICE}$ ,  $f_{EM1}$  and  $f_{EM2}$ ) to the ICE, EM1 and EM2.

Similarly, by resolving the equations (App.6) and (App.7) with torque equations of the PSD and (App.1), (App.2) and (App.4), the following expression can be deduced:

$$T_2' = -J_3 \frac{d}{dt} \Omega_{ICE} - f_3 \Omega_{ICE} + J_4 \frac{d}{dt} \Omega_{PC} + f_4 \Omega_{PC}, \quad (\text{App.9})$$

$$\text{with } T_2' = \frac{1}{k_3 k_4} T_W + k_1 \frac{k_{SS} - 1}{k_{SS}} T_{EM1} + k_2 \frac{k_{SS} - k_{LS}}{k_{SS}} T_{EM2},$$

$$\left\{ \begin{array}{l} J_3 = -k_1^2 \frac{(k_{SS} - 1)}{k_{SS}^2} J_{EM1} + k_2^2 \frac{k_{LS}(k_{LS} - k_{SS})}{k_{SS}^2} J_{EM2} \\ J_4 = \frac{1}{(k_3 k_4)^2} J_W + k_1^2 \left( \frac{k_{SS} - 1}{k_{SS}} \right)^2 J_{EM1} + k_2^2 \left( \frac{k_{SS} - k_{LS}}{k_{SS}} \right)^2 J_{EM2} \\ f_3 = -k_1^2 \frac{(k_{SS} - 1)}{k_{SS}^2} f_{EM1} + k_2^2 \frac{k_{LS}(k_{LS} - k_{SS})}{k_{SS}^2} f_{EM2} \\ f_4 = \frac{1}{(k_3 k_4)^2} f_W + k_1^2 \left( \frac{k_{SS} - 1}{k_{SS}} \right)^2 f_{EM1} + k_2^2 \left( \frac{k_{SS} - k_{LS}}{k_{SS}} \right)^2 f_{EM2} \end{array} \right.$$





These two expressions (App.9) and (App.10) are able to reveal the energy of state variables  $\Omega_{ICE}$  and  $\Omega_{PC}$  through the torques  $T'_1$  and  $T'_2$ :

$$J'_{ICE} \frac{d}{dt} \Omega_{ICE} + f'_{ICE} \Omega_{ICE} = K_{ICE1} T'_1 + K_{ICE2} T'_2 - f''_{PC} \Omega_{PC} \quad (\text{App.11})$$

$$J'_{PC} \frac{d}{dt} \Omega_{PC} + f'_{PC} \Omega_{PC} = K_{PC1} T'_1 + K_{PC2} T'_2 - f''_{ICE} \Omega_{ICE}$$

with,

$$\begin{cases} K_{ICE1} = 1, \quad K_{ICE2} = \frac{J_2}{J_4}, \quad K_{PC1} = \frac{J_3}{J_1} \quad \text{and} \quad K_{PC2} = 1, \\ J'_{PC} = J_4 - K_{PC1} J_2 \quad \text{and} \quad f'_{PC} = f_4 - K_{PC1} f_2, \\ J'_{ICE} = J_1 - K_{ICE2} J_3 \quad \text{and} \quad f'_{ICE} = f_1 - K_{ICE2} f_3, \\ f''_{PC} = -f_2 + K_{ICE2} f_4 \quad \text{and} \quad f''_{ICE} = -f_3 + K_{PC1} f_1 \end{cases}$$

The expression in (App.11) can also be written matrix form as follows:

$$\frac{d}{dt} \begin{bmatrix} \Omega_{ICE} \\ \Omega_{PC} \end{bmatrix} = A \begin{bmatrix} \Omega_{ICE} \\ \Omega_{PC} \end{bmatrix} + B \begin{bmatrix} T'_1 \\ T'_2 \end{bmatrix} \quad (\text{App.12})$$

with

$$A = \begin{bmatrix} f'_{ICE}/J'_{ICE} & f''_{PC}/J'_{ICE} \\ f''_{ICE}/J'_{PC} & f'_{PC}/J'_{PC} \end{bmatrix} \quad \text{and} \quad B = \begin{bmatrix} K_{ICE1}/J'_{ICE} & K_{ICE2}/J'_{ICE} \\ K_{PC1}/J'_{PC} & K_{PC2}/J'_{PC} \end{bmatrix}$$

The moments of inertia ( $J'_{PC}$  and  $J'_{ICE}$ ) and viscous friction ( $f'_{PC}$  and  $f'_{ICE}$ ) are defined in the equations (App.12), which will allow the determination of the time-constant and speeds:

$$\Omega_{ICE} = \frac{K'_{ICE}}{1 + s\tau'_{ICE}} (K_{ICE1}T'_1 + K_{ICE2}T'_2 - f''_{PC}\Omega_{PC}) \quad (\text{App.13})$$

$$\Omega_{PC} = \frac{K'_{PC}}{1 + s\tau'_{PC}} (K_{PC1}T'_1 + K_{PC2}T'_2 - f''_{ICE}\Omega_{ICE})$$

with

$$\begin{cases} \tau'_{ICE} = \frac{J'_{ICE}}{f'_{ICE}} & \text{and } K'_{ICE} = \frac{1}{f'_{ICE}}, \\ \tau'_{PC} = \frac{J'_{PC}}{f'_{PC}} & \text{and } K'_{PC} = \frac{1}{f'_{PC}} \end{cases}$$

Similarly, the torques  $T'_1$  and  $T'_2$  from equations, (App.9) and (App.10) can also be expressed in matrix notation as follows:

$$\begin{bmatrix} T'_1 \\ T'_2 \end{bmatrix} = C \frac{d}{dt} \begin{bmatrix} \Omega_{ICE} \\ \Omega_{PC} \end{bmatrix} + D \begin{bmatrix} \Omega_{ICE} \\ \Omega_{PC} \end{bmatrix} \quad (\text{App.14})$$

with,

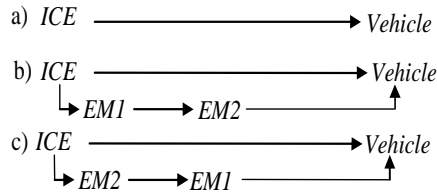
$$C = - \begin{bmatrix} J_1 & -J_2 \\ -J_3 & J_4 \end{bmatrix} \quad \text{and} \quad D = \begin{bmatrix} f_1 & -f_2 \\ -f_3 & f_4 \end{bmatrix}$$

# Appendix D: Power Flows

In this appendix, the remaining power flows for the studied HEVs under the basic and combined operating modes are detailed. To reiterate chapter II, when the position of clutch in military vehicle is locked it has the same power flows as garbage truck. Therefore, in the following discussion, the power flows are shown in such a way to also consider the clutch opening and locking phenomenon.

## 1- Power flows in Operating Modes of Basic Functions

*A) Power flows in ICE Propulsion (F)* – This section will determine the power flows when only the ICE propels the vehicle. In the power flow of this operating mode, the traction energy is supplied only by fuel tank. The possible path flows are:



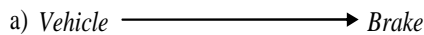
In option a), the ICE power is directly supplied to the wheels and the EMs are either locked or decoupled with a gearbox. In options b) and c), the power is divided into two concurrent paths. The first path goes directly from the ICE to the wheels while the second travels from the ICE through the EMs to the wheels. In the second path, it should be noted that the SOC is constant. Due to this constant SOC, the batteries do not consume any ICE power and the entire ICE energy will be given to the wheels.

*B) Power flows in ICE Charging (C)* – In this power flow, the vehicle is stopped and the speed of the wheels is zero. The possible power flows for charging the batteries from the ICE through the fuel tank are as follows:



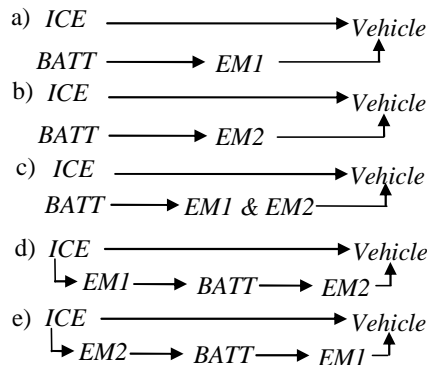
In option a) and b) the EM2 and EM1 is locked in such a way that only one EM is used to charge the batteries. This locking will be done by the gear-box. Furthermore, in the military truck, if the position of the clutch is taken into consideration then it will make no effect on these power flows because the vehicle is already in a rest position.

*C) Power flows in Mechanical Braking (M)* – In mechanical braking, the flow of power is directly given by the driver through the brake pedal to the wheels. This is the simplest power flow and the path is to follow is:



Similar to the power flows in ICE charging, the clutch assembly does not make any effect on the actual path of power.

*D) Power flows in Electric and ICE propulsion (EF)* – Here, the power is supplied by both energy sources, electrical (through EM) and fuel tank (ICE), to propel the vehicle. Following are the possible power flows for this operating mode:

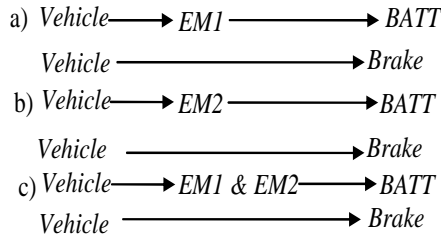


The power flows a), b) and c) are simple because the EM(s) and ICE are used simultaneously to propel the vehicle. The option d) and e) are also called hieratical mode. In this, a part of the ICE goes to the batteries via EM i.e. EM1 or EM2 and a part goes to the wheels, though the batteries also supply energy through the other EM i.e. EM2 or EM1 to wheels.

## **2- Power flows in Operating Modes of Combined Functions**

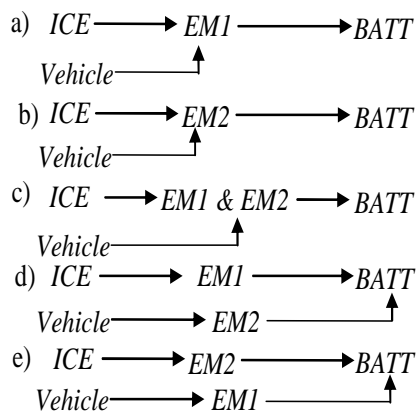
*E) Power flows in Regenerative and Mechanical Braking (RM)* – In this power flow, the vehicle is being stopped by the subsystems of studied HEVs i.e. EM(s) and mechanical brakes. Due to regenerative braking the vehicle is

stopped and as well as charging the batteries through the EM(s). The power flows in this operating mode are:



In option a) and b) only one EM is used to charge the vehicle when the power is less than its design values. The remaining brake power will be compensated with the mechanical brakes through the brake pedal. Here, it should be noted that in the military truck, the clutch should be locked for the regenerative braking power to be delivered to the batteries.

*F) Power flows in Regenerative Braking and ICE Charging (RC)* – In this power flow, the batteries are charged through the EM(s) by the wheels and ICE. Therefore, the following are the possible power flows:

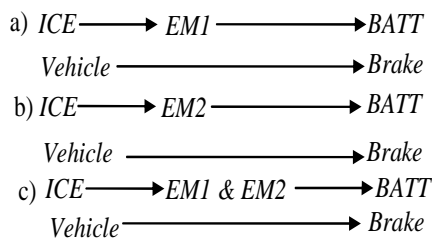


As discussed in the Hybrid Charging operating mode, this operating mode is only viable for very short period of time. To be effective, the regenerative braking has to be sudden and heavy while the vehicle is being propelled by the only the ICE. The ICE cannot stop at once due to the sudden braking thus the ICE must be utilized to charge the batteries with regenerative braking energy instead of propelling the vehicle.

In options a) and b), all of the ICE's power is given to the batteries by utilizing only one EM. This is possible when the other EM is disengaged with the gearbox. Option c) mentions that both EMs are used to charge the batter-

ies with the ICE and braking energy. In options d) and e), the ICE and braking energy each supply directly to one EM to store the energy in the batteries. It should be noted that all of these power flows are dependent on the SOC of the batteries.

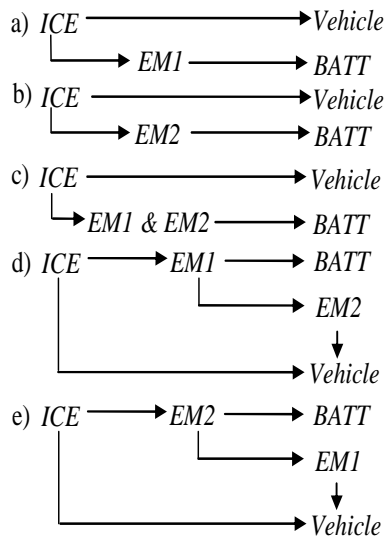
*G) Power flows in Mechanical Braking and ICE Charging (MC)* –These power flows are the combination of power flows shown in the ICE charging and mechanical braking. But similar to the parent power flows in the operating modes of mechanical braking and ICE charging, it would not affect the path of power. This includes the following power flows:



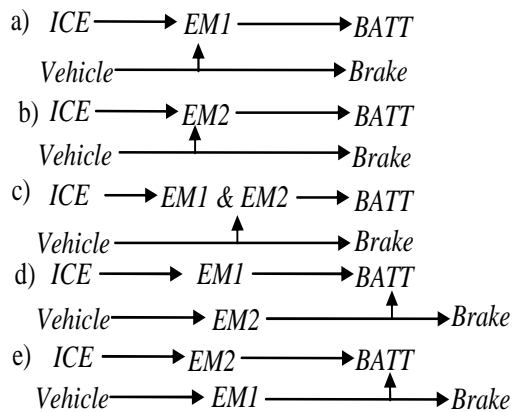
These power flows are useful when the vehicle is propelled by the ICE and the mechanical brakes are applied suddenly by the driver. At that moment, it is impossible to turn off the ICE for minimizing the fuel consumption. Therefore, all of the ICE power should be given to batteries via EM(s) for its charging.

*H) Power flows in ICE Propulsion and Charging (FC)* – In this, the ICE is used to propel the vehicle, but at the same time, it charges the batteries through the EM(s). The possible power flows in this operating mode are:

The first three power flows are clear because they take simple paths to charge the batteries as well as to propel the vehicle. However, the last two cases d) and e) are quite complex for PSDs. For example, in case e), a part from the ICE is directly given to the wheels and another part to routed through the EM1 to propel the vehicle. At the same time, a part from the ICE is given to charge the batteries through EM2.



*D) Power flows in Regenerative and Mechanical Braking with ICE Charging (RMC)* – These power flows will be valid when the vehicle is propelling by the ICE only and then it is stopped by both braking subsystems of HEVs, the EM and mechanical brakes. It holds the following paths in studied HEVs:



A detailed description of these power flows are previously given in E), F) and G) of this appendix. As an additional note, this power flow is very rare because it is used only in safety cases and can be compensated by the power flows E), F) or G).



# Appendix E:

## State Transition Diagram

State Transition Diagrams (STDs) are diagrams made of blocks to represent states and directed line segments to represent transitions between these states. One or more actions (outputs) may be connected with each transition. The diagram signifies a finite state machine. The well-known activity diagram in control engineering also represents finite state machine. However, whereas an activity diagram shows a flow of control from activity to activity across various objects, a state diagram shows the flow of control from state to state within a single object. Furthermore, the STDs are one of five diagrams in Unified Modeling Language (UML) for representing the dynamic aspects of systems [Booch 2005] [Horstmann 2005].

The main objectives of STDs are to represent a system as a series of states and related activities that display the connections amongst the states, show how the system moves from state to state, and document the sequence and priority of the states. They were initially developed to help design compilers. But later, due to its effectiveness in complex systems, they were widely utilized by systems analysts, application and information system engineers to analyze and design real-time and object-oriented systems [O'Docherty 2005].

Like other formalisms, STDs have their own language and notations to represent. In the following through [Fertuck 1994] [Amble 2002] [Booch 2005] and [O'Docherty 2005] the basic definitions of these terms are defined and shown (Fig. App.4) in the following:

*State* – A state is a condition or situation during the life of an object during which some condition is satisfied, some activity is performed, or an events is being waited for. As shown in Fig. App.4, graphically a state is represented by a rectangle with rounded corners.

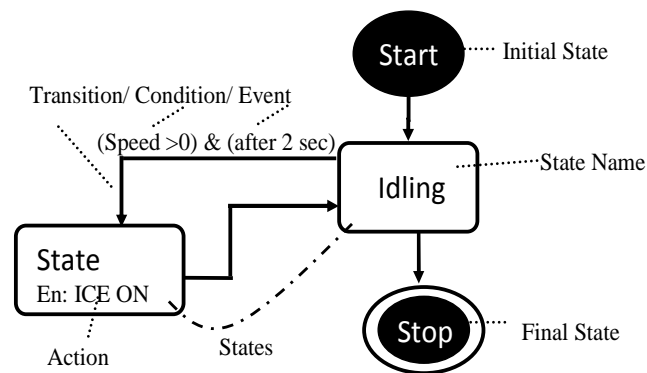
*Event* – An event is the identification of a major occurrence that has a place in time and space. With reference to state machines, an event is an occurrence of a stimulus that can trigger a state transition.

*Transition* – A transition is a relationship between two states that indicates that an object in the first state will do certain actions to advance to

the second state when a specified event occurs and certain conditions are met. It is represented by arrows as shown in Fig. App.4.

*Activity* – An activity diagram shows the flow from activity to activity. An activity is a continuing non-atomic execution within a state machine

*Action* – An action is an executable computation that results in a change in state of the model or the return of a value. A transition is shown as a solid directed line or path from the original state to the new state.



**Fig. App. 3 - State Transition Diagram – Level 1(Idling Function)**

In Fig. App.4, there are two special states that can be defined for an object's state machine. First, a primary state, “START”, that indicates the de-facto starting place for a state machine or sub state. An initial state is represented as a filled black circle. Second, the last state, “STOP”, which indicates that the execution of the state machine or the enclosing state is finished. A final state is represented as a filled black circle surrounded by an unfilled circle (a bull's eye). The remaining figure (Fig. App.4) is elaborated with the constituent needed to build any STD.

# **Acronyms & Abbreviations**



ANR	Agence Nationale de la Recherche
ARCHYBALD	ARChitectures HYBrides Adaptées aux véhicules Lourds à forte Disponibilité / Hybrid Drive Systems for Heavy-Duty Vehicles
ARTEMIS	Assessment and Reliability of Transport Emission Models and Inventory Systems
CO2	Carbon dioxide
CVT	Continuous Variable Transmission
DC	Direct Current
DOD	Depth Of Discharge
E-CVT	Electric Continuous Variable Transmission
ECU	Electronic Control Unit
ED	Electric Drive
EGR	Exhaust Gas Recirculation
EM	Electric Machine
EMR	Energetic Macroscopic Representation
EMS	Energy Management Strategy
EPA	Environmental Protection Agency
ES	Energy Sources
ESS	Energy Storage System
EV	Electric Vehicle
EVT	Electric Variable Transmission
FC	Fuel Cell

GM	General Motors
GPS	Global Positioning System
GVWR	Gross Vehicle Weight Rating
HEV	Hybrid Electric Vehicle
ICE	Internal Combustion Engine
IEA	International Energy Agency
MEGEVH	Modélisation Énergétique et Gestion d'Énergie des Véhicules Hybrides / Energy Modeling and Energy Management of Hybrid Vehicles
NEDC	New European Drive Cycle
OCV	Open Circuit Voltage
OM	Operating Modes
PF	Power Flow
PMSM	Permanent Magnet Synchronous Machine
PSD	Power Split Devices
pu	Per Unit
SOC	State Of Charge
SORT	Standard On-Road Test
STD	State Transition Diagrams
UNFCC	United Nations Framework Convention on Climate Change

# List of Symbols





$A$	Area ( $m^2$ )
$BSFC$	Brake Specific Fuel Consumption (g/kWh)
$c_x$	Drag Coefficient
$DOD$	Depth of Discharge (%)
$E_D$	Energy Density ( $kWh/kg$ )
$f_R$	Coefficient of Rolling Resistance
$f$	Viscous Friction ( $Nms$ )
$g$	Acceleration due to gravity ( $m/s^2$ )
$J$	Moment of Inertia ( $kg.m^2$ )
$k$	Gear ratio
$M$	Mass ( $kg$ )
$p_{cl}$	Position of the clutch (%)
$P$	Power ( $W$ )
$Q$	Storage capacity ( $Ah$ )
$R$	Radii of Clutch ( $m$ )
$T$	Torque of EM1 ( $Nm$ )
$u$	Battery Voltage ( $V$ )
$v$	Vehicle Speed ( $m/s$ )
$X$	Variable name
$\Omega$	Angular speed of EM1 ( $rad/s$ )
$\eta$	Efficiency of ICE (%)
$\rho$	Air density ( $kg/m^3$ )
$\mu$	Friction coefficient of the clutch
$\mu_{stat}$	Static friction coefficient of the clutch

$\alpha_{dyn}$	Dynamic friction coefficient
$X_{bat}$	Variable of batteries
$X_{Brake}$	Variable of brake
$X_{conv}$	Variable of converters
$X_{EM1}$	Variable of EM1
$X_{EM2}$	Variable of EM2
$X_{env.}$	Variable of environment
$X_F$	Frictional related Variable
$X_{ICE}$	Variable of ICE
$X_{IP}$	Variable of Inner Plane
$X_{LS}$	Variable of Large Sun
$X_{mea}$	Measured variable
$X_{PC}$	Variable of Planet Carrier
$X_R$	Variable of Ring gear
$X_{ref}$	Reference variable
$X_{SS}$	Variable of Small Sun
$X_{veh}$	Variable of vehicle
$X_W$	Variable of Wheel

# References



## A

1. [Allaby 2003] M. Allaby, R. Garratt, *“Fog, Smog, and Poisoned rain”*, Facts on File Science Library, ISBN-13: 978-0816047895, May 2003.
2. [Allègre 2010-a] A. L. Allègre, A. Bouscayrol, P. Delarue, P. Barrade, E. Chattot, S. Elfassi, *“Energy storage system with supercapacitor for an innovative subway”*, IEEE Trans. on Industrial Electronics, vol. 57, no. 12, pp. 4001 – 4012, December 2010.
3. [Allègre 2010-b] A. L. Allègre, *“Gestion du stockage mixte de l’énergie pour véhicule hybride électrique”*, PhD thesis (text in French), Université Lille1, Lille (France), (within MEGEVH network), October 2010.
4. [Amble 2002] S. W. Amble, *“The Elements of UML Style (Sigs Reference Library)”*, Cambridge University Press, Edition Illustrated, ISBN-13: 978-0521525473, November, 2002.
5. [Anderson 1995] C. Anderson, E. Pettit *“The effects of APU characteristics on the design of hybrid control strategies for hybrid electric vehicles”*, SAE 950493, pp. 65-71 February 1995.
6. [Anderson 2010] C. D. Anderson, J. Anderson, *“Electric and hybrid cars: a history”*, McFarland publishers, ISBN-13: 978-0786433018, April 2010.
7. [ANL 2012] Argonne National Laboratory, *“PSAT Documentation”*. cited on February 2012, available at: <http://www.transportation.anl.gov/software/PSAT/>,
8. [Ao 2008] S. Ao, O. Castillo, L. Xu, *“Trends in Intelligent Systems and Computer Engineering”*, First Edition, Springer, ISBN-13: 978-0387749341, April, 2008

## B

9. [Babers 2006] C. Babers, *“Architecture Development Made Simple”*,

- Second Edition, LuLu Publishers, ISBN-13: 978-1847288332, August 2006.
10. [Baert 2011] J. Baert, J. Pouget, D. Hissel, M.C. Pera, "*Energetic Macroscopic Representation of a Hybrid Railway Powertrain*", IEEE-VPPC'11, USB-S08-1-105, September 2011, Chicago (USA).
  11. [Barre 2006] P. J. Barre, A. Bouscayrol, P. Delarue, E. Dumetz, F. Giraud, J. P. Hautier, X. Kestelyn, B. Lemaire-Semail, E. Semail, "*Inversion-based control of electromechanical systems using causal graphical descriptions*", IEEE-IECON'06, November 2006, Paris (France).
  12. [Baumann 2000] B. M. Baumann, G. Washington, B. C. Glenn, G. Rizzoni, "*Mechatronic Design and Control of Hybrid Electric Vehicles*", IEEE/ASME Trans. on Mechatronics, vol. 5, no. 1, pp. 58-72, March 2000.
  13. [Bellis 2009] M. Bellis, "*Automobile History, The History of Cars and Engines*", available at: [http://inventors.about.com/od/cstartinventions/a/Car\\_History.htm](http://inventors.about.com/od/cstartinventions/a/Car_History.htm), June 2009.
  14. [Bennett 2005] S. Bennett, "*Heavy Duty Truck Systems*", Edition Fourth, Delmar Cengage Learning publisher, ISBN-13: 978-1401870645, November 2005.
  15. [Berenbrink 2002] P. Berenbrink, A. Brinkmann, C. Scheideler, "*SIMLAB-a simulation environment for storage area networks*", Proceedings on Parallel and Distributed Processing, Mantova, Italy, August 2002
  16. [Beresford 2006] A. R. Beresford, J. Bacon, "*Intelligent Transportation Systems*", IEEE Journal of Pervasive Computing, vol. 5, no. 4, pp. 63 - 67, October 2006
  17. [Bhide 2011] S. Bhide, T. Shim, "*Novel Predictive Electric Li-Ion Battery Model Incorporating Thermal and Rate Factor Effects*", IEEE Trans. on Vehicular Technology, vol. 60, no. 3, pp. 819-829, March 2011.
  18. [Bienaimé 2011] D. Bienaimé, N. Devillers, M.C. Péra, F. Gustin, A. Berthon, M.L. Hopdjanian, "*Energetic Macroscopic*

- Representation of an electric network embedded in a helicopter*”, IEEE-VPPC'11, September 2011, Chicago (USA).
19. [Booch 2009] G. Booch, J. Rumbaugh, I. Jacobson, “*Unified Modeling Language User Guide*”, Addison-Wesley Professional, Second Edition, ISBN-13: 978-0321267979, May, 2009
  20. [Boulanger 2011] A. G. Boulanger, A. C. Chu, S. Maxx, D. L. Waltz, “*Vehicle Electrification: Status and Issues*”, The Proceedings of the IEEE, vol. 99, no. 6, pp. 1116–1138, May 2011.
  21. [Boulon 2009-a] L. Boulon, M. C. Pera, P. Delarue, A. Bouscayrol, D. Hissel, “*Causal fuel cell system model suitable for simulation of transportation applications*”, ASME Journal of Fuel cell science and technology, vol. 7, no. 1, November 2009.
  22. [Boulon 2009-b] L. Boulon, “*Modelisation multiphysique des elements de stockage et de conversion d'energie pour les vehicules electriques hybrides. Approche systemique pour la gestion d'energie*”, Ph. D thesis (text in French), University of Franche Conte, Belfort (France), (within MEGEVH network), July 2009.
  23. [Boulon 2010] L. Boulon, D. Hissel, A. Bouscayrol, M.C. Pera, “*From Modeling to Control of a PEM Fuel Cell Using Energetic Macroscopic Representation*”, IEEE Trans. on Industrial Electronics, vol. 57 , no. 6, pp. 1882 – 1891, June 2010.
  24. [Bouscayrol 2000] A. Bouscayrol, B. Davat, B. de Fornel, B. Francois, J. P. Hautier, F. Meibody-Tabar, M. Pietrzak-David, “*Multimachine multiconverter system: application for electromechanical drives*”, European Physics Journal - Applied Physics, vol. 10, no. 2, pp.131-147, May 2000.
  25. [Bouscayrol 2002] A. Bouscayrol, P. Delarue, “*Simplifications of the Maximum Control Structure of a wind energy conversion system with an induction generator*”, Inter-

- national Journal of Renewable Energy Engineering, vol. 4, no. 2, pp. 479-485, August 2002.
26. [Bouscayrol 2003-a] A. Bouscayrol, "*Formalismes de representation et de commande des systemes electromecaniques multima-chines multiconvertis-seurs*", HDR thesis (text in French), University Lille1, Lille (France), December 2003.
  27. [Bouscayrol 2003-b] A. Bouscayrol, B. Davat, B. de Fornel, B. François, J. P. Hautier, F. Meibody-Tabar, E. Monmasson, M. Pietrzak-David, H. Razik, E. Semail, M. F. Benkhoris, "*Control structures for multi-machine multi-converter systems with upstream coupling*", Mathematics and Computers in Simulation, vol. 63, no. 3-5, pp. 261-270, November 2003.
  28. [Bouscayrol 2005-a] A. Bouscayrol, P. Delarue, X. Guillaud, "*Power strategies for maximum control structure of a wind energy conversion system with a synchronous ma-chine*", Renewable Energy Network, vol. 30, no. 15, pp. 2273-2288, December 2005.
  29. [Bouscayrol 2005-b] A. Bouscayrol, G. Dauphin-Tanguy, R Schoenfeld, A. Pennamen, X. Guillaud, G.-H. Geitner, "*Different energetic descriptions for electromechanical sys-tems*", *EPE'05*, September 2005, Dresden (Germa-ny).
  30. [Bruyere 2009] A. Bruyere, "*Modélisation et commande d'un alter-no-démarrreur heptaphasé pour application automo-bile micro-hybride*", Ph. D thesis (text in French), d'Arts et Métiers, ParisTech, Paris (France), May 2009.
  31. [Burke 2007] A. F. Burke, "*Batteries and Ultracapacitors for Elec-tric, Hybrid, and Fuel Cell Vehicles*", The Proceed-ings of IEEE, vol. 95, no. 4, pp. 806-820, April 2007.
  32. [Butterbach 2010] S. Butterbach,; B. Vulturescu, G. Coquery, C. Forgez, G. Friedrich, "*Design of a supercapacitor-battery storage system for a waste collection vehicle*", IEEE-VPPC'10, September 2010, Lille (France)



## C

33. [Callery 2009] S. Callery, "*Victor Wouk: The Father of the Hybrid Car*", Series: Voices for Green Choices - 2, Crabtree Publishing Company, ISBN-13: 9780778746775, January 2009.
34. [Ceccarelli 2007] M. Ceccarelli, "*Distinguished Figures in Mechanism and Machine Science: Their Contributions and Legacies, Part 1*", Springer, ISBN: 1402063652, September 2007.
35. [Chai 2005] F. Chai, S. Cui, S. Cheng, "*Performance Analysis of Double-Stator Starter Generator for the Hybrid Electric Vehicle*", IEEE Trans. on Magnetics, vol. 44, no. 1, pp. 484-487, January 2005.
36. [Chan 2000] H. L. Chan, "*A New Battery Model for use with Battery Energy Storage Systems and Electric Vehicles Power Systems*", IEEE Meeting on Power Engineering Society, vol. 1, pp 470-475, January 2000.
37. [Chan 2009] C. C. Chan, Y. S. Wong, A. Bouscayrol, K. Chen, "*Powering sustainable mobility: roadmaps of electric, hybrid, and fuel cell vehicles*", The Proceeding of IEEE, vol. 97, no. 4, pp. 603-607, April 2009.
38. [Chan 2010] C. C. Chan, A. Bouscayrol, K. Chen, "*Electric, hybrid and fuel cell vehicles: architectures and modeling*", IEEE Trans. on Vehicular Technology, vol. 59, no. 2, pp. 589 – 598, February 2010.
39. [Chan 2011] C.C. Chan, "*Outlook of Electric, Hybrid and Fuel Cell Vehicles*", Journal of Automotive Safety and Energy, vol. 2, no. 1, pp. 12-24, January 2011.
40. [Chau 2007] K.T. Chau, C.C. Chan, L. Chunhua, "*Overview of Permanent-Magnet Brushless Drives for Electric and Hybrid Electric Vehicles*", IEEE Trans. on Industrial Electronics, vol. 55, no. 6, pp. 2246-2257, June 2008.
41. [Chen 2008] K. Chen, Y. Cheng, A. Bouscayrol, C. C. Chan, A. Berthon, S. Cui, "*Inversion-based control of a hybrid*

- electric vehicle using a split electric variable transmission*”, IEEE-VPPC'08, September 2008, Harbin (China).
42. [Chen 2010] K. Chen, “*Common Energetic Macroscopic Representation and Unified Control Structure for different Hybrid Electric Vehicles*”, PhD thesis, Université Lille1, Lille (France), (within MEGEVH network), May 2010.
43. [Cheng 2009] Y. Cheng, K. Chen, C.C. Chan, A. Bouscayrol, S. Cui, “*Global modeling and control strategy simulation using electric variable transmission in hybrid electric vehicles*”, IEEE Vehicular Technology Magazine, vol. 4, no. 2, pp. 73-79, June 2009.
44. [Cheng 2010] Y. Cheng, A. Bouscayrol, R. Trigui, C. Espanet, “*Inversion-based control of a PM electric variable transmission*”, IEEE-VPPC'11, September 2010, Chicago (USA).
45. [Cho 2006] S. Cho, K. Ahn, J. M. Lee, “*Efficiency of the planetary gear hybrid powertrain*”, Journal of Automobile Engineering , vol. 220, no. 10, pp. 1445-1454 , October 2006.
46. [Chrenko 2009] D. Chrenko, M. C. Pera, D. Hissel, A. Bouscayrol, “*Modeling and control of fuel cell systems by energetic macroscopic representation*”, ASME Journal of Fuel cell science and technology, Vol. 6, no. 2, pp. 4501-450, May 2009.
47. [Colgren 2006] R. D. Colgren, “*Basic MATLAB<sup>®</sup>, Simulink<sup>®</sup> and Stateflow<sup>®</sup>*”, Edition First, AIAA Publishers, ISBN-13: 978-1563478383, December, 2006.

## D

48. [Dagoon 2000] J. D. Dagoon, “*Automotive I*”, Edition First, REX printing Company, ISBN: 971-23-2843-0, 2000
49. [Decon 2005] J. Decon, “*Object-Oriented Analysis and Design*”, Publisher Addison-Wesley, Code: 0-321-26317-0,

- London (UK), 2005.
50. [Delarue 2003] P. Delarue, A. Bouscayrol, A. Tounzi, X. Guillaud, G. Lancigu, “*Modelling, control and simulation of an overall wind energy conversion system*”, *Renewable Energy*, vol. 28, no. 8, pp. 1159-1324, July 2003 (common paper L2EP Lille and Jeumont SA).
51. [Delarue 2010] P. Delarue, A. Bouscayrol, P. Barrade, “*Energetic Macroscopic Representation and PSIM® simulation: application to a DC/DC converter input filter stability*”, IEEE-VPPC’10, Lille (France), September 2010.
52. [Delprat 1999] S. Delprat, G. Paganelli, T. M. Guerra, J. J. Santin, M. Delhorn, E. Combes, “*Algorithm optimization tool for the evaluation of HEV control strategies*,” Electric. Vehicle Symposium, China, 1999.
53. [Delprat 2004] S. Delprat, J. Lauber, T. M. Guerra, J. Rimaux, “*Control of a parallel hybrid powertrain: optimal control*,” IEEE Trans. on Vehicular Technology, Vol. 53, No. 3, pp. 872 - 881, May 2004.
54. [Diegel 2002] S. W. Diegel, S. C. Davis, “*Transportation Energy Databook*”, Edition Twenty-Second, Oak Ridge National Laboratory, September 2002.
55. [Docquier 2002] N. Docquier, S. Candell “*Combustion Control and Sensors: A Review*”, *Progress in Energy and Combustion Science*, vol. 28, no. 2, pp. 107-150, January 2002.

## E

56. [EMR 2012] EMR website, cited on March 2012, available at: <http://emr.univ-lille1.fr/cmsms/>.
57. [Eshani 2005] M. Eshani, Y. Gao, S. E. Gay, A. Emadi, “*Modern electric, hybrid electric and fuel cell vehicles: fundamentals, theory, and design*”, CRC Press, New York, Edition Second, ISBN-10: 0849331544, 2005.

## F

58. [Feroldi 2009] D. Feroldi, M. Serra, J. Riera, “*Design and Analysis of Fuel-Cell Hybrid Systems Oriented to Automotive Applications*”, IEEE Trans. on Vehicular Technology, vol. 58, no. 9, pp. 4720 – 4729, November 2009.
59. [Fertuck 1994] L. Fertuck, “*Systems Analysis and Design with Modern Methods*”, William C Brown Pub, Edition Second, ISBN-13: 978-0697162182, November, 1994.
60. [Fiveland 2000] S. Fiveland, D. Assanis, “*A Four-Stroke Homogeneous Charge Compression Ignition Engine Simulation for Combustion and Performance Studies*”, SAE Technical Paper 2000-01-0332, March 2000.
61. [Foch 1989] H. Foch, et enseignants de l’ENSEEIH, “*Electronique de Puissance - Principes fondamentaux: éléments constitutifs et synthèse des convertisseurs statiques*”, (text in French), Techniques de l’ingénieur, traité de Génie Electrique, D 3152, pp. 1-17, 1989, Paris.
62. [Fritzson 2004] P. Fritzson, “*Principles of Object-Oriented Modeling and Simulation with Modelica 2.1*”, Wiley-IEEE Press, Edition First, ISBN-13: 978-0471471639, January 2004.

## G

63. [Galland 2008] E. Galland, O. Pape, “*Cahier des charges: Véhicule lourd à forte disponibilité*”, Internal Report for ARCHYBALD project, reference: DDO/EAT/440-08/EG, August 2008
64. [Gan 2007] W. Gan, S. Kuo, “*Embedded Signal Processing with the Micro Signal Architecture - An Introduction to Graphical Programming with LabVIEW*”, Wiley-IEEE Press, Edition First, ISBN-13: 978-0471738411, February 2007.
65. [Gao 2006] Y. Gao, M. Ehsani, “*A Torque and Speed Coupling Hybrid Drivetrain — Architecture, Control, and*

- Simulation*”, IEEE Trans. on Power Electronics, vol. 21, no. 3, pp. 741–748, May 2006.
66. [Garret 2001] T. K. Garrett, K. Newton, W. Steeds, “*The Motor Vehicle*”, Edition Thirteen, SAE and Butterworth-Heinemann, ISBN: 978-0-7680-0639-1, January 2001.
67. [Gates 1997] Gates Energy Products, “*Rechargeable Batteries Applications Handbook*”, Newnes publishers, ISBN-13: 978-0750670067, December 1997.
68. [Gielniak 2004] M. J. Gielniak, Z. J. Shen, “*Power management strategy based on game theory for fuel cell hybrid electric vehicles,*” IEEE Vehicular Technology Conference, pp. 4422–4426, September 26–29, 2004.
69. [Gover 2010] J. Gover, M. J. Thompson, C. J. Hoff, “*Design of a Hybrid Electric Vehicle Education Program Based on Corporate Needs*”, IEEE-VPPC’10, September 2010, Lille (France).
70. [Granovskii 2006] M. Granovskii, I. Dincer, M. A. Rosen, “*Economic and environmental comparison of conventional, hybrid, electric and hydrogen fuel cell vehicles*”, Journal of Power Sources, vol. 159, no. 2, pp. 1186–1193, September 2006.
71. [Guzzella 2004] L. Guzzella, C. H. Onder, “*Introduction to Modeling and Control of Internal Combustion Engine Systems*”, Springer-Verlag Berlin Heidelberg, ISBN: 978-3-642-10774-0, May 2004.
72. [Guzzella 2007] L. Guzzella, A. Sciarretta, “*Vehicle Propulsion Systems: Introduction to Modeling and Optimization*”, Springer, ISBN-13: 978-3540746911, October 2007.

## H

73. [Hautier 1996] J. P. Hautier, J. Faucher, “*Le graphe informationnel causal*”, (text in French), Bulletin de l'Union des Physiciens, vol. 90, pp. 167-189, June 1996.
74. [Hautier 2004] J. P. Hautier, P. J. Barre, “*The causal ordering*

- graph - a tool for modelling and control law synthesis*”, Studies in Informatics and Control Journal, vol. 13, no. 4, pp. 265-283, December 2004.
75. [Hoeijmakers 2006] M. J. Hoeijmakers, J. A. Ferreira, “*The electric variable transmission*,” IEEE Trans. on Industrial Applications, vol. 42, n.4, pp. 1092- 1093, August 2006.
76. [Hofman 2007] T. Hofman, M. Steinbuch, R. van Druten, A. Serrarens, “*Rule-based energy management strategies for hybrid vehicles*,” International Journal of Electric and Hybrid Vehicles, vol. 1, no. 1, pp. 71–94, 2007.
77. [Horstmann 2005] C. S. Horstmann, “*Object-Oriented Design and Patterns*”, Wiley, Second Edition, ISBN-13: 978-0471744870, June, 2005
78. [Husain 2003] I. Husain, “*Electric and Hybrid Vehicles, Design Fundamentals*”, CRC, Edition First, ISBN-13: 978-0849314667, March 2003.

## I

79. [IEA 2009] International Energy Agency, “*World Energy Outlook 2009*”, ISBN 978-92-64-06130-9, March 2009

## J

80. [Johnson 2000] V. H. Johnson, K. B. Wipke, D. J. Rausen, “*HEV control strategy for realtime optimization of fuel economy and emissions*”, SAE paper 2000-01-1543, 2000.

## K

81. [Kapila 2007] V. Kapila, “*SimDriveline - [Product spotlight]*”, IEEE Journals on Control Systems, vol. 27 , no. 3, pp. 110-111, 2007
82. [Karnopp 1975] D. Karnopp, R. Rosenberg, “*System dynamics: a unified approach*”, John Wiley & Sons, 1975.
83. [Karris 2007] S. T. Karris, “Introduction to Stateflow with Appli-

- cations”, Edition First, Orchard Publications, ISBN-13: 978-1934404072, August, 2007
84. [Kavalov 2004] B. Kavalov, S. D. Peteves, “*Impacts of the increasing automotive diesel consumption in the EU*”, European Commission publications; EUR-21378, ISBN 92-894-6088-1, 2004.
85. [Kermani 2009] S. Kermani, “*Gestion énergétique des véhicules hybrides : de la simulation à la commande temps réel*”, Ph. D thesis (text in French), Université de Valenciennes et du Hainaut-Cambrésis, Valenciennes (France), (within MEGEVH network), September 2009.
86. [Kessels 2007] J. Kessels, “*Energy management for automotive power nets*”, Ph.D thesis, Eindhoven University of Technology (Netherlands), ISBN: 9038619634, February 2007.
87. [Kessels 2008] J. T. B. A. Kessels, M. W. T. Koot, P. P. J. van den Bosch, D. B. Kok, “*Online Energy Management for Hybrid Electric Vehicles*”, IEEE Trans. on Vehicular Technology, Vol. 57, No. 6, pp. 3428 - 3440, November 2008.
88. [Kestelyn 2009] X. Kestelyn, J. Gomand, A. Bouscayrol, P. J. Barre, “*Control of a symmetrical dual-drive gantry system using Energetic Macroscopic Representation*”, Solid State Phenomena, vol. 144, pp. 181-185, September 2009.

## L

89. [Le Trouher 2009] G. Le Trouher, “*Dispositif de traction hybride pour véhicule lourd*”, Patent (text in French) FR2918003, January 2009.
90. [Lee 1998] H.-D. Lee, S.-K. Sul, “*Fuzzy-logic-based torque control strategy for parallel-type hybrid electric vehicle*”, IEEE Trans. on Industrial Electronics., vol. 45, no. 4, pp. 625–632, August 1998.

91. [Lee 2000] H. Lee, S. Sul, H. Cho, J. Lee, “*Advanced Gear Shifting and Clutching Strategy for a Parallel-Hybrid Vehicle*”, IEEE Trans. on Industry Applications, vol. 6, no. 6, 2000, pp. 26-32, December 2000.
92. [Letrouvé 2010] T. Letrouvé, A. Bouscayrol, W. Lhomme, N. Dollinger, F. Mercier Calvairac, “*Different models of a traction drive for An electric vehicle simulation*”, IEEE-VPPC’10, September 2010, Lille (France).
93. [Lhomme 2007] W. Lhomme, “*Gestion d’énergie de véhicules électriques hybrides basée sur la représentation énergétique macroscopique*”, Ph. D thesis (text in French), Université Lille1, Lille (France), (within MEGEVH network), November 2007.
94. [Lhomme 2008-a] W. Lhomme, R. Trigui, P. Delarue, B. Jeanneret, A. Bouscayrol, F. Badin, “*Switched causal modeling of transmission with clutch in hybrid electric vehicles*”, IEEE Trans. on Vehicular Technology, vol. 57, no. 4, pp. 2081-2088, July 2008
95. [Lhomme 2008-b] W. Lhomme, R. Zanasi, G.-H. Geitner, A. Bouscayrol, “*Different Graphical Descriptions of Clutch Modelling for Traction Systems*”, ElectrIMACS’08, May 2008, Québec (Canada).
96. [Liawa 2004] B. Y Liawa, G. Nagasubramanian, R. G. Jungst, D. H. Doughty, “*Modeling of lithium ion cells—A simple equivalent-circuit model approach*”, International Conference on Solid State Ionics, vol. 175, no. 1-4, pp. 835-839, November 2004.
97. [Lin 2003] C.-C. Lin, H. Peng, J. W. Grizzle, J.-M. Kang, “*Power management strategy for a parallel hybrid electric truck*,” IEEE Trans. Control System Technology, vol. 11, no. 6, pp. 839–848, November 2003.
98. [Litvin 2004] F. L. Litvin, A. Fuentes, “*Gear Geometry and Applied Theory*”, Edition Second, Cambridge University Press, 2004.
99. [Liu 2008] J. Liu, H. Peng, “*Modeling and Control of a Power-Split Hybrid Vehicle*”, IEEE Trans. on Control Sys-



- tems Technology, vol. 16, no. 6, pp. 1242–1251, November 2008.
100. [Locment 2010] F. Locment, M. Sechilariu, “*Energetic Macroscopic Representation and Maximum Control Structure of electric vehicles charging photovoltaic system*”, IEEE-VPPC'10, September 2010, Lille (France).

## M

101. [Maggetto 2000] G. Maggetto, J. Van Mierlo, “*Electric and electric hybrid vehicle technology: a survey*”, IEE Seminar, Electric, Hybrid and Fuel Cell Vehicles, August 2002.
102. [Magyar 2007] G. Magyar, G. Knapp, G. Wojtkowski, J. Zupancic, “*Advances in Information Systems Development: Volume 1*”, Edition First, Springer, ISBN-13: 978-0387707600, October, 2007.
103. [Martinet 2010] S. Martinet, S. Pelissier, “*Tutorial on Batteries for Electric and Hybrid Vehicles: State of the art; Modeling, Testing and Aging*”, IEEE-VPPC'10, September 2010, Lille (France).
104. [MathWorks 2011-a] The MathWorks, “Stateflow user guide”, Accessed on July 2, 2011.
105. [MathWorks 2011-b] The MathWorks, “*Simdriveline<sup>®</sup> Demos*”, Ravigneaux Gear, Accessed on July 29, 2011.
106. [McGraw-Hill 2002] McGraw-Hill, S. P. Parker, “*McGraw-Hill Dictionary of Scientific and Technical Terms*”, Sixth edition, McGraw-Hill Professional Inc., ISBN-13: 978-0070423138, September 2002.
107. [MEGEVH 2011] MEGEVH website, cited on August 2011, available at: <http://l2ep.univ-lille1.fr/megevh/>.
108. [MEGEVH 2007] A. Bouscayrol, S. Delprat, D. Hissel and R. Trigui, “*MEGEVH project: graphical modelling for energy management of hybrid electric vehicles*”, EET'07, Brussel (Belgium), June 2007.
109. [MfE 2011] Ministry for the Environment (MfE), “*Energy Effi-*

*cient Ways*”, cited on March 2011, available at:

<http://www.energyfed.org.nz/Transport.pdf>

110. [Miller 2003] J. M. Miller, “*Propulsion systems for hybrid vehicles*”, Institution of Electrical Engineers, ISBN-13: 978-0863413360, December 2003.
111. [Miller 2006] J. M. Miller, “*Hybrid Electric Vehicle Propulsion System Architectures of the e-CVT Type*”, IEEE Trans. on Power Electronics, vol. 21, no. 3, pp. 756-767, May 2006.

## N

112. [Naunheimer 2011] H. Naunheimer, B. Bertsche, J. Ryborz, W. Novak, A. Kuchle, P. Fietkau , “*Automotive Transmissions: Fundamentals, Selection, Design and Application*”, Springer, Edition Second, ISBN 978-3-642-16213-8, 2011.
113. [Nobrant 2001] P. Nobrant, “*Driveline modelling using Mathmodelica*”, Masters thesis, Linköpings Universitet (Sweden), March 2001.

## O

114. [O'Docherty 2005] M. O'Docherty, “*Object-Oriented Analysis and Design: Understanding System Development with UML 2.0*”, Willey, First Edition, ISBN-13: 978-0470092408, June, 2005.
115. [O'Keefe 2002] M. P. O'Keefe, K. Vertin, “*An analysis of hybrid electric propulsion systems for transit buses*”, Tech. Rep. NREL/MP-540-32858, National Renewable Energy Laboratory, Golden, CO, 2002.
116. [Olah 2006] G. A. Olah, A. Goepfert, G. K. S. Prakash, “*Beyond Oil and Gas: The Methanol Economy*”, First Edition, Wiley-Vch Verlag publishers, ISBN-13: 978-3527312757, March 2006.
117. [Olivé 2007] A. Olivé, “*Conceptual Modeling of Information Systems*”, Edition First, Springer, ISBN-13: 978-

3540393894, October 2007.

118. [Otter 1997] M. Otter, C. Schlegel, H. Elmqvist, “*Modeling and real-time simulation of an automatic gearbox using modelica*”, ESS’97, pp. 115-121, October 1997.

## P

119. [Paganelli 2001] G. Paganelli, G. Ercole, A. Brahma, Y. Guezennec, G. Rizzoni, “*General supervisory control policy for the energy optimization of charge sustaining hybrid electric vehicles*,” Journal of Society Automotive Engineering, Japan, vol. 22, no. 4, pp. 511–518, October 2001.
120. [Pang 2001] S. Pang, J. Farrell, J. Du, M. Barth, “*Battery state-of-charge estimation*,” IEEE American Control Conference, vol. 2, pp. 1644–1649. June 2001, Arlington (USA).
121. [Panwai 2005] S. Panwai, H. Dia, “*Comparative evaluation of microscopic car-following behavior*”, IEEE Trans. on Intelligent Transportation Systems, vol. 6, no. 3, pp. 314-325, September 2005.
122. [Pape 2010] O. Pape, W. Lhomme, D. Depernet, B. Vulturescu, L. Bregeon, “*ARCHYBALD project on new HEV powertrains*”, IEEE-VPPC’10, September 2010, Lille (France).
123. [Paynter 1961] H. Paynter, “*Analysis and design of engineering systems*”, MIT Press, 1961.
124. [Peng 2009] L. Peng, B. Francois, Y Li, “*Improved crowbar control strategy for DFIG based wind turbines to ride-through grid faults*”, IEEE-APEC’09, March 2009, Washington (USA).
125. [Peter 2001] H. Peter, M. Keller, “*Real-world driving cycles for emission measurements: ARTEMIS and Swiss cycles*”, Federal Office for the Environment FOEN, March 2001, Bern (Switzerland), available at: <http://www.bafu.admin.ch>

126. [Phillips 2000] A. M. Phillips, M. Jankovic, K. Bailey, “*Vehicle system controller design for a hybrid electric vehicle*”, IEEE Int. Conf. Control Appl., pp. 297–302, September 25–27, 2000.
127. [Piccolo 2001] A. Piccolo, L. Ippolito, V. Galdi, and A. Vaccaro, “*Optimization of energy flow management in hybrid electric vehicles via genetic algorithms*,” IEEE/ASME Int. Conference on Advance Intelligent Mechatronics, pp. 434–439, July 8–12, 2001.
128. [Pisu 2003] P. Pisu, E. Silan, G. Rizzoni, S. M. Savaresi, “*A LMI-based supervisory robust control for hybrid vehicles*,” American Control Conference, pp. 4681–4686, June 4–6, 2003.
129. [Pisu 2005] P. Pisu, K. Koprubasi, and G. Rizzoni, “*Energy management and drivability control problems for hybrid electric vehicles*,” IEEE Conference on Decision Control, pp. 1824–1830, December 12–15, 2005.
130. [Pisu 2007] P. Pisu, G. Rizzoni, “*A comparative study of supervisory control strategies for hybrid electric vehicles*”, IEEE Trans. on Control Systems Technology, vol. 15, no. 3, pp. 506–518, 2007.
131. [Pop 2008] V. Pop, H. J. Bergveld, D. Danilov, P. P.L. Regtien, P. H. L. Notten, “*Battery Management Systems*”, First Edition, Philips Research Book Series - Volume 9, Springer publishers, ISBN-13: 978-140206945-1, May 2008.

## R

132. [Rahman 2008] S. A. Rahman, N. Zhang, J. Zhu, “*Modeling and simulation of an energy management system for Plug-in Hybrid Electric Vehicles*”, Power Engineering Conference (AUPEC’08), pp. 1 - 6, December 2008.
133. [Rajagopalan 2003] A. Rajagopalan, G. Washington, G. Rizzoni, Y. Guezennec, “*Development of fuzzy logic control and*

- advanced emissions modeling for parallel hybrid vehicles*”, NREL Tech. Rep., NREL/SR-540-32919, December 2003.
134. [Raskin 2006] P A. Raskin, S. Shah, “*The emergence of hybrid vehicles - ending oil's stranglehold on transportation and the economy*”, June 2006, available at: <http://www.calcars.org/alliance-bernstein-hybrids-june06.pdf>
135. [Ravelco 2011] Ravelco website, cited on August 2011, available at [www.ravelcodfw.com/truck\\_classes.htm](http://www.ravelcodfw.com/truck_classes.htm)
136. [Reitze 2010] A. W. Reitze, “*Air pollution control law: compliance and enforcement*”, Environmental Law Institute, ISBN: 9781585761531, January 2010.

## S

137. [Salman 2005] M. Salman, M.-F. Chang, J.-S. Chen, “*Predictive energy management strategies for hybrid vehicles*,” IEEE Conference on Decision Control, pp. 21–25, December 12–15, 2005.
138. [Salmasi 2007] F. R. Salmasi, “*Control Strategies for Hybrid Electric Vehicles: Evolution, Classification, Comparison and Future Trends*”, IEEE Trans. on Vehicular Technology, vol. 56, no. 5, pp. 2393-2404, September 2007.
139. [Sautter 2010] A.C. Sautter, V. Venaille, G. Le Trouher, J.L. Bouysset, O.Pape, “*ARCHYBALD: an hybrid transmission for heavy vehicles*”, IEEE-VPPC’10, September 2010, Lille (France)
140. [Schouten 2002] N. Schouten, M. Salman, N. Kheir, “*Fuzzy logic control for parallel hybrid vehicles*,” IEEE Trans. on Control Systems Technology, vol. 10, no. 3, pp. 460–468, 2002.
141. [Sciarretta 2004] A. Sciarretta, M. Back, L. Guzzella, “*Optimal control of parallel hybrid electric vehicles*,” IEEE Trans. on Control Systems Technology, vol. 12, no. 3, pp.

- 352–363, May 2004.
142. [Serrao 2006] L. Serrao, P. Pisu, G. Rizzoni, “*Analysis and evaluation of a two engine configuration in a series hybrid electric vehicle*”, ASME, International Mechanical Engineering Congress and Exposition, 2006.
143. [Serrao 2009] L. Serrao, “*A Comparative Analysis of Energy Management Strategies for Hybrid Electric Vehicles*”, PhD dissertation, The Ohio State University, 2009.
144. [Serrarens 2004] V. Serrarens, M. Dassen, M. Steinbuch, “*Simulation and Control of an Automotive Dry Clutch*”, IEEE-ACC’04, vol. 5, pp. 4078-4083, July 2004, Boston (USA).
145. [Shumei 2006] C. Shumei, Z. Wei, T. Likun, “*Control Strategy for Double Shaft Parallel Hybrid Electric Vehicle*”, IEEE-VPPC’06, Windsor (UK), pp. 1 – 4, September 2006.
146. [Sokhi 2008] R. S. Sokhi, “*World Atlas of Atmospheric Pollution*”, Anthem Press, Edition First, ISBN-13: 978-1843312895, May 2008.
147. [Srinivasan 2007] S. Srinivasan, “*Automotive Engines*”, Fifth edition, Tata McGraw-Hill Publishing Co. Ltd., ISBN: 0-07-040265-5, 2007.
148. [Stanley 2011] J. K. Stanley, D. A. Hensher, C. Loader, “*Road transport and climate change: Stepping off the greenhouse gas*”, Elsevier Science - Journal of Cleaner Production, vol. 45, no. 10, pp. 1020-1030, December 2011.
149. [Stremersch 2001] G. Stremersch, “*Supervision of Petri nets*”, First Edition, Springer publishers, ISBN-13: 978-0792374862, September 2001.

## T

150. [Tate 1998] E. D. Tate, S. P. Boyd, “*Finding ultimate limits of performance for hybrid electric vehicles*”, SAE Paper: 00FTT-50, 1998.

151. [Taylor 2002] D. G. Taylor, “*Nonlinear Control of Electric Machines: An Overview*”, IEEE Control Systems, vol. 14, no. 6, pp. 41 - 51, August 2002.
152. [Trigui 2011] R. Trigui, “*Approche systémique pour la modélisation, la gestion de l’énergie et l’aide au dimensionnement des véhicules hybrides thermiques - électriques*”, HDR thesis (text in French), Université Lille1, Lille (France), (within MEGEVH network), December 2011.
153. [Tsai 2000] L. W. Tsai, “*Mechanism design: enumeration of kinematic structures according to function*”, CRC Press, Edition First, ISBN-13: 978-0849309014, September 2000.

## U

154. [UITP 2001] International Association of Public Transport (UITP), “*SORTT – Standardized On-Road Tests Cycles*”, 54th UITP International Congress, May 2001, London (UK), cited on February 2012, available at: [http://ec.europa.eu/environment/archives/clean\\_bus/slides/etienne\\_sort.pdf](http://ec.europa.eu/environment/archives/clean_bus/slides/etienne_sort.pdf).

## V

155. [Vasca 2008] F. Vasca, L. Iannelli, A. Senatore, M.T. Scafati, “*Modeling torque transmissibility for automotive dry clutch engagement*”, American Control Conference, pp. 306 – 311, June 2008, Seattle (USA).
156. [Verhille 2006] J. N. Verhille, A. Bouscayrol, P. J. Barre, J. P. Hautier, “*Model validation of the whole traction system of an automatic subway*”, IEEE-VPPC '06, September 2006, Windsor (UK).

## W

157. [Walsh 1999] M. P. Walsh, “*Motor Vehicle Standards and Regulations around the World*”, cited on June 1999, availa-

- ble at:  
[www.walshcarlines.com/pdf/globalregs.pdf](http://www.walshcarlines.com/pdf/globalregs.pdf)
158. [Wang 1998] J. Wang, "*Timed Petri nets: theory and application*", *First Edition*, Springer publishers, ISBN-13: 978-0792382706, October 1998.
  159. [Wankam 2006] Y. D. Wankam, P. Sicard, A. Bouscayrol, "*Maximum control structure of a five-drive paper system using Energetic Macroscopic Representation*", IEEE-IECON'06, November 2006, Paris (France).
  160. [Wipke 1999] K. B. Wipke, M. R. Cuddy, S. D. Burch, "*ADVISOR 2.1: a userfriendly advanced powertrain simulation using a combined backward/forward approach*", IEEE Trans. on Vehicular Technology, vol. 48, no. 6, pp. 1751-1761, November 1999.
  161. [Wirasingha 2011] S. J. Wirasingha, A. Emadi, "*Classification and Review of Control Strategies for Plug-In Hybrid Electric Vehicles*", IEEE Trans. on Vehicular Technology, vol. 60, no. 1, pp. 111-122, January 2011.
  162. [Woodrooffe 2000] J. Woodrooffe, "*Technology Roadmap for the 21st Century Truck Program*", US Department of Energy's (DOE), cited on December 2000, available at: <http://www.osti.gov/bridge/>
  163. [Wu 2009] Z. Wu, D. Depernet, C. Kieffer, F. Dubas, D. Hissel, C. Espanet, "*Electrical motor design for hybrid heavy-duty electrical powertrain*", IEEE-VPPC'09, September 2009, Dearborn (USA).
  164. [Wu 2010] Z. Wu, D. Depernet, C. Espanet, "*Optimal design of electrical drive and power Converter for hybrid electric powertrain*", IEEE-VPPC'10, September 2010, Lille (France)
  165. [Wu 2012] Z. Wu, "*Conception optimale d'un entraînement électrique pour la chaîne de traction d'un véhicule hybride électrique : co-conception des machines électriques, des convertisseurs de puissance et du réducteur planétaire*", PhD thesis (text in French), University of Besancon, Belfort (France), (within ME-



GEVH network), March 2012.

## Y

166. [Yanowitz 2000] J. Yanowitz, R. L. McCormick, M. S. Graboski, “*In-Use Emissions from Heavy-Duty Diesel Vehicles*”, *Environ. Sci. Technol.*, vol.34, no.5, pp. 729–740, January, 2000

## Z

167. [Zachariadis 2001] T. Zachariadis, Z. Samaras, “*Validation of road transport statistics through energy efficiency calculations*”, Elsevier Science - *Journal of Energy*, vol. 26, no. 5, pp. 467–491, May 2001.
168. [Zanasi 1996] R. Zanasi, “*Power-oriented graphs for modeling electrical machines*”, MELECOM'96, Bari (Italy), pp. 1211-1214, May 1996.